UNIVERSITY OF INSUBRIA

Doctoral School of Biological and Medical sciences
Ph.D. Program in Neurobiology

THE PROTEOMIC APPROACH TO INVESTIGATE PARKINSON'S DISEASE: PATHOGENETIC MECHANISMS AND BIOMARKERS DISCOVERY

Tutor:
Prof. Mauro Fasano

Coordinator:
Prof. Daniela Parolaro

Ph.D. thesis of:
Tiziana Alberio

2007-2010

Table of contents

Abstract

The overall goals of basic research in improving the clinical approach to a disease are, on the one hand, to unravel its natural history, finding its cause and developing better treatments and, on the other hand, to find biomarkers that would permit to ameliorate the diagnosis, to distinguish among patient subtypes and to set up clinical trials of new therapeutic agents. The common threads of the two projects developed in this thesis are the technique used, proteomics, and the main object, Parkinson's disease (PD). Proteomics is a powerful methodology to investigate how protein expression is affected in the pathogenesis of a disease process and should be exploited both to investigate PD pathogenetic mechanisms and to discover peripheral biomarkers.

In the first part of this thesis the project "A SH-SY5Y model to investigate PD pathogenetic mechanisms" is discussed. We investigated the expression pattern of cellular proteins following dopamine exposure in catecholaminergic SH-SY5Y human neuroblastoma cells overexpressing α-synuclein by a proteomic approach. Using 2D gel image analysis and ANOVA statistics we identified proteins that correlate with the experimental conditions in our model. Significant changes in specific cellular processes were observed, such as cytoskeleton structure and regulation, mitochondrial function, energetic metabolism, protein synthesis and neuronal plasticity. Proteins were analyzed by a network enrichment tool that automatically enriched the network model in terms of the most relevant proteins that seem to be missing. Moreover, the bioinformatic approach found out the enriched Gene Ontology (GO) categories, allowing us to draw attention to the NF-κB pathway. To validate experimentally the hypothesis of the NF-κB involvement, we performed a luciferase gene reporter assay that revealed a downregulation of the transcription factor activation by α-synuclein increased expression and its complete quenching by dopamine exposure.

Each element arising from the present study could represent a valuable starting point for focused investigations aimed to better understand key issue of PD pathogenesis. For instance, a protein that completely disappeared after dopamine treatment was VDAC2, a porin of the outer mitochondrial membrane. Since the impairment of mitochondrial function is considered among the major pathogenetic factors of neurodegeneration in PD, we further investigated the regulation of VDAC2 degradation and the role of its phosphorylation.

Accumulating evidence supports a specific role of DJ-1 in protecting dopaminergic neurons from dopamine itself. Since this protein act as a pool of different forms possibly associated to

different function and localization, we analyzed DJ-1 2D electrophoresis pattern in SH-SY5Y cells after exposure to dopamine; we observed a specific increase in the most acidic forms in the pattern together with a significant decrease of the most basic spot. Unlike cells exposed to generic oxidative conditions, no additional shift was observed. The results are corroborated by a meta-analysis of the literature showing that in the absence of dopamine treatment the specific acidic form is underrepresented.

The second part of the thesis is focused on the project "Dopamine response of dopaminergic circulating cells: the Jurkat cell model". The functions of immune cells are regulated not only by cytokines, but also by several neurotransmitters. In particular, peripheral blood lymphocytes possess a complex dopaminergic regulatory system. Human T-lymphocytes express all five dopamine receptors (D1-D5), each of which exerts different actions on the regulation of T-cell functions. The Jurkat human leukemia CD4+ T-cell line has been thoroughly used and characterized as a suitable cell model to investigate T-cell signaling and apoptosis, nevertheless its characterization as a model of circulating dopaminergic cells was never reported before. In this regard, we characterized the dopaminergic system in Jurkat cells and through a proteomic approach we analyzed their response to a dopamine challenge in order to highlight metabolic pathways that could specifically reveal alterations linked to PD. A dopamine challenge, with no effect on cell viability (50 μM), induced quantitative changes in the protein expression pattern. The proteins that showed quantitative differences were identified by peptide mass fingerprinting and analyzed in terms of both interaction network and GO classification enrichment. We obtained a significant model for network enrichment and a functional association to GO classification (unfolded protein binding). Eventually, we observed a modification of β-actin and 14-3-3 two-dimensional pattern following dopamine exposure.

In both projects, by combining the experimental and the bioinformatic approach, we fulfilled the expectations for proteomics to generate new hypotheses. Of course, one must consider that models have limitations and that hypotheses need further validation, but they could be a good starting-point to unravel biochemical pathways altered in PD, a disease with a poorly understood etiology.

1. INTRODUCTION

1.1 The proteomic approach to investigate pathogenethic mechanisms and to find biomarkers for Parkinson's disease

The overall goals of basic research in improving the clinical approach to a disease are, on the one hand, to unravel its natural history, finding its cause and developing better treatments and, on the other hand, to find biomarkers that would permit to ameliorate the diagnosis, to distinguish among patient subtypes and to set up clinical trials of new therapeutic agents.

Dealing with neurodegenerative disorders with a complex etiology and a still obscure pathogenesis, it is difficult to generate valuable hypotheses and set up focused investigation to reveal new insights of the disease. This would require an *a priori* speculation on probable causes and pathological cascades that follow. Being the subject of interest a multifactorial condition such as it is the case of Parkinson's disease (PD), the choice of a biased approach is often a dead-end strategy.

Consequently, a recent effort has focused on the use of –omics techniques, *i.e.*, transcriptomics, proteomics, and metabolomics, in order to elucidate many of the pathogenic aspects of PD. As a matter of fact, a more comprehensive investigation of PD and the identification of specific disease networks and molecular pathways involved herein will facilitate our understanding of the disease process and enhance our ability to diagnose and treat this debilitating condition. In general, these techniques can be applied to various biological media, including tissues, cerebrospinal fluid (CSF), blood and blood constituents, urine, as well as others (Caudle et al., 2010).

Proteomics is a powerful methodology to investigate how protein expression is affected in the pathogenesis of a disease process, providing a complement to the information obtained by functional genomics (see Hanash, 2003). Proteomics is a technology-driven approach, and takes advantage from unprecedented advances in separation techniques such as two-dimensional electrophoresis and liquid chromatography, in the design and exploitation of high-sensitivity sources and analyzers for mass spectrometry, and bioinformatics (Tao and Aebersold, 2003). These advances have allowed the quantitative analysis of protein levels and post-translational modifications that altogether help to understand molecular alterations in cells, tissues and biofluids that are associated to disease etiology, progression, outcome, and response to therapy. On the other hand, proteomics provides a high-throughput methodology for the search of new therapeutic targets for diseases with a high social impact like cancer and neurodegenerative diseases with a remarkable prevalence in the elderly (Hanash, 2003). The

term proteome was first introduced (Wasinger et al., 1995) to describe the entire protein complement of the genome in a given compartment at a given time. Proteomics also has the main goal to understand protein localization, modification, trafficking, interactions, and eventually function. This wealth of information cannot be obtained by genomics and transcriptomics alone, since the actual function of a gene depends on the activity of the translated, processed protein (Lee, 2003). The emerging field of neuroproteomics promises to provide powerful strategies to further characterize neuronal dysfunction and cell loss associated with neurodegenerative diseases (Becker et al., 2006; Fasano and Lopiano, 2008).

Although the proteomic approach in neuroscience research is very recent, several papers have been published in the last four years on the investigation of pathogenetic mechanisms of neurodegenerative disorders by proteomics (Fasano et al., 2007; Fasano and Lopiano, 2008; Schulenborg et al., 2006; Sheta et al., 2006). Moreover, the field of clinical proteomics is especially well suited for the discovery of biomarkers; indeed, proteins that show reproducible changes either in levels or in post-translational modifications are potential drug targets or disease biomarkers. The latter are particularly useful if they are present in body fluids, like blood (plasma and blood cells) or urine, which are easy to obtain (Dorsey et al., 2006; Fasano et al., 2008b; Sheta et al., 2006; Michell et al., 2004).

Altogether, the proteomic methods are a valuable toolbox for either the analysis of pathogenetic mechanisms in neurodegenerative disorders and (cell and animal) models thereof, or the search for suitable biomarkers that should be useful for early and differential diagnosis as well as for therapy assessment. For these reasons, this thesis is focused on the two main goals of neuroproteomics mentioned above, in order to better understand the main actors of PD pathogenetic mechanisms and to reveal possible protein responders to dopamine-related alterations at T-cells level.

1.2 Parkinson's disease

Parkinson's disease is a neurodegenerative disorder characterized by motor symptoms (tremor, bradykinesia and rigidity) that develop as a consequence of the degeneration of dopaminergic neurons of the substantia nigra pars compacta (SNpc) (Thomas and Beal, 2007). No single causative factor has been yet identified for PD, which may originate from the interaction of various pathogenic mechanisms, including mitochondrial defects, enhanced

formation of reactive oxygen species (ROS) and aberrant protein aggregation (Van Laar and Berman, 2009).

The traditional view of PD as a single clinical entity is under scrutiny. Clinically, the disease is heterogeneous, and subtypes may be recognized on the basis of age of onset, predominant clinical features and progression rate. Two major clinical subtypes exist: a tremor predominant form that is often observed in younger people, and a type known as "postural imbalance and gait disorder" (PIGD) that is often observed in older people (>70 years old) and is characterized by akinesia, rigidity, and gait and balance impairment. In very general terms, the first subtype leads to a slow decline of motor function, whereas the latter worsens more rapidly (Obeso et al., 2010). Different clinical subtypes of PD are distinguished due to predominant motor symptoms: a tremor-dominant type (TDT), an akinetic rigid type (ART), and a predominant postural instability and gait difficulty (PIGD) type. Several studies suggest that the different subtypes may have different patterns of disease progression: whereas motor function deteriorates more rapidly in ART, it has a more benign course in TDT (Jankovic et al., 1990; Roos et al., 1996). The development of PIGD becomes a major cause of disability and dependence (Shulman et al., 2008). A different neuropathological substrate for these subtypes of PD has also been described (Jellinger et al., 1999). Patients with TDT have been reported to have less depression and cognitive deterioration (Lewis et al., 2005). A recent SPECT study of cerebral dopamine transporters revealed significant differences between TDT and ART at the same stage of PD (Spiegel et al., 2007). Patients with PIGD suffer significantly more from orthostatic hypotension than TDT patients (Allcock et al., 2006).

Although Parkinson's disease is classically diagnosed by the onset of motor manifestations, the concept of premotor Parkinson's disease has gained support (Hawkes et al., 2008; Langston, 2006). There is increasing evidence that olfactory dysfunction, sleep abnormalities, cardiac sympathetic denervation, constipation, depression and pain may antedate the onset of motor signs of Parkinson's disease (O'Sullivan et al., 2008). Affected nondopamine neurons include monoaminergic cells in the locus coeruleus (Zarow et al., 2003) and raphe nuclei, cholinergic cells in the nucleus basalis of Meynert (associated with cognitive deficits) (Hilker et al., 2005) and the pedunculopontine tegmental nucleus (which may be related to gait problems) (Rinne et al., 2008), and hypocretin cells in the hypothalamus (which likely mediate the sleep disorders seen in Parkinson's disease) (Thannickal et al., 2007). Approximately 30–50% of these nondopamine cells have been lost by end-stage Parkinson's disease. The pathological model proposed by Braak and colleagues (Braak et al., 2003)

reflects the stepwise progression of Lewy body (LB) pathology in the brain. These authors have suggested a caudorostral gradient of LB formation from the lower brainstem to the neocortex (Braak et al., 2006). This suggests that once the disease has started, there is a single progression wave, and that the onset of dementia, generally late in the course of Parkinson's disease, is due to cortical LB (Braak et al., 2005).

LB are mainly composed by α-synuclein and extensively ubiquitinylated proteins; these intracytoplasmic inclusions are also immunoreactive for 3-nitrotyrosine and neurofilament (Devine and Lewis 2008; Thomas and Beal 2007). Histological evidence shows that the more pigmented neurons are the first ones to degenerate, suggesting thus that neuromelanin depletion does not occur at random (Hirsch et al., 1988); conversely, it has been reported that the less pigmented ventral tier of SN is the first to degenerate in PD, with a more extended cell loss with respect to heavily pigmented regions (Gibb, 1992; Kastner et al., 1992). It has been proposed that neuromelanin, that confers the dark pigmentation to dopaminergic neurons, may act as a scavenger of redox-active transition metals and of toxic catechol intermediates (Fedorow et al., 2005; Youdim et al., 1994; Zecca et al., 2003). Other factors that may selectively affect SNpc neurons compared to other catecholaminergic cells include differences in their handling of ionic fluxes -less capacity for calcium buffering (Esteves et al., 2010) and increased reliance on L-type calcium channels (Chan et al., 2007)- and in their expression of specific transcription factors that regulate cell fate and survival (Alavian et al., 2008). Currently, there is no definitive explanation for why these abnormalities affect dopaminergic neurons earlier and more profoundly than other cell types. One major common theme for most mutations and toxins is the impairment of mechanisms related to cellular energy production leading to oxidative stress. It may be that the selective vulnerability of nigrostriatal cells is determined by their profuse arborization, which may result in high levels of energy consumption. It has been estimated that nigrostriatal dopaminergic neurons can form as many as 40,000 synapses, whereas neurons in the ventral tegmental area only make up to 3,000 contacts. It is known that aging decreases energetic cellular efficiency as well as the synthesis and activity of neuronal growth factors. This could explain the enhanced vulnerability with aging and even the trend toward reduction of regional vulnerability. Dietary habits and lifestyles associated with reduced risk of Parkinson's disease (for instance, smoking, coffee drinking, and diets high in uric acid or greater levels of physical activity in midlife) could somehow modify the cellular processes affected in the pathology and reduce the risk to develop Parkinson's disease (Obeso et al., 2010).

1.2.1. Epidemiology and Genetics

PD affects over 1% of the population above the age of 65 but early onset PD (EOPD) patients develop symptoms before age 50 years (Schrag and Schott, 2006; Lesage and Brice, 2009). EOPD patients have an increased likelihood of a genetic etiology of the disease compared with patients with late-onset PD, however it has been suggested that also late-onset PD may have a substantial familial component (Payami et al., 2002; Kay et al., 2006).

About 10-15% of patients with the typical clinical picture of PD have a positive family history compatible with a mendelian (autosomal dominant or autosomal recessive) inheritance. As a rule, age at onset in many (but not all) of these patients is younger than that of patients with sporadic disease, but no other specific clinical signs or symptoms distinguish familial from sporadic cases (Gasser, 2009). Although the different mutations and loci identified so far appear to be directly responsible in only a relatively small number of families each, there is accumulating evidence that the molecular pathways identified may be common to more than one genetic form of PD and may also play a role in the common sporadic disease (Gasser, 2009).

Autosomal recessive forms of parkinsonism are linked to mutations in *parkin* (PARK2, the most common), *PINK1* (PTEN-induced putative kinase 1; PARK6), *DJ-1* (PARK7), *ATP13A2* (PARK9), *PLA2G6* (PARK14) and *FBXO7* (PARK15) genes, and are characterized by age at onset usually before 40 years. As for the autosomal dominant forms, mutations in five genes have been identified: *α-synuclein* (PARK1 and PARK4), *UCHL1* (ubiquitine C-terminal ligase L1; PARK5), *LRRK2* (leucine-rich repeat kinase 2; PARK8), *GIGYF2* (PARK11) and *OMI/HtrA2* (PARK13) (Lesage and Brice, 2009; Gasser, 2009) (see Table 1).

The most common monogenic cause of EOPD is due to mutations in the parkin gene on chromosome 6q. The disease is autosomal recessive, and numerous mutations in parkin have been described to date. About half of all patients with familial PD with onset before age 45 years and a family history compatible with autosomal recessive inheritance have composite mutations in the parkin gene, and it causes about 10–20% of apparently sporadic cases with onset before age 45 years (Schrag and Schott, 2006, Lesage and Brice, 2009).

The *PARK8* gene encodes for dardarin (LRRK2). Different LRRK2 mutations have been described, with the G2019S mutation, a founder haplotype in several European populations, being found in up to 5-6% of several large cohorts of families with PD-affected members and even in 1-2% of patients with apparently sporadic late-onset PD. The clinical features and

epidemiology of LRRK2-related PD have yet to be fully elucidated, but mutations are present in various populations (Schrag and Schott, 2006; Gasser, 2009). Most patients have onset above age 50 years, and penetrance seems to be age related (Schrag and Schott, 2006). Nonetheless, several cases of EOPD are associated with LRRK2 mutations, including a recent report of a mutation in a 28-year old with apparently sporadic disease (Kay et al., 2006). Additionally, some cases of apparently idiopathic EOPD may also be due to either very rare and atypical genetic abnormalities, or to as yet unidentified genetic defects (Schrag and Schott, 2006).

Table 1: Loci, genes and susceptibility factors involved in parkinsonism.

PARK loci	Form of PD	GENE
PARK1	EOPD AD	α-synuclein (mut)
PARK2	Juvenile and EOPD AR	Parkin
PARK3	LOPD AD	SPR (?)
PARK4	EOPD AD	α-synuclein (dupl./tripl.)
PARK5	LOPD AD?	UCHL1
PARK6	AR	PINK1
PARK7	EOPD AR	DJ-1
PARK8	LOPD AD and sporadic	LRRK2, dardarin
PARK9	Juvenile AR Kufor–Rakeb syndrome and EOPD	ATP13A2
PARK10	non-Mendelian	?
PARK11	LOPD AD	GIGYF2
PARK12	non-Mendelian	?
PARK13	AD	OMI/HtrA2
PARK14	AR, Juvenile AR levodopa-responsive dystonia-parkinsonism	PLA2G6
PARK15	AR, EO AR parkinsonian-pyramidal syndrome	FBXO7

EO, early-onset; LO, late-onset, AD, autosomal dominant; AR, autosomal recessive; PD, Parkinson's disease; PINK1, PTEN-induced kinase 1; LRRK2, Leucine-Rich Repeat Kinase 2; SPR, sepiapterin reductase; UCHL1, ubiquitin carboxy-terminal hydrolase; GIGYF2, GRB10-interacting GYF protein 2; PLA2G6, group VI phospholipase A2 (adapted from Lesage and Brice, 2009).

1.3 Alteration of dopamine homeostasis and oxidative stress

Oxidative stress is classically defined as a redox imbalance with an excess formation of oxidants or a defect in antioxidants. Although the body in general has developed several defense mechanisms to counteract oxidative stress, the brain appears to be more susceptible to this damage than any other organ, as it consumes about 20% of the resting total body oxygen. The ability of the brain to withstand oxidative stress is limited because of the presence of high amounts of polyunsaturated fatty acids, low levels of antioxidants such as glutathione(GSH) and vitamin E and the elevated content of iron in specific areas such as the globus pallidus and the substantia nigra (Chinta and Andersen, 2008). Moreover, being postmitotic, neurons in the brain once damaged may be permanently dysfunctional (Calabrese et al., 2005). Post-mortem studies on brains from PD patients have consistently implicated the role of oxidative damage in the pathogenesis of PD. It is not clear whether accumulation of ROS in PD is a primary event or a consequence of other cellular dysfunctions (Chinta and Andersen, 2008).

There is much evidence to suggest that ROS derived from the combined presence of dopamine (DA), low GSH, and high iron are a major cause of the loss of dopaminergic cells in the brains of individuals with PD (Jenner and Olanow, 1996; Youdim and Riederer, 1997). The metabolism of dopamine gives rise to various molecules that can act as endogenous toxins (Dodson and Guo, 2007; Lotharius and Brundin, 2002; Zhang et al., 2000). Indeed, dopamine is chemically unstable and can auto-oxidize at neutral pH with the formation of quinone species and hydrogen peroxide, which can be reduced into cytotoxic hydroxyl radicals in a reaction catalyzed by iron, whose levels are higher in SNpc than in other brain regions, oxygen, or enzymes such as tyrosinase (Barnham et al., 2004; Chinta and Andersen, 2008; Lotharius and Brundin, 2002; Zecca et al., 2001). The electrophilic quinones themselves can act as oxidants thus supporting ROS formation. Auto-oxidation of dopamine may be increased in the early stages of the disease when dopamine turnover is increased to compensate for dying dopaminergic neurons (Scherman et al., 1989). Other dopamine metabolites such as 3, 4-dihydroxyphenylacetic acid (DOPAC) can undergo further two-electron oxidation to generate ROS and DOPAC-quinones (Gluck and Zeevalk, 2004).

Many of the genetic factors linked to PD lead to an impairment of dopamine homeostasis by interfering with the vesicular storage and release mechanisms. Dopamine auto-oxidation in the cytosol determines oxidative stress conditions that are magnified by the impairment of the antioxidant defence of the cell (Devine and Lewis, 2008; Fasano et al., 2006; Fasano and

Lopiano, 2008; Gasser, 2009; Lesage and Brice, 2009; Maguire−Zeiss et al., 2005; Thomas and Beal, 2007).

Normally, ROS are eliminated by intracellular antioxidant systems, which might be impaired as a result of the aging process or in disease states. Although GSH is not the only antioxidant molecule reported to be altered in PD, the magnitude of GSH depletion appears to parallel the severity of the disease and is the earliest known indicator of nigral degeneration, reportedly preceding detectable losses in both mitochondrial complex I activity and striatal dopamine. GSH depletion has been demonstrated to result in complex I inhibition (Chinta et al., 2007). Depletion of GSH has also been reported to result in inhibition of glutathione reductase activity (the enzyme which converts oxidized glutathione or GSSG into reduced GSH) via direct oxidation of its two active site cysteine residues. This would result in further increases in GSH loss and alteration of the cellular redox state as the GSH/GSSG ratio is further decreased.

These data indicate that not only can complex I inhibition result in increased dopamine oxidation, but dopamine oxidation itself might affect complex I function leading to mitochondrial dysfunction (Chinta and Andersen, 2008).

Studies with toxins able to induce parkinsonian syndromes in experimental models further suggest a possible role for free oxygen in selective loss of SN dopaminergic neurons in the disease. For instance, 6-hydroxydopamine (6-OHDA) is known to destroy dopaminergic neurons through free radical-mediated mechanisms. Similarly, 1-methyl-4-phenyl-1,2,3,6-tetrahydropyridine (MPTP)-induced impairment of the mitochondrial respiratory chain via inhibition of complex I enhances superoxide formation that then can initiate neuronal death (Liu et al., 2010).

As a whole, in a disease where the etiology is still unknown, many of the genetic and environmental factors variously linked to it contribute to a redox imbalance that seem to have the strongest effect on the more sensitive dopaminergic SN cells.

1.4 α-Synuclein

Mutations in the α-synuclein gene have an historical relevance as responsible for the first monogenic PD form identified. Three single point mutations, duplication and triplication of the gene were reported and linked to familial forms of Parkinson's disease (PARK1 and PARK4, respectively – see Table 1) (Gasser, 2009). α-Synuclein, a small 14 kDa protein, is a major constituent of LB where it assumes a fibrillary, β-pleated-sheet conformation and binds

other proteins such as the 14-3-3 chaperonin, an anti-apoptotic factor that antagonizes α-synuclein and shares 40% sequence conservation with the N-terminal region of α-synuclein (Goedert, 2001; Ostrerova et al., 1999; Spillantini et al., 1997). Early studies revealed that 14-3-3 binds to and activates tyrosine hydroxylase (TH) (Ichimura et al., 1988), the rate-limiting enzyme in catecholamine synthesis. α-Synuclein, like 14-3-3, may also bind to TH but, in contrast, inhibits its activity (Perez et al., 2002). This finding suggests that a loss of α-synuclein by its aggregation or its decreased expression, as occurs in PD, may selectively disrupt DA homeostasis and negatively impact dopaminergic neuronal survival (Perez et al., 2002).

As explained in Paragraph 1.3, oxidative imbalance is supposed to be the main pathogenetic event in triggering neurodegeneration in PD. α-Synuclein can variously contribute to oxidative stress. Expression of either wild-type or mutant protein in different cell lines has demonstrated that α-synuclein modulates DA toxicity, associated to reactive oxygen species (ROS) arising from DA oxidation (Fasano and Lopiano 2008; Wood-Kaczmar et al., 2006;) (see Figure 1). Several studies indicate that α-synuclein protofibrils can modify the permeability of vesicles by formation of pores similar to those generated by pore-forming bacterial toxins (Lashuel et al., 2002; Volles et al., 2001; Volles et al., 2002). The altered membrane permeability could cause unregulated calcium flux and leakage of DA into the cytoplasm that leads to cell death (Lotharius and Brundin, 2002, Volles et al., 2001;) (see Figure 1). DA quinone reacts with α-synuclein to form covalent adducts that slows the conversion of protofibrils to fibrils (Conway et al., 2001). This finding suggests that cytosolic DA in dopaminergic neurons promotes the accumulation of toxic α-synuclein protofibrils, which might explain why these neurons are most vulnerable to degeneration in PD (Rochet et al., 2004). Cross-linking promoted *in vitro* by DA-derived radicals was already suggested to occur in neurofilament subunits and several other proteins (Hao et al., 2007; Montine et al., 1995). Noteworthy, evidence for cross-linking of α-synuclein to oxidized, polymerized DA (*i.e.*, neuromelanin) was found in SNpc of PD patients (Fasano et al., 2003; Fasano et al., 2006).

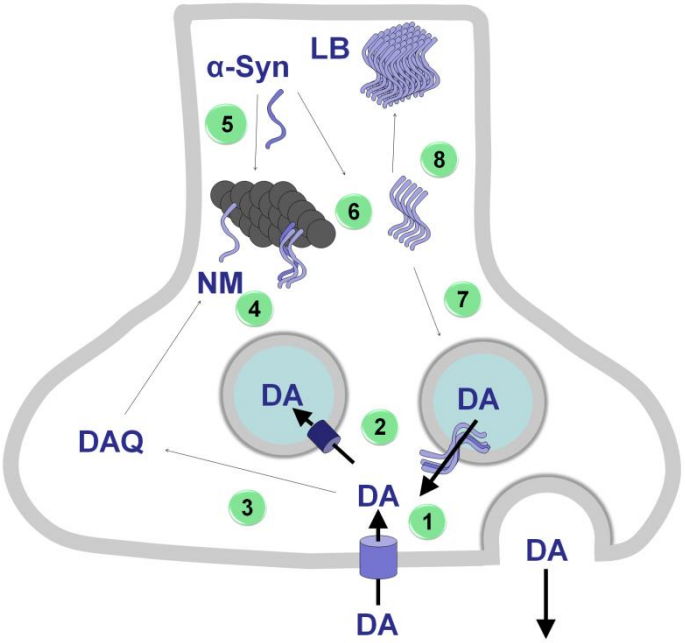

Figure 1: Dopamine, α-synuclein and neurodegeneration Dopamine (DA), either synthesized or reuptaken from synaptic space (1), is stored into vesicles by the vesicular monoamine transporter (2), so that the concentration of cytosolic DA is kept low. Cytosolic DA is auto-oxidized to yield dopamine quinone (DAQ) (3) and eventually forms neuromelanin (NM) (4), α-Synuclein (α-Syn) may cross-link with the growing NM polymer to yield a melanoproteic adduct (5), or aggregate into soluble protofibrils (6) able to form pores through the membrane of vesicles and consequently to release stored DA (7); eventually, α-Syn protofibrils assemble together with other proteins to form Lewy bodies (LB) (8). Adapted from Fasano and Lopiano, 2008.

PD-characteristic aggregates of α-synuclein have been found not only in the central nervous system (CNS), but also in the enteric nervous system, that is connected to the CNS via the vagal nerve. According to the pathogenetic hypothesis proposed by Braak and coworkers, as already explained in Paragraph 1.2, α-synuclein progressively accumulates in the brain starting from defined induction sites (medulla oblongata/pontine tegmentum and olfactory bulb/anterior olfactory nucleus) and advancing in a topographically predictable sequence, with motor symptoms becoming appreciable only when α-synuclein starts to assemble into the very first LB in SNpc melanized neurons (Braak et al., 2004).

The role of α-synuclein in cell death is unclear as is the form the protein has when it causes cell death. α-Synuclein conformation can range from unfolded state in solution, to α-helical in the presence of lipid-containing vesicles, to β-pleated sheet or amyloid structure in fibrils (see

Fasano and Lopiano, 2008). The presence of LB within cells has been taken as an indication that toxic α-synuclein acts intracellularly to initiate apoptotic pathways, but the viability of cells with aggregated forms of α-synuclein suggests that these cells are resistant to the toxicity of this form of the protein. This leaves to the possibility that intracellular α-synuclein is only toxic under certain conditions (Brown, 2010). Aggregates of α-synuclein can take on a variety of forms. Most commonly noted are the fibrillar forms of the protein. Other forms include oligomeric species and small protofibrils. These alternative forms of aggregates can take on distinct forms such as rings or stellate spheres (Wright et al., 2009). The conditions under which these different aggregates form is, therefore, of considerable importance. The most reliable factor in this regard is molecular crowding (Uversky, 2002). The higher the intracellular concentration of α-synuclein, the more likely it is to form aggregates. Considerable evidence suggests that oligomers, formed as prefibrillar intermediates, may be the toxic component (Danzer et al., 2007; Karpinar et al., 2009; Outeiro et al., 2008; Volles et al., 2001; Wright et al., 2009). Studies of aggregation using recombinant α-synuclein lead to the investigation of factors that increase the rate or extent of aggregation. One of the factors identified was the presence of metal ions (Uversky et al., 2001). In particular, copper has been shown in numerous studies to greatly enhance the aggregation of α-synuclein (Brown, 2010). There are clear evidences that high levels of α-synuclein can be damaging, but it is equally true that raising the level of the same protein from low to moderate is beneficial (Quilty et al., 2006). Cookson proposed a J shaped model to explain the dual role of α-synuclein (Figure 2; Cookson, 2006). At low levels, lack of α-synuclein is detrimental for cell viability, and there is a moderate amount of expression where synuclein expression maximally improves neuronal viability (many of the toxins that are commonly used to generate experimental parkinsonian syndromes – rotenone, MPP^+, 6-hydroxydopamine and dopamine itself – all increase α-synuclein expression), which tails off as expression levels increase above the doubling seen in the genomic triplication. If a neuron forms an inclusion body and deposits fibrillary α-synuclein into an insoluble Lewy body, then the probability of the cell survival is improved. It is worth stressing that the concentration responses have narrow ranges. In this vision, the normal function of α-synuclein is partially neuroprotective and the upregulation seen in chronic neurodegenerative diseases is a deliberate action on the part of the neuron to protect itself. Clearly, it becomes central to understand normal functions of this protein to better explain this phenomenon. Indeed, whether synuclein is toxic or beneficial will depend on regional and temporal influences, as well as expression levels (Cookson, 2006).

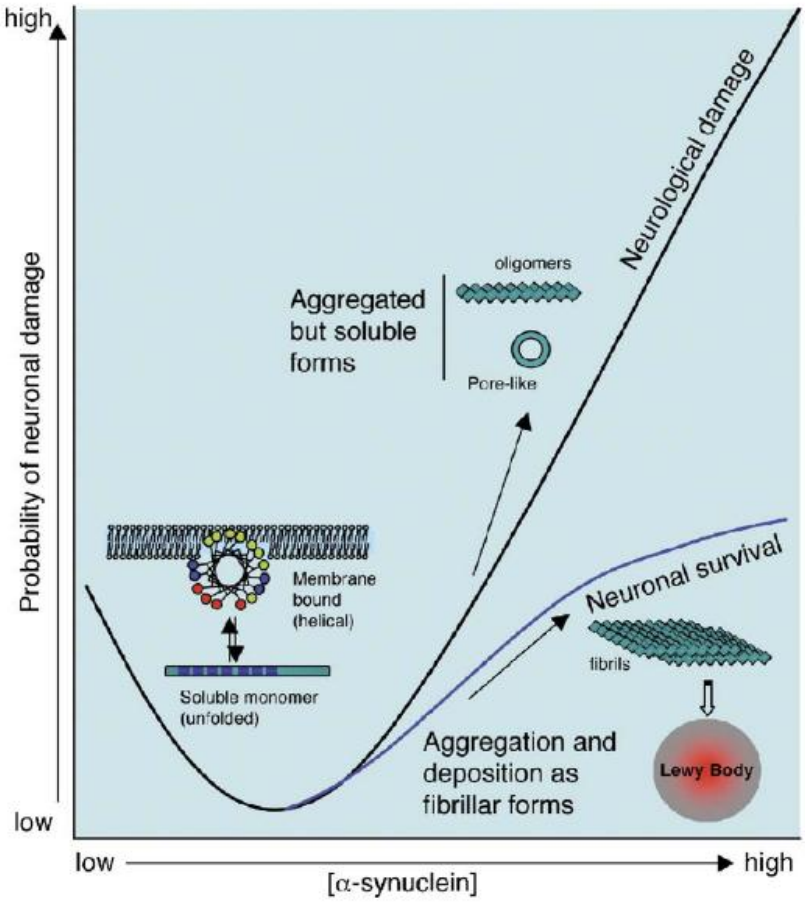

Figure 2: α-Synuclein's J-shaped curve. The relationship between α-synuclein and cell survival is complex and involves a number of factors including time, amount of expression and neuronal phenotypes. This schematic representation emphasizes the effects of α-synuclein expression levels on cell survival. Moderate expression levels (moving towards the centre of the x-axis) seem to promote cell survival, but high expression levels are associated with pathological events including inclusion body formation and cell loss (towards the right of the same axis). It is also important to note that some of these events seen at high expression levels can be dissociated from each other. To show this schematically, the two lines diverge at higher expression levels. A current, if controversial, hypothesis in the field is that more soluble forms of α-synuclein are toxic. These are represented as oligomers and pore-like annular structures and would be associated with cell death. An alternative route is that α-synuclein can form fibrils and be deposited into inclusion bodies (Lewy bodies shown here). While this may come at the cost of decreased function, this may also be permissive for neuronal survival (blue line). Taken from Cookson, 2006.

1.5 DJ-1

DJ-1/PARK7 is an ubiquitous, highly conserved protein that was originally identified because of its ability to transform NIH3T3 mouse cells in cooperation with Ras (Nagakubo et al., 1997). Starting from the association between loss-of-function mutations in the DJ-1 gene and PARK7, a monogenic, autosomal-recessive form of PD (Bonifati et al., 2003), an accumulating body of evidence pinpointed the important role of DJ-1 in this neurodegenerative condition. Very recently, it has been shown that oxidized dopamine can covalently modify DJ-1 (Van Laar et al., 2009); however, whether this can affect dopamine cell degeneration is unknown. Some hints may come from the involvement of DJ-1 into many cellular functions, including evidence linking this protein to oxidative stress response – a fact well known even before the association of DJ-1 with PD (Mitsumoto et al., 2001) – mitochondrial function (Zhang et al., 2005) and transcription (Zhong and Xu, 2008), nuclear transcription (Xu et al., 2005), mRNA binding and protein interaction (Hod et al., 1999; Van der Brug et al., 2008) and protein degradation (Xiong et al., 2009).

Mirroring the involvement of DJ-1 in multiple cellular activities, this protein has been found in complex with multiple molecular partners, including DJ-1 itself (Tao and Tong, 2003), PINK-1 and Parkin (Xiong et al., 2009), alpha-synuclein (Meulener et al., 2005), HSP70 (Li et al., 2005), DJBP (Niki et al., 2003), PIASx alpha (Takahashi et al., 2001), ASK1 (Waak et al., 2009), histone deacetylase 6 (Olzmann et al., 2007), androgen receptor (Tillman et al., 2007), DAXX (Junn et al., 2005), and Abstrakt (Sekito et al., 2005).

DJ-1 has been shown to modulate dopamine toxicity in cellular models of oxidative stress with reference to PD (Fasano et al., 2008a; Kim et al., 2005). Dopamine exposure leads to upregulation of DJ-1 that in turn increases cell resistance to dopamine itself and reduces intracellular oxidants (Lev et al., 2008; Lev et al., 2009). On the other hand, α-synuclein overexpression leads to upregulation of DJ-1, and DJ-1 overexpression protects cells from α-synuclein toxicity (Batelli et al., 2008; Colapinto et al., 2006; Zhou and Freed, 2005). Besides being in complex with a number of different partners, DJ-1 is often post-translationally modified. DJ-1 modifications mainly include oxidations at different sites, which is related to its antioxidant role (Choi et al., 2006; Kinumi et al., 2004; Mitsumoto et al., 2001), but there are also evidences of ubiquitination (Olzmann et al., 2004, Olzmann et al., 2007) and SUMOylation (Small Ubiquitin-like MOdifier) (Shinbo et al., 2006).

Not unexpectedly, DJ-1 binding to its molecular counterparts, and thus its pleiotropic effects, are affected by DJ-1 posttranslational modification. For example, oxidation regulates homodimerization (Ito et al., 2007) and affects DJ-1 binding to mRNA (van der Brug et al., 2008), ASK1 (Waak et al., 2009), HSP70 (Li et al., 2005), parkin (Moore et al., 2005), while ubiquitination mediates the binding to histone deacetylase 6 (Olzmann et al., 2007).

Multiple DJ-1 modified forms are simultaneously present, so that DJ-1 can be better considered as a pool of different forms, with different modifications and in different amounts. It is very likely that, instead of the total amount of DJ-1 or of a defined DJ-1 form, the composition of this pool and the precise balance between different forms is the main factor determining DJ-1 global activity (Alberio et al., 2010a).

In particular, alterations of this pool, instead of DJ-1 mutations, are expected to play a role in those non-genetic conditions correlated to DJ-1 activity, including idiopathic PD. Indeed, since many different DJ-1 forms can be separated on the basis of their pI, it is a common finding that DJ-1 oxidation, correlated to ageing, Parkinson's and Alzheimer's diseases, produces an increase in DJ-1 species of acidic pH, and a decrease in basic species, so that these conditions are characterized by a pool of DJ-1 forms different than that observed in controls. Up to 10 different DJ-1 forms, including the acidic forms (pI 5.5 and 5.7) of DJ-1 monomer and the basic forms (pI 8.0 and 8.4) of SDS-resistant DJ-1 dimer, were reported to selectively accumulate in PD and AD frontal cortex tissues compared with age-matched controls (Choi et al., 2006, Canet-Avilés et al., 2004, Meulener et al., 2006). Ubiquitination and SUMOylation of DJ-1, on the other side, affects also the molecular weight of the modified species, and are thus separated by mono-dimensional electrophoresis accordingly (Olzmann et al., 2004, Olzmann et al., 2007, Shinbo et al., 2006).

1.6 Cellular models to investigate dopamine and α-synuclein toxicity

Proteomic technologies have been widely used in the investigation of neuronal differentiation and neurodegeneration, particularly in the detection of differences between healthy individuals and patients suffering from neurodegenerative diseases. However, human tissue samples, while exceedingly important for studying neurodegeneration, are heterogeneous from patient to patient, which increases the difficulty of identifying changes in protein expression for a specific disease state. Another important point is that patient tissue samples often can provide information at the terminal stage of a disease, owing to the difficulty in

collecting tissues undergoing disease development. To deal with this cellular complexity and to overcome heterogeneity and problems in sample collection, the use of cellular culture models has been considered (Johnson et al., 2005). Among the most frequently used continuous cell lines in neurobiology are SH-SY5Y, C-1300, NSC34, MES.

As described in Paragraph 1.3, dopaminergic neurons are particularly exposed to oxidative stress because the metabolism of DA gives rise to various molecules that can act as endogenous toxins. On this basis several efforts have been made to develop cell models for dopamine toxicity. The majority of data about the degeneration of melanized dopamine containing neurons has come from animal and cell cultures studies that employ neurotoxins such as rotenone (Shastry, 2001) and 6-hydroxydopamine (6-OHDA), which replicate many characteristics of the parkinsonian syndrome. 6-OHDA is widely used because it selectively kills catecholaminergic neurons and induces cellular responses relevant to the naturally occurring disease such as mitochondrial dysfunction, oxidative stress and apoptotic death (Dauer and Przedborski, 2003, Marti et al., 2002, Walkinshaw, 1994). In any case, it would be advisable to explore the effects of misregulated dopamine homeostasis that is the most probable trigger of dopaminergic neuron death in sporadic PD, rather than those of toxins that act in a less specific way (6-OHDA) or target specific proteins (rotenone on mitochondrial complex 1).

The catecholaminergic SH-SY5Y human neuroblastoma cell line is a valuable model to explore dopamine toxicity and its accumulation in the cytosol. Indeed, these cells express the DA transporter (DAT) and DA receptors and are able to form storage vesicles, although the low activity of the vesicular monoamine transporter type 2 (VMAT-2) impairs DA storage into vesicles. For this reason, SH-SH5Y cytoplasmic DA concentration may be raised by administering extracellular DA in the culture medium (Gomez-Santos et al., 2003). Moreover, addition of catalase is able to markedly improve cell survival (Colapinto et al., 2006) even in the presence of 1 mM DA, in agreement with a similar observation on PC12 cells (Blum et al., 2000). Thus, it is possible to investigate dopamine effects in these models, eliminating aspecific effects due to H_2O_2 generation in the extracellular space.

Specific mitochondrial proteins covalently modified by dopamine and its oxidized form, dopamine-quinone, have been identified in rat isolated mitochondria and in SH-SY5Y cells, using a proteomic analysis (Van Laar et al., 2009).

As explained in Paragraph 1.4, despite the association between α-synuclein and various diseases, it remains unknown as to how the protein can cause the diseases or initiate neuronal

death. Several authors increased the level of α-synuclein by transient or conditional expression, observing extensive protein aggregation and increased susceptibility to DA toxicity (Junn and Mouradian, 2002; Kanda et al., 2000; Lee et al., 2001; Tabrizi et al., 2000; Tanaka et al., 2001; Xu et al., 2002). Zhou et al. employed quantitative proteomics in conjunction with isotope-coded affinity tags (ICAT) to identify the proteins associated with soluble α-synuclein that might promote its aggregation (Zhou et al., 2004). More than 250 proteins associated with Nonidet P-40 soluble α-synuclein were identified, and at least 51 of these proteins displayed significant differences in their relative abundance in α-synuclein complexes under conditions where rotenone was cytotoxic and induced formation of cytoplasmic inclusions immunoreactive to anti α-synuclein (Zhou et al., 2004). To characterize the exact biological role of α-synuclein other authors evaluated changes in whole genome expression in SH-SY5Y caused by reductions of 90% in α-synuclein RNA levels and of 59% in α-synuclein protein levels as a result of RNA interference (Häbig et al., 2008). The expression of 361 genes was altered, with 82 up-regulated and 279 down-regulated. The differentially expressed gene products are involved in the regulation of transcription, cell cycle, protein degradation, apoptosis, neurogenesis, and lipid metabolism.
Wright et al. used SH-SY5Y cells to demonstrate the toxicity of α-synuclein oligomers. Only the aggregated protein generated in the presence of copper was toxic. Analysis with electron microscopy demonstrated that these oligomers were present only when α-synuclein was bound to copper (Wright et al., 2009).

1.7 Parkinson's disease as a mitochondrial disease

Strong evidence now exists to support a role for aberrant mitochondrial form and function, as well as increased oxidative stress (see Paragraph 1.3), in the pathogenesis of PD (Schapira, 2008). A complex interplay occurs between mitochondria and other cellular machinery that affects cell survival, as mitochondria not only have a key role in electron transport and oxidative phosphorylation, but they are also the main cellular source of free radicals, and they are involved in calcium homeostasis and in the regulation and instigation of cell-death pathways (Henchcliffe and Beal, 2008) (Figure 3).

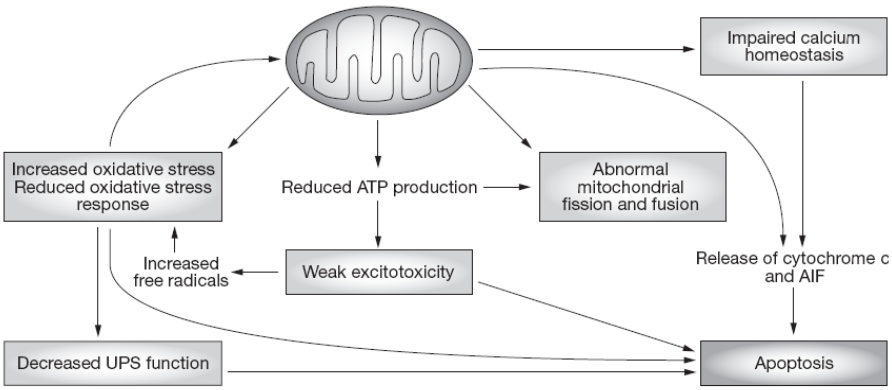

Figure 3: Mitochondrial dysfunction affects diverse cellular processes that can culminate in cell death. Mitochondrial dysfunction affects a number of cellular pathways, leading to damage of intracellular components and to cell death. Abnormal metabolic function, abnormal morphology, and impaired fission–fusion balance have all been observed in mitochondria in at least some forms of Parkinson disease. Mitochondria are a major source of free radicals in the cell, resulting in oxidative stress, but mitochondria are also integral to the oxidative stress response. Increased oxidative stress can lead to impaired function of the UPS, thereby further affecting cell survival. Mitochondria also sequester calcium when intracellular calcium levels rise during the excitotoxic process. The threshold for excitotoxicity might decrease if mitochondrial ATP production is impaired. Mitochondria also have a pivotal role in apoptotic cell death. Mitochondrial release of cytochrome c and other 'pro-apoptotic factors', such as AIF, into the cytoplasm triggers a cascade of events, culminating in cell death. Abbreviations: AIF, apoptosis-initiating factor; UPS, ubiquitin–proteasomal system (Henchcliffe and Beal, 2008).

The most direct evidence for disrupted mitochondrial metabolism has come from studies of autopsy tissue and other tissue samples and in vitro cell cultures derived from patients with PD. The activity of complex I, a major component of the electron transport chain, is decreased in SN (Schapira et al., 1990) and frontal cortex (Parker et al., 2008) in patients with PD. Moreover, increased oxidative damage and reduced electron transfer rates through complex I subunits has been demonstrated in these individuals (Keeney et al., 2006). This abnormality is predicted to render cells more vulnerable to Bax-induced apoptosis and conceivably contributes to the dysfunction of cells during the PD disease process. Electron transport chain impairment might actually be systemic, as decreased complex I activity has been demonstrated in platelets (Haas et al., 1995), and defective oxidative phosphorylation has been suggested to occur in skeletal muscle (Penn et al., 1995). Moreover, magnetic resonance

spectroscopy studies have demonstrated metabolic abnormalities consistent with mitochondrial dysfunction and a shift to anaerobic metabolism in vivo in humans with PD (see Henchcliffe et al., 2008).

Several complex I inhibitors, such as MPTP, rotenone and paraquat, replicate some of the key motor features of PD and cause death of dopaminergic neurons. The precise role of environmental complex I inhibitors in PD remains to be defined, but the effect observed following complex I inhibitors help to corroborate concerns over other environmental toxins (Henchcliffe and Beal, 2008).

Mitochondrial dysfunction leads to increased oxidative stress, which in turn induces α-synuclein aggregation and impairs proteasomal ubiquitination and degradation of proteins (Jenner et al., 2003).

Additionally, mitochondria have an integral role in the apoptotic cell death pathway; when the outer mitochondrial membrane is rendered permeable by the action of 'death agonists', such as Bax, cytochrome c is released into the cytosol, leading to caspase activation and apoptosis (Green et al. 2004). Similar pathways are also activated by opening of the mitochondrial permeability transition pore, an event that can occur under conditions of oxidative stress or electron transport chain inhibition, leading to collapse of the mitochondrial membrane potential (Henchcliffe and Beal, 2008).

The products of several PD-associated genes, including α-synuclein, Parkin, PINK1, DJ-1, LRRK2 and HTR2A, show a degree of localization to the mitochondria under certain conditions (see Figure 4).

Oxidative damage to α-synuclein affects the protein's aggregation, an effect that might partially explain the cellular toxicity of the protein (see Paragraph 1.4). The α-synuclein protein contains an amino-terminal mitochondrial targeting sequence (Devi et al., 2008) and acidification of the cytosol or overexpression of α-synuclein can cause the protein to become localized to mitochondria (Cole et al., 2008; Devi et al. 2008).

A number of mutations in the parkin gene (also known as PARK2) lead to autosomal recessive PD. Parkin acts as a ubiquitin E3 ligase within the UPS, and this activity is vulnerable to oxidative damage. Parkin also seems to have a fundamental role in mitochondrial function (Kuroda et al., 2006). In particular, very recently it was shown that parkin translocates to mitochondria upon dissipation of the mitochondrial membrane potential ($\Delta\Psi m$) by the uncoupler carbonyl cyanide m−chlorophenylhydrazone (CCCP) or in response to ROS (Narendra et al., 2008). As a result, damaged mitochondria are removed by

autophagic degradation (mitophagy). This year Geisler and coworkers unraveled that functional PINK1, a mitochondrial serine-threonine kinase that affords protection against oxidative stress, is a prerequisite to induce translocation of the E3 ligase parkin to depolarized mitochondria. In addition, the autophagic adaptor p62/SQSTM1 is recruited to mitochondrial clusters and is essential for the clearance of mitochondria. Strikingly, they identified VDAC1 (voltage-dependent anion channel 1) as a target for parkin-mediated Lys27 poly-ubiquitinylation and mitophagy. Moreover, pathogenic parkin mutations interfere with distinct steps of mitochondrial translocation, ubiquitinylation and/or final clearance through mitophagy. Thus, these data provide functional links between PINK1, Parkin and the selective autophagy of mitochondria, which is implicated in the pathogenesis of PD (Geisler et al., 2010). Moreover, PINK1 acts with parkin to regulate the balance of mitochondrial fission and fusion (Yang et al., 2008).

The leucine-rich repeat serine-threonine-protein kinase 2, LRRK2, associates, at least in part, with the outer mitochondrial membrane; its precise function in that location is unclear, but it is thought to interact with parkin (West et al., 2005).

High temperature requirement protein A2, HTRA2, is a mitochondrial serine protease, the release of which might be involved in apoptotic cell death. Under conditions of oxidative stress DJ-1 is relocated to the mitochondrial matrix and intermembrane space acting there as a neuroprotective factor (Zhang et al., 2005).

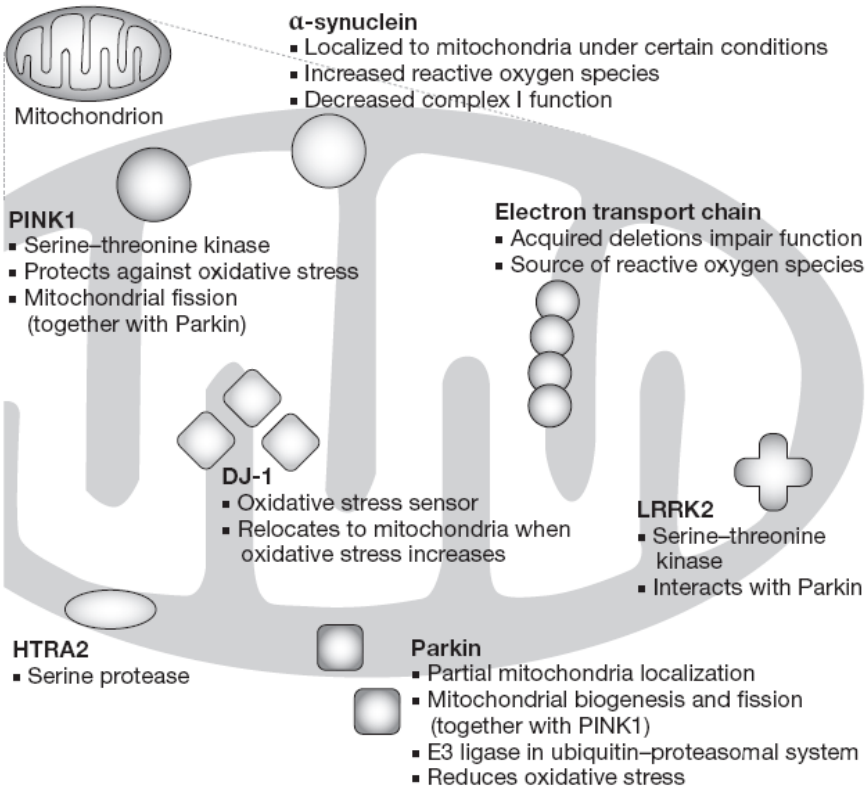

Figure 4: Products of PD-associated genes that affect mitochondrial function and oxidative stress. Acquired somatic mutations affect mitochondrial electron transport chain function, and such mutations are increased in the SN in patients with PD. Rare inherited mutations in genes encoding electron transport chain components have been associated with parkinsonism. Parkin, α-synuclein, PINK1, DJ-1, LRRK2 and HTRA2, are all encoded by nuclear genes, mutations in which can lead to PD, and all show a degree of localization to the mitochondria (adapted from Henchcliffe and Beal, 2008).

1.8 Biomarkers for Parkinson's disease

In the absence of reliable and readily available laboratory tests, the diagnosis of PD is currently based on the clinical manifestations of the disease. Diagnostic features of PD are asymmetrical onset, rigidity, bradikynesia, unilateral tremor at rest and acute L-DOPA response (Jankovic et al., 2008). The picture is made more complicated by a large heterogeneity in terms of predominance of one of the motor symptoms over the others and in terms of disease progression.

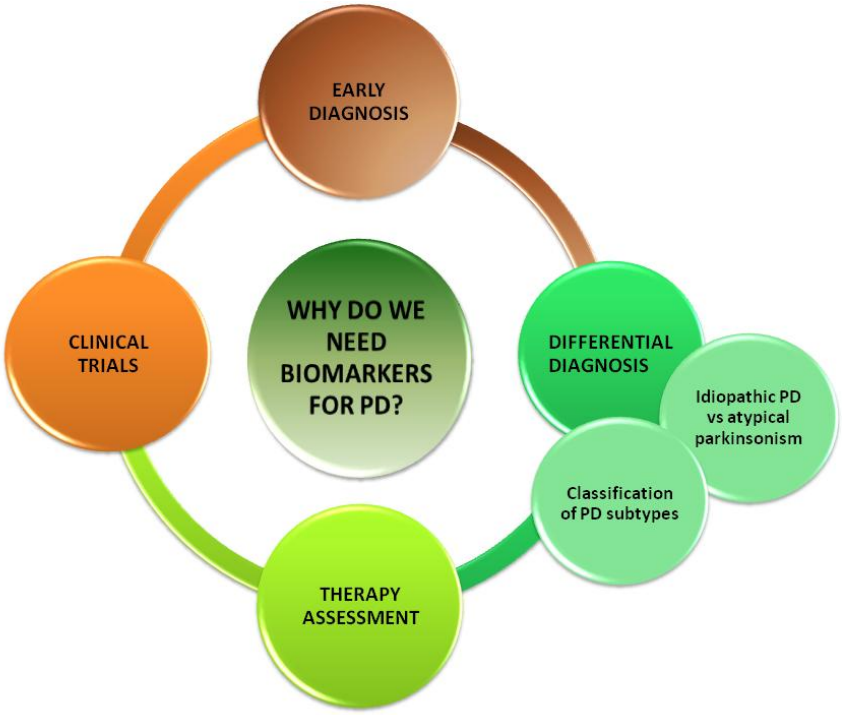

Figure 5: Peripheral biomarkers are required to accomplish different tasks: early diagnosis, possibly at a pre-motor stage; differential diagnosis of parkinsonian syndromes and of PD subtypes that may require different therapeutic plans; assessment of a personalized therapeutic plan; objective measurement of the actual extent of neurodegeneration so that neuroprotective and/or neurorestorative interventions could be monitored (adapted from Fasano et al., 2008b).

The availability of peripheral PD biomarkers would have a dramatic feedback. They would allow the differentiation of susceptible individuals from normal ones before motor symptoms appear (early diagnosis), and would help the identification of true idiopathic PD from atypical degenerative parkinsonisms (differential diagnosis). Moreover, the differentiation of patients in terms of their response to a pharmacological treatment would be possible (therapy assessment) (Michell et al., 2004). Eventually, biomarkers correlated to different PD subtypes would be an useful tools for the correct classification of PD patients so to start as soon as possible the appropriate therapeutic plan (Bogdanov et al., 2008) (see Figure 5).

The onset of motor symptoms is a late event in the neurodegenerative process at the ground of PD (Braak et al., 2004); as a consequence, the search for potential biomarker candidates is usually performed on patients that show the clinical signs of the disease and therefore could not show any longer the presence of peripheral indicators occurring in the early stages of PD. Moreover, no protective or restorative therapies could be attempted at a stage when more than 80% nigral neurons are lost (Dauer and Przedborski, 2003). On the other hand, it would be desirable to have available a panel of biomarkers that not only allow the diagnosis of PD at an early, pre-motor stage, but possibly correlate with the progression of the neurodegeneration progress. This would allow researchers to develop neuroprotective or neurorestorative agents and to follow directly their efficacy. Drugs that are now under clinical scrutiny as neuroprotective agents include molecules that combine one or more of the following properties: monoamine oxidase inhibition (*e.g.*, rasagiline, safinamide), mitochondrial enhancement (*e.g.*, coenzyme Q10, creatine), antiapoptotic activity, anti-inflammatory activity, protein aggregation inhibition, and neurotrophic activity (Bonuccelli and Del Dotto, 2006). Although this is still far from actuality, clinical trials on new PD treatments cannot be foreseen in the absence of affordable biomarkers.

The discovery of new PD markers should basically tackle two main objectives: the identification of molecular biomarkers in biological fluids and the identification of clinical or functional signs, both possibly anticipating motor symptoms. Imaging biomarkers targeting the premotor period are critical to elucidate both the onset and progression of premotor PD. Widespread data have demonstrated that functional imaging can detect PD subjects at the motor symptom threshold. Novel strategies combining functional imaging of the integrity of the dopaminergic neurotransmission (*e.g.*, scanning of the DAT using a suitable tracer) with known genetic mutations for PD or early clinical signs and PD-associated symptoms, such as olfactory loss and sleep disturbances like REM behavior disorder, have begun to be used to

identify individuals at risk for PD before motor symptoms become manifest. Early studies also have used imaging techniques targeting norepinephrine, serotonin, cholinergic, or other neuronal systems to focus on early cardiac, cognitive, and behavioral symptoms. Imaging of nondopaminergic targets such as inflammation or α-synuclein deposition may provide further insight into the etiology of PD. Given the multiple genetic etiologies for PD already identified, the marked variability in the loss of dopaminergic markers measured by imaging at motor symptom onset, and the clear heterogeneity of clinical symptoms at PD onset, it is certain that many imaging biomarkers with a focus ranging from clinical symptoms to PD pathobiology to molecular genetic mechanisms, will be necessary to fully map PD risk (Marek and Jennings., 2009).

1.8.1 Rationale for peripheral PD biomarkers

Several evidences sustain the rationale to search for peripheral biomarkers of PD as early reporters of central neurodegeneration. First, up-regulation and/or genetic/post-translational modifications of α-synuclein and PD-related proteins should be appreciable even at the peripheral level, either in plasma, blood cells, or cerebrospinal fluid (CSF). Moreover, the immune system may sensibly reflect specific mechanisms of PD pathogenesis occurring at the central level. In particular, peripheral blood lymphocytes (PBLs) share with SNpc cells all the molecular machinery that makes functional a dopaminergic cell and may therefore represent sensitive reporters of PD pathogenesis (Fasano et al., 2008b).

Altered α-synuclein metabolism in the CNS may be reflected in peripheral tissues. α-synuclein has been found in body fluids including CSF and plasma. Although α-synuclein lacks an endoplasmic reticulum targeting signal sequence and is considered to be exclusively a cytoplasmic protein, recent findings support the hypothesis of physiological secretion and consequently the possibility to detect it in plasma or other body fluids (see Fasano et al., 2008b). Further support to the systemic extension of PD comes from the pathogenetic hypothesis of Braak and coworkers (Braak et al., 2004) (see Paragraph 1.2 and 1.4). Motor symptoms become appreciable only at Braak's stage 3, *i.e.*, when α-synuclein starts to assemble into the very first LB in SNpc neurons. Characteristic aggregates of α-synuclein have been found not only in the CNS, but also in the enteric nervous system, that is connected to the CNS via the vagal nerve (Braak et al., 2004). Although the precise topographic sequence has not yet been established, there are increasing evidences of peripheral autonomic dysfunction anticipating pathologic events in the CNS. Indeed, autonomic failure before the

diagnosis of PD and dementia with LB has been described (Kaufmann et al., 2004). While enriched in neurons, α-synuclein was also detected in peripheral cells such as skin, platelets, vascular cells, and PBLs (Fasano et al., 2008b). As a word of caution, it should be taken into account that the symptomatic therapy administered to PD patients may dramatically induce oxidative modifications of proteins and metabolites at the peripheral level. Therefore, biomarker discovery and validation processes always need to consider dependence of observed modifications from the dose of medications being administered (Fasano et al., 2008b).

1.8.2 Potential source for peripheral biomarkers of PD: Peripheral blood lymphocytes

PBLs are easy to obtain from patients with little discomfort and may represent sensitive cellular sensors to be used for the evaluation of gene expression modification in physiological and pathological conditions, providing a unique and easily available biological model for integrated studies of gene expression in humans (Borro et al., 2007). Several evidences link PBLs to PD, sustaining the rationale for their use as a suitable pool of biomarkers. First, genetic traits may lead to changes in protein expression that bring to neurodegeneration in CNS and to some other specific functional alteration in PBLs. Moreover, PBLs may report on the activation of an immune response at the central level, either a primary event leading to cell death, or a secondary response to neuronal injury. Indeed, the hypothesis of a neuroimmune component of PD was also taken into account. Eventually, PBLs are circulating dopaminergic cells, therefore they could highlight alterations of genetic, environmental, or any other origin that become evident specifically in dopaminergic cells because of their marked oxidative challenge (Fasano et al., 2008b).

The dogma of the immune privilege of the CNS has been challenged, based on the following observations: 1) the immune system patrols the CNS through continuous migration of leukocytes (Ransohoff et al., 2003); 2) the adaptive immune system affects cognitive performance and behavior (Kipnis et al., 2004); 3) the immune system, through T lymphocytes-sustained autoimmune mechanisms, may promote neuroprotective responses (see Cohen and Schwartz., 1999; Schwartz., 2000; Schwartz,.2001). Immune cells (PBLs, in particular) may mirror a systemic “trait”, possibly of genetic origin. Immune mechanisms may contribute to neuronal damage, as suggested by the immune disturbances reported in PD

(Fiszer, 2001), as well as by the demonstration of chronic neuroinflammatory processes in the brain of PD patients (McGeer and McGeer, 2004). This observation, coupled with the need for reliable and possibly manageable bio-markers of the disease, has prompted extensive investigation outside the CNS, particularly in peripheral blood cells, which have been shown to exhibit some of the changes observed at the nigral level – *e.g.*, decreased complex I activity or increased oxidative stress (Blandini et al., 2003; Blandini et al., 2006; Martignoni et al., 1999; Migliore et al., 2002).

Among T lymphocytes, $CD4^+CD25^+$ T regulatory (T_{reg}) cells seem to play a key role in autoimmune neuroprotection, and the neurotransmitter dopamine represents, at present, one of the few endogenous modulators of T_{reg} function (Kipnis et al., 2004). Interestingly, a decreased $CD4^+$:$CD8^+$ T-cell ratio, less $CD4^+CD25^+$ T cells and a significantly increased ratio of IFN-gamma-producing to IL-4-producing T cells were observed in PD patients (Baba et al., 2005).

Mutations in the parkin gene (PARK2) render PBLs more susceptible to dopamine- and iron-mediated apoptosis (Jimenez Del Rio et al., 2004). PBLs show altered alpha-synuclein expression in PD patients, and alpha-synuclein appears to induce apoptosis in PBLs by enhanced expression of glucocorticoid receptor, caspase activation (caspase-8, caspase-9), CD95 up-regulation, and reactive oxygen species production (Kim et al., 2004). Oxidative-stress-induced apoptosis has been reported in PBLs of two patients carrying the A53T alpha-synuclein mutation (Battisti et al., 2008). The expression of transcription factor Nurr-1, which is critical in the development and maintenance of the dopaminergic system in the CNS, is reduced both in PD midbrains and in PBLs of parkinsonian patients (Jankovic et al., 2005).

The functions of T cells are regulated not only by cytokines, but also by neurotransmitters, with a peculiar role exerted by dopamine (Pacheco et al., 2009). T lymphocytes express the same dopamine receptors expressed by neurons (D1 to D5), although the effect of dopamine stimulation on the same receptor may be different in different cells (Pacheco et al., 2009). T cells are capable of synthesizing and/or capturing dopamine. PBLs, unlike monocytes, express tyrosine hydroxylase and store catecholamines into vesicles that are released through a synaptic-like mechanism (Cosentino et al., 2003; Cosentino et al., 2007; Marino et al., 1999). T cells possess transporters like DAT and VMAT, therefore they can internalize dopamine into specific vesicular storages similar to that impaired in PD pathogenesis (Cosentino et al., 2003; Cosentino et al., 2007; Marino et al., 1999; Pacheco et al., 2009).

A marked alteration in calcium homeostasis has been reported in PBLs of PD patients showing levodopa-induced dyskinesias with respect to patients under levodopa treatment that do not show dyskinetic movements (Blandini et al., 2008). Recently, infiltration of both $CD4^+$ and $CD8^+$ T cells, but not B cells, has been reported in SN specimens from PD patients and in a MPTP mouse model of PD, further supporting the functional link between neurodegeneration and immune system (Brochard et al., 2009).

Indeed, modifications of dopaminergic receptor expression has been described in PBLs from PD patients (Barbanti et al., 1999; Nagai et al., 1996). Dopamine D1-like and D2-like receptors on PBLs in 50 de novo PD patients, in 36 neurological control subjects, and in 26 healthy control subjects were assayed by radioligand binding assay techniques, showing a greater density of dopamine D1-like and D2-like receptors on PBLs in de novo PD patients than in either healthy control subjects or patients affected by different neurological diseases. Interestingly, treatment with L-DOPA or bromocriptine induced a down-regulation of both receptors to values comparable to those of control subjects (Barbanti et al., 1999). This up-regulation, followed by a normalization after therapy, closely resembles the changes in the expression of putaminal D2-like receptors early demonstrated by PET studies in untreated PD patients (Antonini et al., 1994) and may suggest the existence of an adaptive response of peripheral receptors to the central dopaminergic deficit. These changes in the expression of dopamine D1-like and D2-like receptors on PBLs are therefore closely associated with PD and seem to represent a specific trait of such patients (Barbanti et al., 1999).

In addition to the reported changes in DA receptor populations, DA transporters also appear to change significantly in PD. A recent study reported that measurement of DAT expression in PBLs allows to discriminate, possibly in the early clinical stages, PD patients from those affected by essential tremor, a neurological disorder characterized by postural and intentional tremor with slight signs of rigidity, that is not accompanied by central dopaminergic damage (Pellicano et al., 2007). DAT immunoreactivity was measured by densitometric analysis in PBLs from de novo PD or essential tremor patients with respect to healthy subjects, showing a reduction in PD that parallels that reported at the striatal level by SPECT (Benamer et al., 2000). Therefore, the pathophysiological mechanisms underlying PD progression could directly or indirectly modify the expression of DAT at peripheral level (Pellicano et al., 2007). The observation is in agreement with a previous report that showed a reduction of dopamine transporter immunoreactivity in PBLs in the early clinical stages of the disease (Caronti et al., 2001).

In another study proteomics was used to search differentially expressed proteins in PBLs from sporadic PD patients in order to identify peripheral candidate biomarkers of substantia nigra degeneration using two-dimensional electrophoresis and mass spectrometry protein identification (Fasano et al., 2008b; Mila et al., 2009). To evaluate whether the pharmacological therapy could specifically affect the expression of responsive proteins, proteome maps from PD patients under dopaminergic drug treatment were matched with those from controls and from patients under deep brain stimulation of the subthalamic nucleus whose administered l-DOPA dose was significantly reduced. Three proteins were up-regulated in PD patients and were respectively identified as cofilin 1, actin, and mitochondrial ATP synthase beta subunit, whereas in PD patients tropomyosin and gamma-fibrinogen were down-regulated. None of the selected spot volumes correlated with the administered l-DOPA dose. A linear combination of these spots was found that correctly classifies 7 out of 8 control subjects and 13 out of 13 PD patients selected in the study. Moreover, the level of a fibrinogen fragment linearly decreased with the years after onset, *i.e.*, with the disease progression, regardless of the l-DOPA dosage (Mila et al., 2009).

For all the reasons listed above, it is realistic that biochemical alterations at the SNpc level caused by genetic defects may also have a counterpart at the PBLs level (Fasano et al., 2008b). In other words, mutations that lead to specific damage of dopaminergic neurons may lead to functional alterations in dopaminergic peripheral cells (*i.e.*, T cells).

2. AIM OF THE PROJECT

The emerging field of neuroproteomics promises to provide powerful strategies to further characterize neuronal dysfunction and cell loss associated with neurodegenerative diseases. Moreover, it could be a valuable tool for the biomarkers discovery phase. These potentialities are due to the fact that proteomics is an unbiased approach.

The common threads of the two projects developed in this thesis are the technique used and the main subject, Parkinson's disease.

In particular, two cell models are exploited:

- SH-SY5Y neuroblastoma cell line, to investigate biochemical pathways altered by dopamine toxicity and α-synuclein overexpression. Altered dopamine homeostasis is a thoroughly accepted mechanism in the pathogenesis of Parkinson's disease, and α-synuclein overexpression and impaired disposal contribute to this mechanism.

  Through this cell model we want to characterize from a molecular point of view pathogenetic mechanisms at the basis of neuronal cell death in PD.
- Jurkat T-cell leukemia cell line, to understand proteome perturbations in peripheral dopaminergic cells, *i.e.*, T-cells, after a non-oxidative, saturating dopamine stimulus.

  This investigation aims at substantiating the use of T-cells as an appropriate source of peripheral biomarkers and of Jurkat cells as a cell culture model to investigate dopamine-activated biochemical processes in T-cells. Eventually, the set of proteins whose level is modified by dopamine in Jurkat cells might represent by itself a reporter of dopaminergic functionality at the peripheral level, for instance in T-cells of PD patients whether or not stimulated with dopamine.

3. MATERIALS AND METHODS

3.1 A SH-SY5Y MODEL TO INVESTIGATE PD PATHOGENETIC MECHANISMS

3.1.1 Cell cultures and transfection

Human neuroblastoma **SH-SY5Y** cells were cultured in 5% CO_2 humidified atmosphere at 37 °C in high-glucose Dulbecco's modified Eagle's medium (DMEM) with 10% fetal bovine serum (FBS), 100 U/ml penicillin, 100 μg/ml streptomycin, and 2 mM L-glutamine.
The complete wild-type α-synuclein coding sequence (aminoacids 1-140) was subcloned into the mammalian expression vector pcDNA3.1 (Invitrogen Ltd, Paisley, UK) yielding plasmid pcDNA-Syn (Colapinto et al., 2006). SH-SY5Y cells were transfected with pcDNA-Syn by using Lipofectamine 2000 (Invitrogen). Briefly, cells were grown to 80% confluence in 24-well plates for 24 h in complete growth medium without antibiotics and then exposed to a mixture of 2 μl/well lipofectamine and 0.8 μg/well pcDNA-Syn. Transfected cells were selected with 500 μg/ml geneticin (Life Technologies, Paisley, UK) added to cell culture 48 h after transfection. α-Synuclein-expressing cells (α-syn) were further expanded in the presence of 200 μg/ml geneticin. Cells transfected with the pcDNA-β-gal plasmid, containing the β-galactosidase complete sequence, were used as control (β-gal). Intentionally, cell lines were not cloned. This avoided working with only a few clones but, instead, resulted in an ensemble average of different clones.

3.1.2 Cell viability

The dopamine effect on cell viability was assessed by the MTT assay using the Celltiter 96 non-radioactive cell proliferation assay (Promega, Madison, WI, USA), according to the manufacturer's instructions. Briefly, 4.0×10^4 cells/well were seeded onto 96-well plates, grown for 24 h and exposed for further 24 h to different dopamine concentrations (0.125-1.00 mM) in the presence of 700 U/ml catalase, in order to eliminate aspecific effects due to H_2O_2 arising from dopamine auto-oxidation (Blum et al., 2000). At the end of the treatment, cells were washed twice with Phosphate Buffer Saline (PBS) to eliminate aspecific reduction of tetrazolium by dopamine and then incubated with the dye solution at 37 °C for 4 h; formazan crystals, formed by mitochondrial reducing activity, were dissolved in Solubilization/Stop Solution and the absorbance was read at 570 nm, using a Universal Microplate reader Model

550 (Bio-Rad, Hercules, CA, USA). Cell viability was calculated as follows: Abs_{570} dopamine treated cells/ Abs_{570} control cells. All experiments were run in triplicate.

3.1.3 2-DE electrophoresis and statistical analysis

α-Syn and β-gal cells treated or not with 0.25 mM dopamine in the presence of catalase (700 U/ml) for 24 h were collected by centrifugation, lysed with 200 µl lysis solution (7 M urea, 2 M thiourea, 4% w/v CHAPS, 0.5 µl protease inhibitor mix; Sigma-Aldrich, Milan, Italy) and centrifuged (13000 *g*, 30 min, 10 °C). Proteins were collected in the supernatant and their concentration was determined using the Bio-Rad Protein Assay (Bio-Rad).

2-DE was performed according to Görg (Görg et al., 2000), with minor modifications. Samples (about 200 µg) were diluted to 250 µl with a buffer containing 7 M urea, 2 M thiourea, 4% CHAPS, 0.5% IPG buffer 3-10, 2 mM tributylphosphine and traces of bromophenol blue, and loaded on 13 cm IPG DryStrips with a non-linear 3-10 pH gradient by in-gel rehydration (1 h at 0 V, 10 h at 50 V). IEF was performed at 20°C on IPGphor (GE Healthcare, Little Chalfont, UK) according to the following schedule: 2 h at 200 V, 2 h linear gradient to 2000 V, 2 h at 2000 V, 1 h of linear gradient to 5000 V, 2 h at 5000 V, 2 h linear gradient to 8000 V and 2 h and 30 min at 8000 V. IPG strips were then equilibrated for 2 × 30 min in 50 mM Tris-HCl pH 8.8, 6 M urea, 30% glycerol, 2% SDS and traces of bromophenol blue containing 1% DTT for the first equilibration step and 2.5% iodoacetamide for the second one. SDS-PAGE was performed using 13% 1.5 mm thick separating polyacrylamide gels without stacking gel, using Hoefer SE 600 system (GE Healthcare). The second dimension was carried out at 45 mA/gel at 18°C. Molecular weight marker proteins (11-170 kDa from Fermentas, Burlington, Canada) were used for calibration.

Gels were stained according to MS-compatible silver staining method (Gromova et al., 2006), scanned with an Epson Perfection V750 Pro transmission scanner (Epson, Nagano, Japan) and analyzed with ImageMaster 2D Platinum V5.0 software package (GE Healthcare). Spots were detected automatically by the software and manually refined hereafter; gels were then matched and the resulting clusters of spots confirmed manually. Unmatched spots among the experimental groups were considered as qualitative differences. Synthetic images ("average gels") comprised of spots present in more than 80% of the gels were built for each group and then compared; spots have been quantified on the basis of their relative volume (spot volume normalized to the sum of the volumes of all the representative spots) and those

that consistently and significantly varied among the different populations were identified by ANOVA analysis with a threshold of $p \leq 0.05$ using the StatistiXL software (http://www.statistixl.com).

3.1.4 LC-MS-MS analysis for protein identification

Silver-stained spots were manually excised and destained (1 × 10 min 50 µl $K_3[Fe(CN)_6]$ 30 mM and $Na_2S_2O_3$ 100 mM, 6 × 10 min 100 µl deionized water, 1 × 20 min 100 µl NH_4HCO_3 200 mM, 1 × 20 min 100 µl deionized water), dehydrated with acetonitrile (1 × 40 min 100 µl) and then dried at 37°C by vacuum centrifugation. The gel pieces were then swollen in 10 µl digestion buffer containing 50 mM NH_4HCO_3 and 12.5 ng/µl modified porcine trypsin (sequencing grade, Promega). After 10 min 30 µl of 50 mM NH_4HCO_3 were added to the gel pieces and digestion allowed to proceed at 37° C overnight. The supernatants were collected and peptides were extracted in an ultrasonic bath for 10 min (twice 100 µl 50 % acetonitrile, 50 % H_2O, 1% formic acid v/v; once 50 µl acetonitrile). All the supernatants were collected in the same tube, dried by vacuum centrifugation and dissolved in 20 µl 2% acetonitrile, 0.1 % formic acid in water.

Peptide mixtures were separated by using a nanoflow-HPLC system (Agilent Technologies series 1200, Santa Clara, CA, USA). A sample volume of 10 µl was loaded onto a 2 cm fused silica pre-column (75 µm I.D.; 375 µm O.D.) at a flow rate of 2 µl/min. Peptides were eluted at a flow rate of 200 nl/min with a linear gradient from Solution A (2% acetonitrile; 0.1% formic acid) to 50% of Solution B (98% acetonitrile; 0.1% formic acid) in 40 minutes over the pre-column in-line with a homemade 15 cm resolving column (75 µm I.D.; 375 µm O.D.; Zorbax 300-SB C18, Agilent Technologies). Peptides were eluted directly into a Esquire 6000 Ion Trap mass spectrometer (Bruker-Daltonik, Bremen, Germany). Capillary voltage was 1.5-2 kV and a dry gas flow rate of 10 l/min was used with a temperature of 230 °C. The scan range used was from 300 to 1800 m/z. The tandem mass spectra were annotated and peak list files were generated, commonly referred to as .MGF files, by running DataAnalysis version 3.2 (Bruker-Daltonik) using default parameters. Protein identification was manually performed by searching the National Center for Biotechnology Information non-redundant database (NCBInr 20081021; 709593 sequences actually searched) using the Mascot MS/MS Ion Search program (version 27 Oct 2008; http://www.matrixscience.com). The following parameters were set: enzyme trypsin,

complete carbamidomethylation of cysteines and partial oxidation of methionines, peptide Mass Tolerance ± 0.9 Da, Fragment Mass Tolerance ± 0.9 Da, missed cleavages 2, species restriction to human. All identified proteins have a Mascot score greater than 69, corresponding to a statistically significant ($p < 0.05$) confident identification. Among the positive matches, only protein identifications based on at least two different non-overlapping peptide sequences of more than 6 amino acids and with a mass tolerance <0.9 Da were accepted.

3.1.5 Bioinformatics enrichment and network clustering

Identified proteins were clustered in two groups. The first one corresponds to proteins that displayed significant changes in their levels following dopamine treatment. The second one groups together proteins that showed quantitative alterations in response to α-synuclein overexpression, or that differentially responded to dopamine exposure as a function of α-synuclein overexpression. Lists were fed to *PPI spider* (http://mips.helmholtz-muenchen.de/proj/ppispider/) in order to determine a statistically-significant interaction network as well as statistically-significant functional association to Gene Ontology (GO) classifications (Antonov et al., 2009).

3.1.6 Apoptosis analysis

The induction of apoptotic cell death was analyzed by flow cytometry with the Annexin V-FITC apoptosis detection kit (BD, Becton-Dickinson, Franklin Lakes, NJ, USA). Briefly, cells treated or not with 0.250 mM dopamine in the presence of catalase (700 U/ml) for 24 h were resuspended (1×10^6 cells/ml) in binding buffer; 1×10^5 cells were incubated with Annexin V-FITC and propidium iodide for 15 min at room temperature (RT) in the dark. Samples properly diluted were analyzed with a FACSCalibur flow cytometer (BD) equipped with a 15-mW, 488-nm, air-cooled argon ion laser. At least 10,000 events were analyzed for each sample and data were processed using CellQuest software (BD). Fluorescent emission of propidium iodide and Annexin V-FITC were collected through a 575 and a 530/30 band-pass filter, respectively. The percentage of apoptotic cells in each sample was determined based on

the fraction of Annexin V positive cells, whereas the percentage of necrotic cells was determined based on the fraction of propidium iodide positive cells.

3.1.7 Transient transfection and luciferase gene reporter assay

β-Gal and α-syn cells (60% confluent in six-well plates) were transfected with pNF-κB-Luc plasmid (Stratagene, Santa Clara, CA, USA) (150 ng/well) and phRL-CMV, containing Renilla luciferase cDNA (5 ng/well), using Lipofectamine and OptiMEM medium (Invitrogen, Carlsbad, CA). In pNF-κB-Luc the expression of the firefly luciferase is controlled by a synthetic promoter containing five NF-κB binding sites. After 7 hours incubation, the transfection mixture was replaced with complete DMEM containing or not 0.25 mM dopamine, in the presence of 700 U/ml catalase. Cells were harvested after 2 and 24 hours, lysed and the cell lysates were tested for luciferase activities by using the Dual-Luciferase reporter assay system (Promega), according to manufacturer's instruction. Experiments were performed in duplicate and repeated three times with nearly identical results in order to gain statistical significance (verified by Student's t-test). NF-κB-dependent luciferase activity was normalized to the Renilla luciferase activity present in each sample.

3.1.8 Western blotting of α-synuclein, HSP70 and 14-3-3

Expression of **α-synuclein**, **HSP70** and **14-3-3** was determined by Western blotting. β-Gal and α-syn cells treated or not with 0.250 mM dopamine in the presence of catalase (700 U/ml) for 24 h were lysed in RIPA buffer (25 mM Tris-HCl pH 7.4, 0.15 M NaCl, 0.1% SDS, 1% Triton X-100, 1% sodium deoxycholate). Proteins (80 μg) were resolved by SDS-PAGE on a 16% polyacrylamide gel and then transferred to a PVDF membrane (Roth, Karlsruhe, Germany) at 25 V for 2h. The membrane was incubated with different primary antibodies (see Table 2) diluted in 5% nonfat dry milk in TBS-T (10 mM Tris HCl pH 8, 150 mM NaCl, 0.05% Tween 20) for 1.5 h at RT. Protein bands were visualized using a peroxidase-conjugated IgG secondary antibody (see Table 3) and the ECL plus western blotting detection system (Millipore, Billerica, MA, USA). Relative levels of α-synuclein, HSP70 and 14-3-3 were calculated by densitometric analysis (ImageJ software; http://rsb.info.nih.gov/ij) and normalized to β-actin.

Table 2: List of primary antibodies, the dilution used and the supplier.

Antibody	Dilution	Supplier
Mouse anti-α-synuclein	1:1000	BD Transduction Laboratories, Franklin Lakes, USA
Mouse anti-HSP70	1:1000	Zymed Laboratories, San Francisco, USA
Rabbit anti-14-3-3	1:1000	Zymed Laboratories, San Francisco, USA
Mouse anti-β-actin	1:3000	GeneTex, Irvine, USA

Table 3: List of HRP conjugated secondary antibodies, the dilution used and the supplier.

Antibody	Dilution	Supplier
Anti rabbit polyclonal IgG-HRP conjugated	1:1000	Millipore, Tamekula, CA, USA
Anti mouse polyclonal IgG-HRP conjugated	1:3000	GeneTex, Irvine, USA

3.1.9 Cell cycle analysis

The effect on cell cycle distribution by 24 h exposure to 0.25 mM dopamine was analyzed by flow cytometry. α-Syn and β-gal cells treated or not with 0.25 mM dopamine in the presence of catalase (700 U/ml) were detached by trypsinization, washed in phosphate-buffered saline (PBS) and fixed in ice-cold 70% ethanol for 20 min at -20°C. After a further wash in PBS, DNA was stained with 50 μg/ml propidium iodide (PI) in PBS in the presence of RNAse A (30 U/ml) at 37°C for 30 minutes.

All samples were analyzed with a FACSCalibur flow cytometer (BD) equipped with a 15-mW, 488-nm, air-cooled argon ion laser. At least 10,000 events were analyzed for each sample and all data were processed using CellQuest software (BD). Fluorescent emission of PI was collected through a 575 band-pass filter, acquired in linear mode for cell cycle analysis.

Through the flow cytometry analysis it is possible to distinguish among cells with 2n DNA content (G_1 phase), cells with 4n DNA content (G_2/M phase) and cells with an intermediate DNA content (S phase).

3.1.10 Western blotting of Voltage Dependent Anion Channels (VDACs)

MONODIMENSIONAL WESTERN BLOTTING (TIME COURSE)

SH-SY5Y wild type cells were treated or not with 0.25 mM dopamine in the presence of catalase (700 U/ml) for 4, 7, 12 and 24 h. Cells were then harvested and proteins extracted as described in Paragraph 3.1.8. Thirty micrograms of total proteins were resolved by SDS-PAGE on a 13% polyacrylamide gel and then transferred to a PVDF membrane (see paragraph 3.1.8).

The membrane was incubated with anti VDACs, anti-grp75 or anti-HSP60 primary antibodies (see Table 4) diluted in 5% nonfat dry milk in TBS-T overnight at 4°C. Protein bands were visualized using a peroxidase-conjugated IgG secondary antibody (see Table 5) and the ECL plus western blotting detection system. Relative levels of VDAC1, VDAC2 and VDAC3 were calculated by densitometric analysis (ImageJ software) and normalized to β-actin.

Table 4: List of primary antibodies, the dilution used and the supplier.

Antibody	Dilution	Supplier
Rabbit anti VDAC1	1:1800	Abcam, Cambridge, UK
Goat anti VDAC2	1:2000	Abcam, Cambridge, UK
Chicken anti VDAC3	1:500	Abcam, Cambridge, UK
Rabbit anti-grp75	1:10000	Santa Cruz Biotech., Santa Cruz, USA
Goat anti-HSP60	1:1000	Santa Cruz Biotech., Santa Cruz, USA

Table 5: List of HRP conjugated secondary antibodies, the dilution used and the supplier

Antibody	Dilution	Supplier
Anti goat polyclonal IgG-HRP conjugated	1:3000	Millipore, Tamekula, CA, USA
Anti rabbit polyclonal IgG-HRP conjugated	1:1000	Millipore, Tamekula, CA, USA
Anti chicken polyclonal IgG-HRP conjugated	1:5000	Millipore, Tamekula, CA, USA

VDAC2 TWO-DIMENSIONAL WESTERN BLOTTING

SH-SY5Y wild type cells were treated or not with 0.250 mM dopamine in the presence of 700 U/ml catalase for 4 or 7 h. Cells were lysed using UTC (see Paragraph 3.1.3). Sixty micrograms of total proteins were loaded onto 7 cm IPG DryStrip with a non-linear 7-11 pH gradient by in-gel rehydration (1 h at 0 V, 10 h at 25 V). IEF was performed at 20° C according to the following schedule: 0,5 h linear gradient to 300 V, 3 h at 300 V, 3,5 h of linear gradient to 3500 V, 3500 V to 20000 Vhrs. IPG strips were then equilibrated as described in Paragraph 3.1.3. SDS-PAGE, transfer of proteins on PVDF membrane and immunodetection were performed as detailed in Paragraph 3.1.10.

3.1.11 Tetramethylrhodamine methyl ester (TMRM) staining

Inside a healthy, non-apoptotic cell, the lipophilic tetramethylrhodamine methyl ester (TMRM, Molecular Probes, Invitrogen Co.) dye, bearing a delocalized positive charge, enters the negatively charged mitochondrion where it accumulates in an inner-membrane potential-dependent manner. When the mitochondria collapse in apoptotic or otherwise depolarized cells, the TMRM potentiometric dye no longer accumulates inside the mitochondria and becomes evenly distributed throughout the cytosol. When dispersed in this manner, overall cellular fluorescence levels decrease dramatically and this event can easily be visualized by fluorescence microscopy or quantitated by flow cytometry or fluorescence plate reader analysis techniques.

4×10^5 SH-SY5Y cells were seeded on 24 mm coverslip and grown for 24 hours. Afterwards, they were treated or not with 0.25 mM dopamine in the presence of 700 U/ml catalase for 24 h. For measurement of the mitochondrial membrane potential ($\Delta\Psi m$), cells were loaded with 10 nM TMRM for 30 min at 37°C in KRB/Ca^{2+} solution and then placed in a thermostated chamber on the stage of a Zeiss Axiovert 200 inverted microscope equipped with a BD Carv-

II confocal head and a high sensitivity back-illuminated EM-CCD camera (Cascade 512b, Photometrics). Images were taken with a 63× 1.4 N.A. Plan-Apochromat objective with 500 ms exposure time. TMRM intensity was quantified by measuring the average pixel intensity of the whole cell on background-corrected images after thresholding with the Metamorph 7.5 **software.**

3.1.12 Measurement of Ca^{2+} flux to mitochondria using Aequorin

Aequorin is a 21 kDa protein isolated from Aequorea sp. Jellyfish, which emits blue light in the presence of calcium ions (Shimomura, 1988). In its active form the photoprotein includes an apoprotein and a covalently bound prosthetic group, coelenterazine. When calcium ions bind to the three high affinity EF hand sites, coelenterazine is oxidized to coelenteramide, with a concomitant release of carbon dioxide and emission of light. Reconstitution of an active aequorin (expressed recombinantly) can be obtained also in living cells by simple addition of coelenterazine to the medium. Coelenterazine is highly hydrophobic and has been shown to permeate cell membranes of various cell types.
Recombinant aequorin can be targeted to the mitochondria (mtAEQ) thanks to a targeting presequence of subunit VIII of human cytochrome c oxidase fused to the aequorin cDNA (Porcelli et al., 2001). Additionally, the aequorin D119A mutant is used, which has the high affinity calcium binding site inactivated so that calcium concentrations in the range of 10 to 100 µM can be measured (Kendall et al., 1992).

CELL PREPARATION, CALCIUM-PHOSPHATE TRANSFECTION PROCEDURE AND RECONSTITUTION OF FUNCTIONAL AEQUORIN

One day before the transfection step, SH-SY5Y cells were plated on a 13 mm round coverslip at 30-50% confluence. Just before the transfection procedure, cells were washed with 1 ml of fresh medium.
For 1 coverslip, 5 µl of 2.5 M $CaCl_2$ were added to 4 µg of DNA dissolved in 45 µl of Tris-EDTA (TE= 10mM Trizma-base, 1mM EDTA, pH 8). The solution was mixed by vortexing with 50 µl of HEPES Buffered Solution (HBS= 280 mM NaCl, 50 mM Hepes, 1.5 mM Na_2HPO_4, , pH 7.12) and incubated for 30 min at RT. The solution was then added directly to

the cell monolayer. After 24 h, cells were washed with PBS (2 or 3 times until the excess precipitate is completely removed).
Once expressed, the recombinant aequorin must be reconstituted into the functional chemiluminescent protein. This is accomplished by incubating cells with synthetic coelenterazine (5 µM) at 37°C in fresh DMEM medium supplemented with 1% FCS for 1 h.
Cells were then treated or not with 0.25 mM dopamine in the presence of 700 U/ml catalase for 4 or 24 h.

LUMINESCENCE DETECTION AND Ca^{2+} MEASUREMENT

The aequorin detection system is based on the use of a low noise photomultiplier placed in close proximity (2-3 mm) of aequorin expressing cells. The cell chamber, which is on the top of a hollow cylinder, is adapted to fit a 13-mm diameter coverslip. The volume of the perfusing chamber is kept to a minimum (about 200 µl). The chamber is sealed on the top with a coverslip, held in place with a thin layer of silicone. Cells are continuously perfused via a peristaltic pump with medium thermostated via a water jacket at 37°C. The photomultiplier (EMI 9789 with amplifier-discriminator) is kept in a dark box. The output of the amplifier-discriminator is captured by an EMIC600 photon-counting board in an IBM compatible microcomputer and stored for further analysis.
The coverslip with transfected cells is transferred to the luminometer chamber and perfused with KRB saline solution in the presence of 1 mM $CaCl_2$ and 1g/l glucose to remove the excess of coelenterazine. Bradykinin (100 nM) was added to the perfusing medium.
Luminescence values are reported as a function of time following calcium release induced by bradykinin. Statistical significance was verified by Student's t test.

3.1.13 Two-dimensional Western blotting of DJ-1

For two-dimensional electrophoresis, 3.5×10^6 SH-SY5Y cells were seeded in 3% FBS and treated with 0.1 mM dopamine in the presence of 700 U/ml catalase in the medium to remove exogenous H_2O_2 (Blum et al., 2000). Cells treated for 15 min with 1.0 mM H_2O_2 were used as positive control of a generic oxidative stress. After 24 h incubation cells were scraped, collected by centrifugation and lysed with 200 µl UTC containing protease inhibitors, and sonicated for 15 seconds. After 90 min DNase I and RNase A (Sigma-Aldrich) were added,

and after further 10 min specimens were centrifuged (13000×g, 30 min, 10°C). The protein concentration was estimated by Bradford assay (Bio-Rad).

2-DE was performed as described in Paragraph 3.1.3. Gels were transferred to PVDF membranes at 25 V for 2 h. Membranes were saturated in 5% non-fat milk in TBS-T and incubated with goat anti-DJ-1 polyclonal antibody (Abcam), 1:1000 dilution in 5% milk-TBS-T for 1.5 h at room temperature or with mouse anti-β-actin monoclonal antibody (see Table 2). Membranes were then washed with TBS-T and incubated with peroxidase-conjugated secondary antibodies (see Tables 3 and 5) for chemiluminescence detection (Pierce, Rockford, IL, USA). Photographic films were scanned with a Epson Perfection V750 Pro transmission scanner (Epson) and images were analyzed using ImageJ (http://rsb.info.nih.gov/ij/). Statistical significance was verified by Student's t test.

3.1.14 2-DE gel alignment and "metagel" production

2-DE images in the literature (Bandopadhyay et al., 2004; Canet-Avilés et al., 2004; Colapinto et al., 2006; Motani et al., 2008) showing DJ-1 spots have been rescaled and registered on the reference pI/MW grid, background-subtracted, segmented for the spots and binarized (Natale et al., 2010). The 6 binarized images were used to get a "metagel", *i.e.*, an average intensity projection image, wherein each pixel stores the average intensity over the 6 original images at corresponding pixel location. The color scale of this metagel accounts for the occurrence frequency of each spot in the considered experiments, with less frequent spot positions in blue and more frequent spot positions in white.

3.2 DOPAMINE RESPONSE OF DOPAMINERGIC CIRCULATING CELLS: THE JURKAT CELL MODEL

3.2.1 Cell culture

The **Jurkat** T-cell leukemia cell line was maintained at 37°C in a 5% CO_2 humidified atmosphere in RPMI 1640, supplemented with 10% fetal bovine serum (FBS), 100 U/ml penicillin, 100 µg/ml streptomycin, and 2 mM L-glutamine. Stock flasks were transferred for culture twice weekly or as required to maintain optimal cell growth. All cell culture media and reagents were from PAA (Pashing, Austria).

3.2.2 RNA extraction, retrotranscription and PCR

RNA was extracted using NucleoSpin RNA II (Macherey-Nagel, Düren, Germany) following manufacturer's instructions and treated with rDNase in order to remove genomic DNA. Five micrograms of RNA were reverse transcribed into first-strand cDNA in a 20 µl final volume using the Maxima™ First Strand cDNA Synthesis Kit (Fermentas). PCR was performed by Real-Time PCR (DNA Engine Opticon 2; MJ Research, Waltham, MA, USA) using a SYBR Green PCR mix (5Prime, Hamburg, Germany). The expression of D1 receptor (DRD1), D2 receptor splicing variants 1 and 2 (DRD2_1 and DRD2_2), D3 receptor splicing variant a (DRD3_a), D4 receptor (DRD4), D5 receptor (DRD5), dopamine transporter (DAT), vesicular monoamine transporter 1 and 2 (VMAT1, VMAT2) and tyrosine hydroxylase (TH) was evaluated using primers reported in Table 6. Optimal PCR conditions were identified for each primer pair. Reactions were incubated at 95°C for 2 min, then 40 cycles of 95°C for 15 sec, 62°C for 20 sec, 68°C for 20 sec. As positive control, cDNA from the catecholaminergic human neuroblastoma SH-SY5Y cell line was used and amplified under the same conditions. The specificity of the amplified products was checked by the melting temperature curve analysis and the expected size of the fragments was further visualized in a 2% agarose gel stained with ethidium bromide. Results were confirmed by three independent replicates. Furthermore, PCR efficiency was determined using serial dilution of control templates obtained by the amplification of positive controls. The dilutions were used as templates for PCR reactions. C(t) values were plotted against the $\log_{10}$ number of template and the slope of

the obtained line defines the reaction efficiency calculated as equal to $10^{(-1/slope)}$. All PCR reactions, thus, displayed similar and optimal efficiency for each primer specific amplification protocol.

PRIMER DESIGN

Primer design was performed by using Primer3 software (http://primer3.sourceforge.net/) and manually adjusted if needed. Primer pairs were designed to avoid the amplification of undesired sequences that share high identity degree and the amplification of common sequences among the splicing variants of the same transcript. Moreover, primers were designed to have comparable melting temperature and reaction efficiency. Primer specificity was tested by BLAST (http://blast.ncbi.nlm.nih.gov/Blast.cgi) and experimentally by the positive control amplification.

Table 6: Sequences of specific primers: F = forward primer; R = reverse primer.

Gene	Primer Sequence	Amplicon size (bp)
D1 F	ATGGACGGGACTGGGCTGGT	91
D1 R	GGAGCGTGGACAGGATGAGCA	
D2_1 F	AGCCTCCACTCTCCGCCTG	102
D2_1 R	CCACTAAAGGGCAACTGTACTCACC	
D2_2 F	CGCCGGGCAGCCTCCTTTAG	156
D2_2 R	CCATCGTCTCCTTCTACGTGCCC	
D3_a F	GGCACTCCCCGAGGTTGCAG	116
D3_a R	CGGAATTCCCTGAGTCCCACC	
D4 F	GCCGACCTCCTCCTCGCTCT	169
D4 R	CGAACCTGTCCACGCTGATGG	
D5 F	TCTACCGCATCGCCCAGGTG	189
D5 R	GCAGCCAGCAACACACGAAGA	
VMAT1 F	GCTTTCTTCAACAGCCACGGTG	170
VMAT1 R	CTGTGGTGGTGCCAATTGTGC	
VMAT2 F	CCATTGCGGATGTGGCATTT	166
VMAT2 R	TCTTCTTTGGCAGGTGGACTTCG	
DAT1 F	AGCCTGCCTGGGTCCTTTCG	106
DAT1 R	AGTGGCGGAGCGTGAACTGG	
TH F	CGACCCTGACCTGGACTTGGA	142
TH R	GGCAATCTCCTCGGCGGTGT	

3.2.3 2-DE electrophoresis and quantitative analysis

Jurkat cells treated or not with 50 μM dopamine in the presence of 140 U/ml catalase (Blum et al., 2000) for 24 h were collected by centrifugation, lysed with 200 μl UTC + 0.5 μl protease inhibitor mix and centrifuged (13000 g, 30 min, 10 °C). Proteins were collected in the supernatant and their concentration was determined using the Bio-Rad Protein Assay (Bio-Rad).

2-DE was performed as described in Paragraph 3.1.3. SDS-PAGE was performed using 11% separating polyacrylamide gels. Gels were stained with Coomassie Brilliant Blue R-350, scanned with an Epson Perfection V750 Pro transmission scanner (Epson) and analyzed with ImageMaster 2D Platinum V5.0 software package (GE Healthcare). Spots that consistently and significantly varied between controls and dopamine-treated samples were identified by Student's t-test analysis with a threshold of $p \leq 0.05$.

3.2.4 Protein identification by matrix-assisted laser desorption ionization time-of-flight (MALDI-TOF) mass spectrometry

Protein spots were excised manually from the gel, washed with high-purity water and destained twice with 100 μl of 50 mM NH_4HCO_3/50% acetonitrile for 10 min. Spots were dehydrated with 100% acetonitrile and swollen at RT in 20 μl of 40 mM NH_4HCO_3/10% acetonitrile containing 25 ng/μl trypsin (Trypsin Gold, mass spectrometry grade; Promega). After 1 h, 50 μl of 40 mM NH_4HCO_3/10% acetonitrile were added and digestion proceeded overnight at 37°C. The generated peptides were extracted with 50% acetonitrile/5% trifluoroacetic acid (TFA; two steps, 20 min at RT each), dried by vacuum centrifugation, suspended in 0.1% TFA, passed through micro ZipTip C18 pipette tips (Milllipore) and eluted directly with the MS matrix solution (10 mg/ml α-cyano-4-hydroxycinnamic acid in 50% acetonitrile/1% TFA). Mass spectra of the tryptic peptides were obtained using a Voyager-DE MALDI-TOF mass spectrometer (Applied Biosystems, Foster City, CA, USA). Peptide mass fingerprinting database searching was performed using the mascot search engine (http://www.matrixscience.com) in the NCBInr/Swiss-Prot databases. Parameters were set to allow one missed cleavage per peptide, a mass tolerance of 0.5 Da and considering

carbamido-methylation of cysteines as a fixed modification and oxidation of methionines as a variable modification.

3.2.5 Bioinformatics enrichment and network clustering

The list of identified proteins was fed to PPI spider (http://mips.helmholtz-muenchen.de/proj/ppispider/) in order to determine a statistically-significant interaction network as well as statistically-significant functional association to Gene Ontology (GO) classifications (Antonov et al., 2009).

3.2.6 Two-dimensional Western blotting of 14-3-3 and β-actin

2-DE was performed as described in Paragraph 3.1.3. Western blotting conditions for 14-3-3 and β-actin detection are detailed in Paragraph 3.1.8. Images were acquired using two different exposure times, in order to discriminate differences in both low- and high-abundance species. By saturating the main component, we were able to observe minor spots. By lowering the exposure time, on the other hand, minor spots disappear and the most abundant isoforms appeared as resolved spots. Photographic films were scanned with a Epson Perfection V750 Pro transmission scanner (Epson) and images were analyzed using ImageJ (http://rsb.info.nih.gov/ij/).

4. RESULTS

4.1 A SH-SY5Y MODEL TO INVESTIGATE PD PATHOGENETIC MECHANISMS

4.1.1. Dopamine toxicity in β-gal and α-syn SH-SY5Y cells

To obtain a cellular model of α-synuclein overexpression, the human neuroblastoma cell line SH-SY5Y was stably transfected with the plasmid containing human α-synuclein cDNA (α-syn) and, as a control, SH-SY5Y cells stably transfected with the plasmid containing β-galactosidase cDNA were used (β-gal) (see Materials and Methods, Paragraph 3.1.1).
The optimal dopamine concentration to be used in this study was determined by MTT assay.
The dopamine effect on cell viability was assessed exposing both β-gal and α-syn SH-SY5Y cells to different dopamine concentrations (0.125, 0.25, 0.5, 1 mM) for 24 h (see Figure 6). Dopamine treatment was always performed in combination with catalase, in order to eliminate extracellular hydrogen peroxide, formed by dopamine oxidation (Blum et al., 2000). Results are reported as the mean percentage of viable cells, obtained by the Abs_{570} ratio of dopamine treated cells (β-gal and α-syn cells treated with 700 U/ml catalase + different dopamine concentrations) and controls (β-gal and α-syn cells treated with 700 U/ml catalase only) of three independent experiments.

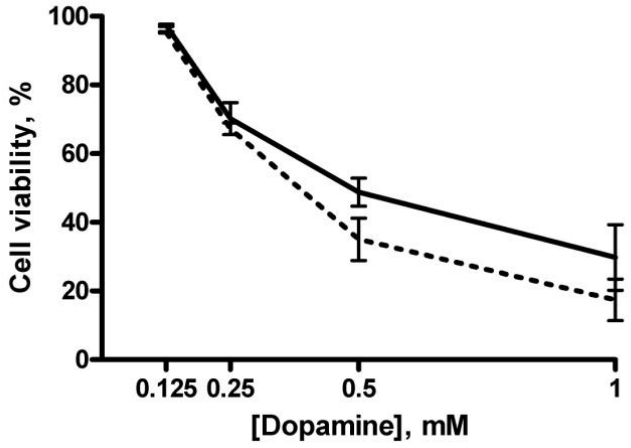

Figure 6: Dose dependent dopamine effect on cell viability measured by MTT assay. Continuous line: β-gal cells. Dashed line α-syn cells. All experiments were performed in the presence of 700 U/ml catalase. Values are the means ± SD of three independent experiments. For details and experimental conditions see Materials and Methods, Paragraph 3.1.2.

Figure 6 shows that dopamine is toxic in the range 0.125-1 mM on both β-gal and α-syn cells. Incrising concentrations of dopamine reduced progressively cell viability. Moreover, α-syn cells were less resistant to higher dopamine concentrations (0.5 and 1 mM).

Since the percentage of viable cells was still acceptable to conduct the proteomic analysis (70±5%) and the toxicity was almost identical for the two cell lines, the concentration chosen for all further experiments was 0.25 mM.

4.1.2 Dopamine increases the expression of α-synuclein to a threshold

Quantification of α-synuclein overexpression was performed by Western blot, revealing a significant 1.5-fold increase in α-synuclein expression in α-syn cells with respect to β-gal cells (Figure 7).

As dopamine upregulates α-synuclein expression (Gómez-Santos et al., 2003), α-synuclein level was measured in α-syn cells with respect to β-gal cells in the presence of catalase only (cat) or in the presence of catalase and 0.25 mM dopamine (DA) for 24 h. Dopamine treatment significantly increased 1.5-fold the expression of α-synuclein in β-gal control cells (SH-SY5Y β-gal DA), but not in α-syn cells that already overexpress it as a consequence of transfection (SH-SY5Y α-syn DA) (Figure 7).

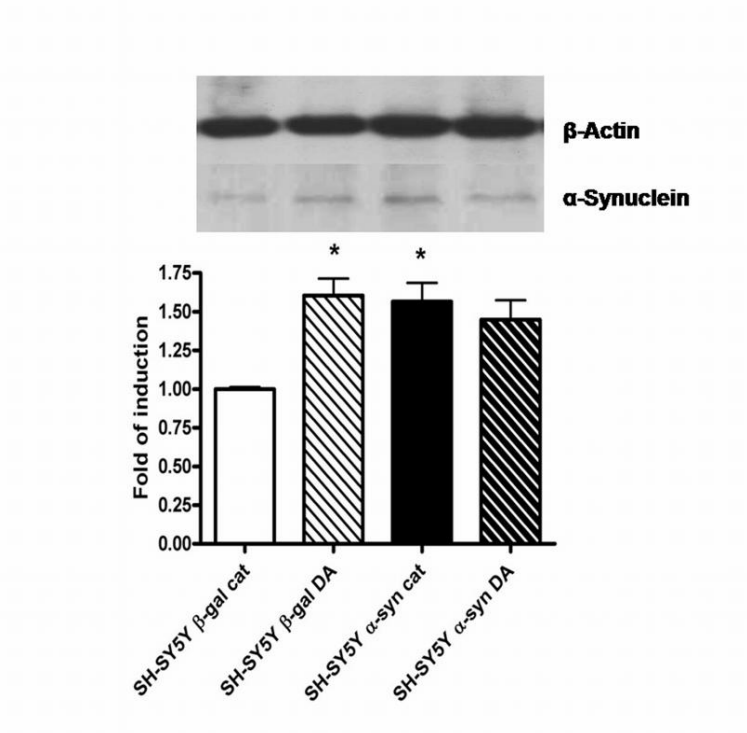

Figure 7: Relative expression of α-synuclein in β-gal and α-syn cells in response to dopamine treatment. Results are indicated as fold of induction relative to expression observed in β-gal cells treated with catalase (SH-SY5Y β-gal cat, set to 1). Values (density of α-synuclein bands normalized to β-actin) are the mean ± SE of three independent experiments. * $p < 0.005$ vs. β-gal cat cells.

4.1.3 Proteomics analysis reveals quantitative changes in 23 proteins

Proteomic investigations were conducted on β-gal and α-syn cells treated or not with dopamine as described in Materials and Methods, Paragraph 3.1.3. Statistical analysis (by two-way ANOVA) of silver-stained gel images revealed 28 spots whose intensity was significantly different in at least one of the four groups considered here (Figure 8).

Two groups of spots showing remarkable changes in the isoform pattern in the four conditions were easily assigned to glyceraldehyde-3-phosphate dehydrogenase and to mitochondrial ATP synthase alpha subunit by comparison with 2-DE maps available in the SWISS 2D-PAGE database (http://www.expasy.org/swiss 2dpage). Additionally, 21 differentially expressed proteins were identified by LC-MS-MS (see Table 7 and Table 8).

After **dopamine** treatment one spot completely disappeared (VDAC-2) and 10 proteins (pyruvate kinase, RPLP2, eIF5A, parathymosin, L7/L12, annexin A2, Annexin A5, aldolase A, fascin 1, and peroxyredoxin 1) displayed quantitative differences (see insets in Figure 8; black vs. white bars). Dopamine-responsive proteins are involved in protein synthesis, energetic metabolism, calcium-dependent phospholipid binding, cytoskeleton regulation, redox homeostasis and mitochondrial electrochemical balance.

Regardless of treatment, overexpression of **α-synuclein** significantly affected the levels of 4 proteins (stathmin 1, GSTπ, Ran 1 binding protein, C1q binding protein), related to cell signaling, apoptosis and cytoskeleton regulation (see insets in Figure 8; shaded vs. white bars).

On the other hand, 6 proteins were regulated in a more **complex** way (see insets in Figure 8; 4-bar histograms), *i.e.*, α-synuclein overexpression modulated the dopamine effect (profilin 1, enolase 1, RuvB-like 1, CRMP4, lamin A/C, mitofilin). These proteins deal with regulation of cytoskeleton, transcription and cell growth, signal transduction and mitochondrial trafficking.

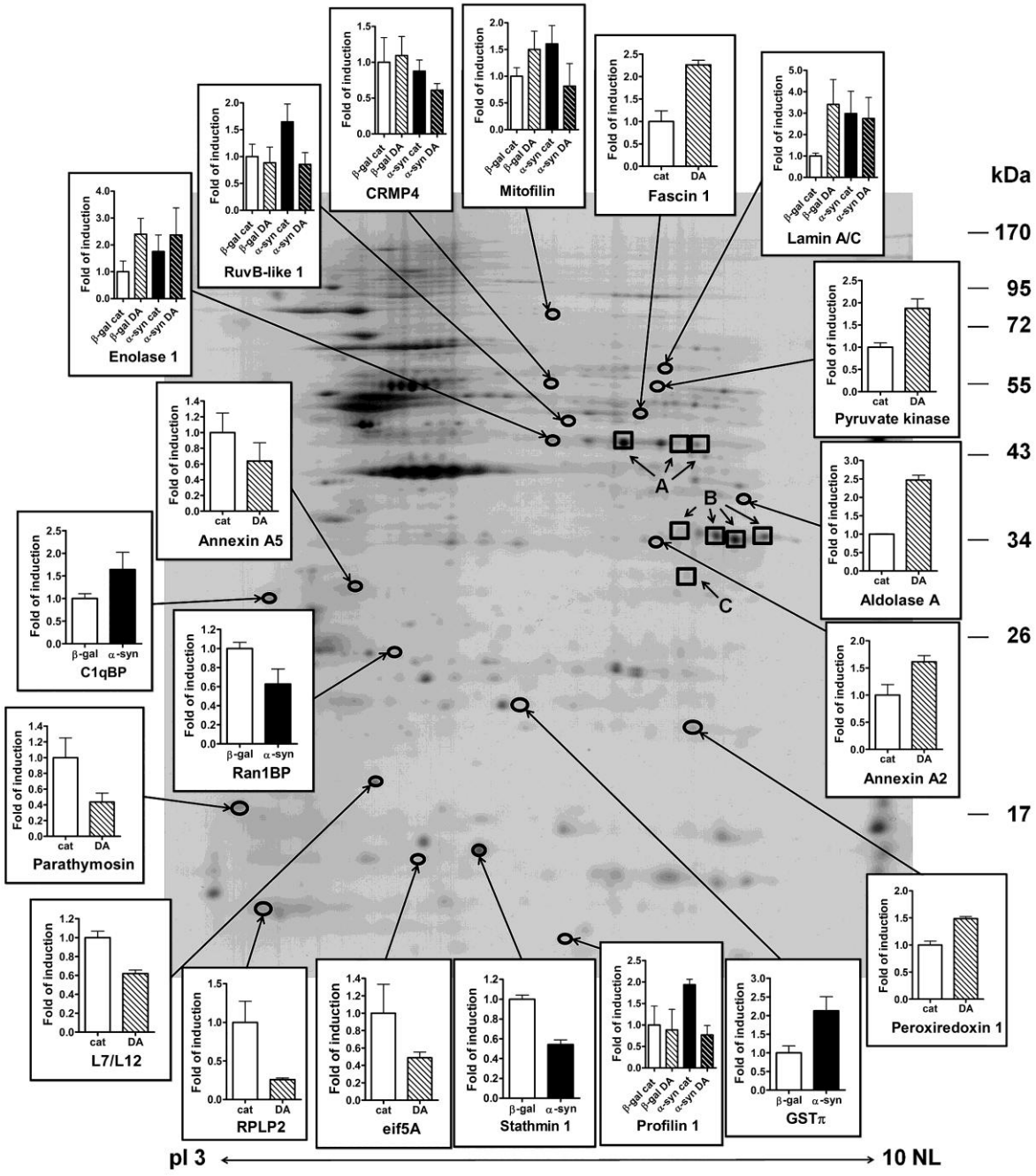

Figure **8**: A representative silver-stained 2-DE gel of proteins extracted from β-gal cat cells. Qualitative differences are indicated by squares (A: ATP synthase α; B: GAPDH; C: VDAC2), whereas circles indicate spots whose levels change significantly as indicated by insets. Values (fold of induction with respect to the reference condition) are the mean ± SD of three different gels in 4-bars histograms and of six gels in 2-bars histograms. For protein identification see Table 7.

Table 7: Identification of differentially expressed proteins. Protein spots in silver-stained gels were analyzed by ANOVA. DA: proteins that showed increased (↑) or decreased (↓) expression following dopamine treatment. α-Syn: proteins that displayed increased (↑) or decreased (↓) expression as a consequence of α-synuclein overexpression. Complex: proteins that displayed altered levels as a result of the association of dopamine treatment with α-synuclein overexpression (see insets in Figure 8).

Protein	Swiss-Protein ID	M_r (kDa)[a]	pI[a]	Identified peptides	Mascot score	Sequence coverage (%)	F[b]	P[b]	Observed change
RPLP2	P05387	11.7	4.42	4	268	53	8.41	0.020	DA ↓ × 3.9
Parathymosin	P20962	11.4	4.14	2	88	22	12.14	0.008	DA ↓ × 2.3
eIF5A isoform B	P63241	16.8	5.08	2	70	7	12.72	0.007	DA ↓ × 2.1
L7/L12, mitochondrial	P52815	21.4	5.37	3	140	11	9.28	0.016	DA ↓ × 1.6
Peroxiredoxin 1	Q06830	22.1	8.27	9	431	45	10.39	0.012	DA ↑ × 1.5
Annexin A5	Q6FHB3	35.9	4.83	13	720	52	6.72	0.032	DA ↓ × 1.6
Annexin A2	Q8TBV2	38.6	7.57	6	299	20	5.25	0.050	DA ↑ × 1.6
Aldolase A	P04075	39.3	8.34	5	210	20	36.86	0.001	DA ↑ × 2.5
Fascin 1	Q16658	54.5	6.84	7	333	16	5.88	0.042	DA ↑ × 2.3
Pyruvate kinase	P14618	57.8	7.95	12	521	29	7.22	0.028	DA ↑ × 1.9
VDAC-2	P45880.2	31.4	7.66	6	268	17	–[d]	–[d]	Absent in DA
Stathmin 1	P16949	17.3	5.76	7	305	32	15.24	0.005	α-Syn ↓ × 1.8
Ran1BP	P43487	23.2	5.19	4	206	21	10.38	0.012	α-Syn ↓ × 1.6
GSTπ	P09211	23.4	5.43	8	474	43	6.29	0.037	α-Syn ↑ × 2.1
C1qBP	Q07021	23.8	4.32	5	306	21	9.81	0.014	α-Syn ↑ × 1.6
Profilin 1	P07737	15.0	8.44	4	170	41	6.92	0.030	Complex
Enolase 1	P06733	47.1	7.01	8	481	24	6.94	0.03	Complex
RuvB-like 1	Q9Y265	50.2	6.02	10	343	28	11.58	0.009	Complex
CRMP4	Q14195	61.9	6.04	2	81	4	13.02	0.007	Complex
Lamin A/C	Q5TCJ3	72.2	6.40	11	536	22	10.91	0.011	Complex
Mitofilin, p32	Q16891	83.7	6.08	5	241	9	12.10	0.008	Complex
GAPDH	P04406	35.9	8.58	–[c]	–[d]	–[d]	–[d]	–[d]	Change in pattern
ATP synthase α	P25705	55.2	8.28	–[c]	–[d]	–[d]	–[d]	–[d]	Change in pattern

[a] Theoretical values. [b] *F* and *P* refer to ANOVA. [c] Identified from SWISS 2D-PAGE database. [d] Not applicable.

Table 8: MS/MS peptide sequence analysis of successfully identified proteins. The protein name, the MS/MS data, the Mascot ion score and the Sequence Coverage are reported. [a] start-end positions of identified peptides were calculated against complete amino acid sequence of the protein.

Protein ID	m/z	charge state	start-end [a]	sequence	Ion Score	Seq Cov (%)
profilin 1	822.41	2+	39 – 54	TFVNITPAEVGVLVGK	38	41
	736.31	2+	57 – 70	SSFYVNGLTLGGQK	45	
	813.30	2+	76 – 89	DSLLQDGEFSMDLR	58	
	690.32	2+	92 – 105	STGGAPTFNVTVTK	29	
60S acidic ribosomal protein P2	709.26	2+	26 – 38	ILDSVGIEADDDR	91	53
	591.62	3+	26 – 41	ILDSVGIEADDDRLNK	35	
	628.80	2+	50 – 61	NIEDVIAQGIGK	81	
	925.50	3+	62 – 94	LASVPAGGAVAVSAAPGSAAPAAGSAPAAAEEK	61	
Eukaryotic initiation factor 5A isoform B	671.37	2+	110 – 121	EDLRLPEGDLGK	34	7
	414.58	2+	114 – 121	LPEGDLGK	36	
stathmin 1	772.87	2+	14 – 27	RASGQAFELILSPR	30	32
	694.89	2+	15 – 27	ASGQAFELILSPR	47	
	771.86	2+	28 – 41	SKESVPEFPLSPPK	54	
	663.84	2+	30 – 41	ESVPEFPLSPPK	36	
	537.74	2+	44 – 52	DLSLEEIQK	47	
	601.80	2+	44 – 53	DLSLEEIQKK	38	
	583.23	2+	86 – 95	AIEENNNFSK	56	
parathymosin	538.23	2+	5 – 15	SVEAAAELSAK	64	22
	680.30	2+	82 – 93	AAEEEDEADPKR	26	
L7/L12, mitochondrial	680.80	2+	151 – 162	NYIQGINLVQAK	47	11
	642.30	2+	163 – 173	KLVESLPQEIK	58	
	578.26	2+	164 – 173	LVESLPQEIK	34	
Glutathione-S-transferase π	734.82	2+	1 – 12	MPPYTVVYFPVR	50	43
	669.32	2+	2 – 12	PPYTVVYFPVR	72	
	638.76	2+	20 – 30	MLLADQGQSWK	68	
	867.86	2+	31 – 45	EEVVTVETWQEGSLK	67	
	942.43	2+	56 – 71	FQDGDLTLYQSNTILR	84	
	706.28	3+	83 – 101	DQQEAALVDMVNDGVEDLR	41	
	767.83	2+	104 – 116	YISLIYTNYEAGK	71	
	719.03	3+	104 – 121	YISLIYTNYEAGKDDYVK	20	
Ran binding protein 1	691.26	2+	40 – 50	TLEEDEEELFK	60	21
	668.29	2+	58 – 68	FASENDLPEWK	43	
	517.70	2+	142 – 150	FLNAENAQK	52	
	593.82	2+	179 – 189	VAEKLEALSVK	52	
C1q binding protein	642.31	2+	77 – 87	AFVDFLSDEIK	61	21
	849.35	2+	77 – 90	AFVDFLSDEIKEER	73	
	819.30	2+	101 – 115	MSGGWELELNGTEAK Oxidation (M)	53	
	1144.08	2+	151 – 170	VEEQEPELTSTPNFVVEVIK	39	
	757.27	2+	204 – 216	EVSFQSTGESEWK	79	

annexin A5	670.75	2+	7 – 18	GTVTDFPGFDER	66	52
	852.90	2+	30 – 45	GLGTDEESILTLLTSR	71	
	723.84	2+	64 – 76	DLLDDLKSELTGK	67	
	501.20	2+	109 – 117	VLTEIIASR	52	
	587.27	2+	152 – 161	MLVVLLQANR Oxidation (M)	54	
	886.75	3+	162 – 186	DPDAGIDEAQVEQDAQALFQAGELK	68	
	477.58	2+	194 – 201	FITIFGTR	32	
	910.36	2+	213 – 227	YMTISGFQIEETIDR Oxidation (M)	68	
	807.42	2+	228 – 242	ETSGNLEQLLLAVVK	38	
	875.38	2+	246 – 260	SIPAYLAETLYYAMK Oxidation (M)	47	
	578.26	2+	261 – 271	GAGTDDHTLIR	44	
	553.75	2+	277 – 285	SEIDLFNIR	59	
	645.78	2+	291 – 301	NFATSLYSMIK Oxidation (M)	48	
annexin A2	544.24	2+	38 – 47	DALNIETAIK	51	20
	556.27	2+	69 – 77	QDIAFAYQR	57	
	611.75	2+	105 – 115	TPAQYDASELK	46	
	688.91	3+	179 – 196	RAEDGSVIDYELIDQDAR	43	
	518.69	2+	197 – 205	DLYDAGVKR	40	
	711.25	2+	314 – 324	SLYYYIQQDTK	71	
aldolase A	717.79	2+	2 – 13	PYQYPALTPEQK	31	20
	666.76	2+	29 – 42	GILAADESTGSIAK	71	
	745.74	2+	44 – 56	LQSIGTENTEENR	44	
	671.82	2+	88 – 99	ADDGRPFPQVIK	31	
	758.34	3+	112 – 134	GVVPLAGTNGETTTQGLDGLSER	33	
enolase 1	902.94	2+	33 – 50	AAVPSGASTGIYEALELR	99	24
	640.75	2+	93 – 103	LMIEMDGTENK	49	
	572.27	2+	184 – 193	IGAEVYHNLK	55	
	980.95	2+	203 – 221	DATNVGDEGGFAPNILENK	44	
	778.82	2+	240 – 253	VVIGMDVAASEFFR.S Oxidation (M)	80	
	713.33	2+	270 – 281	YISPDQLADLYK	53	
	763.82	2+	359 – 372	LAQANGWGVMVSHR	60	
	452.70	2+	413 – 420	IEEELGSK	40	
RuvB-like 1	650.83	2+	34 – 46	QAASGLVGQENAR	64	28
	540.80	2+	65 – 76	AVLLAGPPGTGK	43	
	693.33	2+	77 – 90	TALALAIAQELGSK	49	
	577.72	2+	109 – 117	TEVLMENFR.R Oxidation (M)	31	
	638.80	2+	172 – 182	LDPSIFESLQK	34	
	867.89	2+	185 – 201	VEAGDVIYIEANSGAVK	30	
	844.42	2+	318 – 333	ALESSIAPIVIFASNR	33	
	650.54	3+	340 – 357	GTEDITSPHGIPLDLLDR	18	
	775.36	3+	379 – 400	AQTEGINISEEALNHLGEIGTK	14	
	765.89	2+	405 – 418	YSVQLLTPANLLAK	33	
fascin 1	573.74	2+	23 – 32	YLTAEAFGFK	31	16
	571.73	2+	91 – 100	FLIVAHDDGR	50	
	557.21	2+	101 – 109	WSLQSEAHR	48	
	607.32	3+	202 – 217	LVARPEPATGYTLEFR	58	
	595.75	2+	230 – 241	YLAPSGPSGTLK	40	
	537.71	2+	399 – 408	KVTGTLDANR	45	
	769.76	2+	480 – 493	ASAETVDPASLWEY	60	
pyruvate kinase	599.28	2+	33 – 43	LDIDSPPITAR	54	29
	822.40	3+	93 – 115	TATESFASDPILYRPVAVALDTK	28	
	607.26	2+	142 – 151	ITLDNAYMEK.C Oxidation (M)	56	
	731.86	2+	174 – 186	IYVDDGLISLQVK	64	
	890.84	2+	189 – 206	GADFLVTEVENGGSLGSK	21	
	589.24	3+	207 – 224	KGVNLPGAAVDLPAVSEK	35	
	818.89	2+	208 – 224	GVNLPGAAVDLPAVSEK	60	
	833.39	2+	280 – 294	FDEILEASDGIMVAR	61	
	571.26	2+	295 – 305	GDLGIEIPAEK	51	
	510.14	2+	368 – 376	GDYPLEAVR	32	
	644.63	3+	384 – 399	EAEAAIYHLQLFEELR	26	
	821.82	2+	476 – 489	DPVQEAWAEDVDLR	35	
Collapsin response mediator protein 4	655.34	2+	158 – 170	QIGDNLIVPGGVK	32	4
	821.35	2+	611 – 625	GMYDGPVFDLTTTPK	49	

lamin A/C	680.29	2+	12 – 25	SGAQASSTPLSPTR	44	22
	815.31	2+	29 – 41	LQEKEDLQELNDR	40	
	566.18	2+	33 – 41	EDLQELNDR	38	
	545.69	2+	51 – 60	SLETENAGLR	41	
	574.73	2+	63 – 72	ITESEEVVSR	69	
	514.69	2+	241 – 249	LADALQELR	50	
	751.81	2+	250 – 261	AQHEDQVEQYKK	54	
	877.35	2+	281 – 296	NSNLVGAAHEELQQSR	60	
	487.66	2+	379 – 386	LLEGEEER	25	
	602.23	2+	440 – 450	VAVEEVDEEGK	80	
	754.30	2+	528 – 541	TALINSTGEEVAMR.K Oxidation (M)	54	
Mitofilin, p32	764.37	2+	211 – 223	VVSQYHELVVQAR	55	9
	792.36	2+	229 – 242	ELDSITPEVLPGWK	38	
	605.72	2+	359 – 368	SEFEQNLSEK	37	
	575.23	2+	369 – 377	LSEQELQFR	68	
	936.49	2+	434 – 452	TSSAETPTIPLGSAVEAIK	43	
peroxiredoxin 1	490.63	2+	8 – 16	IGHPAPNFK	26	45
	582.73	2+	17 – 27	ATAVMPDGQFK	35	
	470.69	2+	28 – 35	DISLSDYK	32	
	811.85	2+	94 – 109	QGGLGPMNIPLVSDPK	66	
	554.21	2+	111 – 120	TIAQDYGVLK	32	
	447.56	2+	121 – 128	ADEGISFR	52	
	460.62	2+	129 – 136	GLFIIDDK	52	
	606.76	2+	414 – 451	QITVNDLPVGR	69	
	598.75	2+	159 – 168	LVQAFQFTDK	67	
Voltage-dependent anion channel 2	636.29	1+	42 – 46	DIFNK	14	17
	714.75	2+	123 – 135	LTFDTTFSPNTGK	63	
	778.85	2+	123 – 136	LTFDTTFSPNTGKK	50	
	647.27	2+	251 – 262	YQLDPTASISAK	45	
	701.74	3+	263 – 282	VNNSSLIGVGYTQTLRPGVK	36	
	508.67	2+	283 – 292	LTLSALVDGK	61	

4.1.4 Network enrichment highlights the involvement of the NF-κB pathway

Experimentally identified proteins were analyzed in terms of both interaction network and GO classification enrichment using PPI spider, a network enrichment algorithm based on known protein-protein physical interactions (Antonov et al., 2009). Figure 9 shows significant ($p<0.05$) network models for proteins that displayed significant changes following dopamine treatment, regardless of α-synuclein overexpression (A), and for proteins that displayed significant changes as a consequence of α-synuclein overexpression or as a result of the association of dopamine treatment with α-synuclein overexpression (B). The same analysis performed on all identified proteins was able to correctly cluster them in the two classes described above.

Statistically-significant ($p < 0.05$) functional association to Gene Ontology (GO) classifications was obtained from PPI spider starting from proteins grouped as above (Tables 9 and 10).

In both cases, bioinformatic analysis revealed that the **NF-κB** pathway could be involved in determining the effects of dopamine treatment and α-synuclein overexpression.

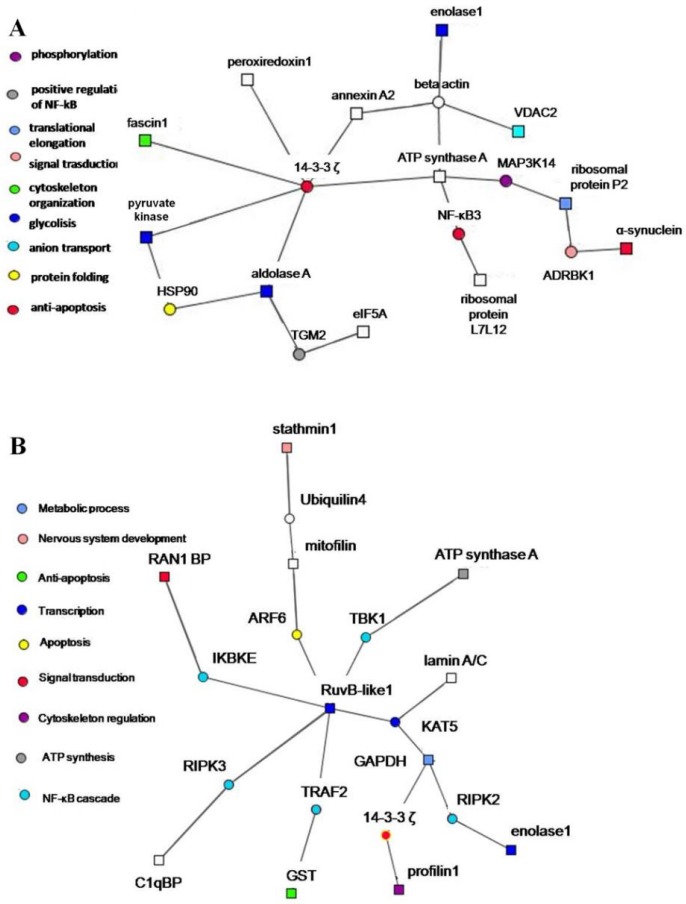

Figure 9: Enriched protein networks. (A) Proteins that displayed significant changes following dopamine treatment. (B) Proteins that displayed significant changes as a consequence of α-synuclein overexpression or as a result of the association of dopamine treatment with α-synuclein overexpression. Experimentally identified proteins are indicated by filled squares. Open circles indicate common interactors as predicted by PPI Spider, $p < 0.05$. Colors indicate different cellular processes, reported in the related legends.

Table 9: Enriched GO categories starting from proteins that displayed significant changes following dopamine treatment, regardless of α-synuclein overexpression. Statistically-significant ($p < 0.05$) functional association to Gene Ontology (GO) classifications was obtained from PPI spider (http://mips.helmholtz-muenchen.de/proj/ppispider/) starting from proteins that displayed significant changes in their levels following dopamine treatment (labeled as DA, see Table 7). Genes are labeled with their accession name in the NCBI Gene database.

GO term	Description	Input genes
GO:0043123	Positive regulation of I-κB kinase/NF-κB cascade	TBK1 MAP3K3 RELA TGM2 TRAF6 RIPK2 IKBKE

Table 10: Enriched GO categories starting from proteins that displayed significant changes following α-synuclein overexpression or in a more complex way. Statistically-significant ($p < 0.05$) functional association to Gene Ontology (GO) classifications was obtained from PPI spider (http://mips.helmholtz-muenchen.de/proj/ppispider/) starting from proteins that show quantitative alterations in response to α-synuclein overexpression (labeled as α-Syn, see Table 7), or that differentially respond to dopamine exposure as a function of α-synuclein overexpression (labeled as Complex, see Table 7). Genes are labeled with their accession name in the NCBI Gene database.

GO term	Description	Input genes
GO:0043123	Positive regulation of I-κB kinase/NF-κB cascade	MAP3K7IP2 TBK1 MAP3K3 RELA TNFRSF1A TRAF6 RIPK2 IKBKE
GO:0006916	Anti-apoptosis	CDC2 GSTP1 NFKB1 SNCA YWHAZ RELA VHL
GO:0004871	Signal transducer activity	MAP3K7IP2 TBK1 MAP3K3 RELA TRAF2 TRAF6 RIPK2 IKBKE STMN1
GO:0004674	Protein serine/threonine kinase activity	RIPK3 TBK1 MAP3K3 MAPK1 MAPK3 MAP3K7 RIPK2 MAP3K14
GO:0006468	Protein amino acid phosphorylation	RIPK3 TBK1 PRKCA MAPK1 MAPK3 MAP3K7 RIPK2 MAP3K14 IKBKE CDC2

4.1.5 Dopamine-induced apoptosis is not affected by α-synuclein

The suggestions obtained from enriched GO categories (Table 10) and the ambiguous role of α-synuclein (see Introduction, Paragraph 1.4) prompted us to evaluate apoptotic cell death in our experimental setting by Annexin V assay (see Material and Methods, Paragraph 3.1.6).
Comparing white and black bars of Figure 10, panel A, it is possible to notice that the basal level of apoptotic cells was not significantly different in α-syn cells (20.0±1.6%) with respect to β-gal cells (23.1±0.7%), in agreement with cell viability assays (see Paragraph 4.1.1). Remarkably, also the percentage of necrotic cells was not significantly affected by α-synuclein overexpression (β-gal cat 16.6±1.3; α-syn cat 14.1±1.5; Figure 10, panel B).
Dopamine triggered apoptotic cell death to the same extent in both α-syn (α-syn DA, 45.8±2.6%), and β-gal cells (β-gal DA, 50.9±2.7%), (Figure 10, panel A). Also propidium iodide positive cells show similar levels in α-syn (α-syn DA, 51.2±5%), and β-gal cells (β-gal DA, 51.7±5%), (Figure 10, panel B).

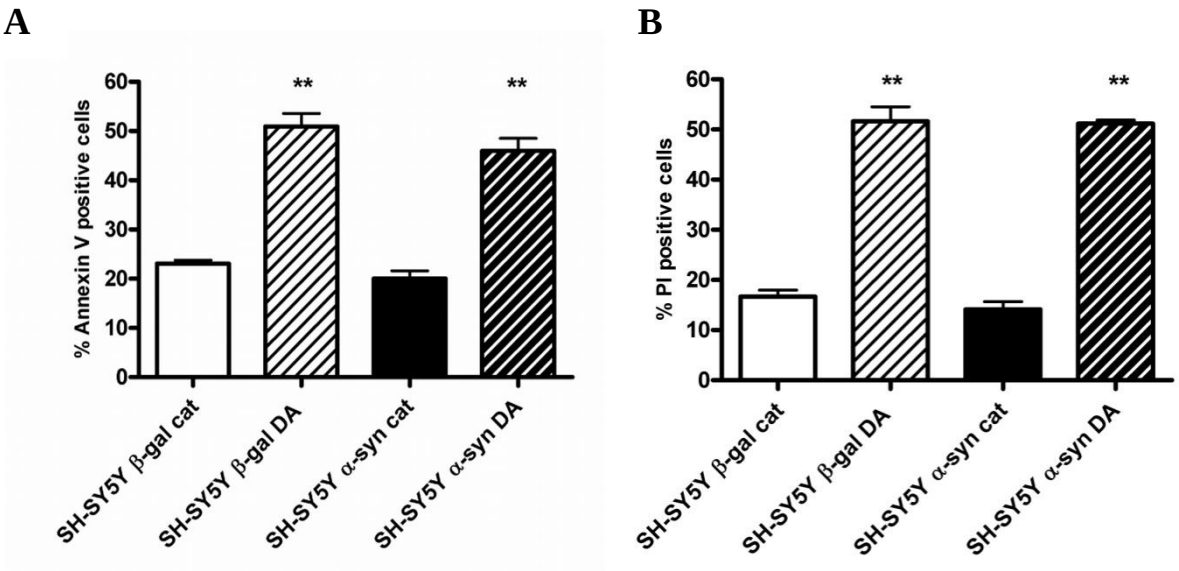

Figure 10: A) Induction of apoptosis. Apoptotic β-gal and α-syn cells are measured as percentage of annexin V positive cells in response to dopamine treatment. ** $p < 0.001$ cat vs. DA cells. Values are the mean ± SE of three independent experiments. B) Percentage of PI positive cells.
White bars: β-gal cells; black bars: α-syn cells; open bars: 24 h treatment in the presence of 700 U/ml catalase only (cat); dashed bars: 24 h treatment in the presence of 700 U/ml catalase and 0.25 mM dopamine (DA). Values are the mean ± SE of three independent experiments. ** $p < 0.001$ cat vs. DA cells.

4.1.6 Dopamine and α-synuclein affect the NF-κB pathway

In order to functionally assess the involvement of the NF-κB pathway as suggested by the network enrichment procedure of proteomic data (see Paragraph 4.1.4), we transfected β-gal and α-syn cells with the pNF-κB-Luc gene reporter and measured the NF-κB-dependent luciferase activity (for further experimental detailed see Materials and Methods, Paragraph 3.1.7).

As shown in Figure 11, the basal activation of NF-κB was significantly ($p < 0.001$) lower in α-syn cells (SH-SY5Y α-syn cat) than in β-gal cells (SH-SY5Y β-gal cat), since the luciferase related activity was reduced by 30% (±5%).

Additionally, after 24 h dopamine treatment, the expression of the reporter gene in β-gal and α-syn cells was dramatically decreased, the luciferase activity being reduced by a factor of 10 ($p < 0.001$). After 2 h dopamine treatment we did not observe any significant change, neither in β-gal nor in α-syn cells (data not shown).

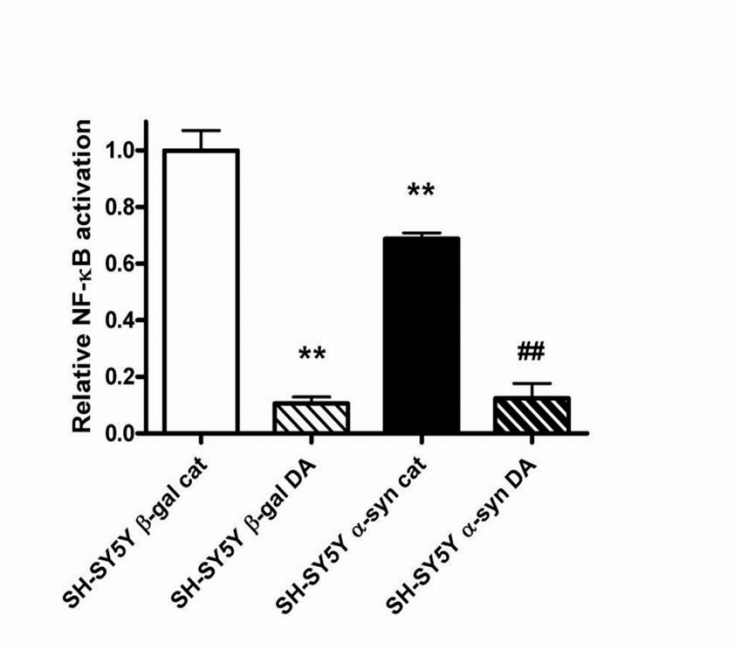

Figure 11: Activation of the NF-κB pathway. NF-κB activity measured by luciferase gene reporter assay relative to β-gal cells treated with catalase (set to 1). ** $p < 0.001$ vs. β-gal cat cells. ## $p < 0.001$ vs. α-syn cat cells.

4.1.7 Dopamine, not α-synuclein overexpression, increases the expression of HSP70

HSP70 is known to be induced by several stress conditions in the nervous system (Calabrese et al., 2004; Garrido et al., 2001) and to inhibit NF-κB activation (Malhotra et al., 2002; Salminen et al., 2008). Thus, we measured by Western blotting HSP70 levels in β-gal and α-syn cells treated or not with dopamine (0.25 mM, 24 h).

Figure 12 shows that HSP70 basal levels were similar in α-syn (SH-SY5Y α-syn cat) and β-gal cells (SH-SY5Y β-gal cat). However, dopamine increased HSP70 level 1.5-fold, regardless of α-synuclein overexpression (SH-SY5Y β-gal DA and SH-SY5Y α-syn DA).

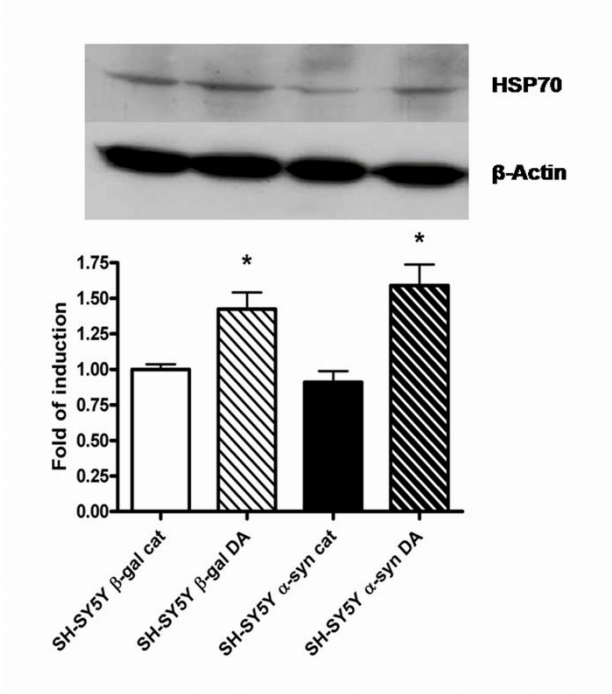

Figure 12: Expression of the NF-κB regulator HSP-70 relative to expression observed in β-gal cat cells (set to 1). * $p < 0.005$ vs. β-gal cat cells. Values are the mean ± SE of three independent experiments.

4.1.8 Dopamine does not influence total level of 14-3-3

14-3-3 proteins are ubiquitous eukaryotic acidic polypeptides of ~32 kDa that binds to serine or threonine residues of phosphorylated proteins and play a regulatory role in intracellular signal transduction, cell-cycle progression, differentiation and apoptosis. In addition, 14-3-3 shows sequence similarity to α-synuclein, which in turn can bind to 14-3-3, and both α-synuclein and 14-3-3 have many common interactors (see Introduction, Paragraph 1.4). Remarkably, network enrichment revealed a central role for 14-3-3 after both dopamine treatment and α-synuclein overexpression (see Paragraph 4.1.4 and Figure 9). Thus, we measured 14-3-3 levels by Western blotting in β-gal and α-syn cells treated or not with dopamine (0.25 mM, 24 h). As reported in Figure 13, 14-3-3 total levels are similar in α-syn (SH-SY5Y α-syn cat) and β-gal cells (SH-SY5Y β-gal cat), even after dopamine treatment (SH-SY5Y β-gal DA and SH-SY5Y α-syn DA).

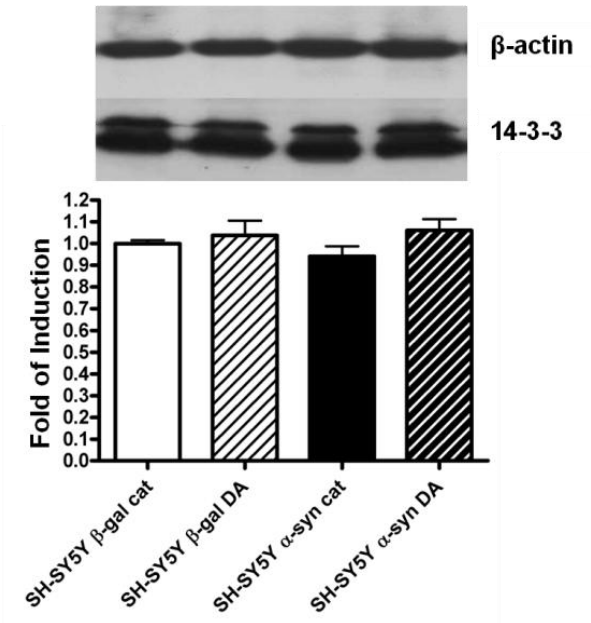

Figure 13: Expression of 14-3-3 chaperone proteins relative to expression observed in β-gal cat cells (set to 1). Values are the mean ± SE of three independent experiments.

4.1.9 Dopamine effect on cell cycle

In order to avoid biased conclusions about dopamine toxicity in our model, we considered potential differences in cell cycle distribution in our experimental conditions.

The effects of dopamine (0.25 mM with catalase 700 U/ml) on cell cycle distribution of α-syn and β-gal cells are reported in Figure 14. The only detectable effect was a slight increase (10%) in the S ($p<0.05$) and a decrease in the G_2/M phase cell subpopulations after 24 h exposure to dopamine in β-gal cells. Noticeably, α-synuclein overexpression does not affect cell cycle distribution of SH-SY5Y cells.

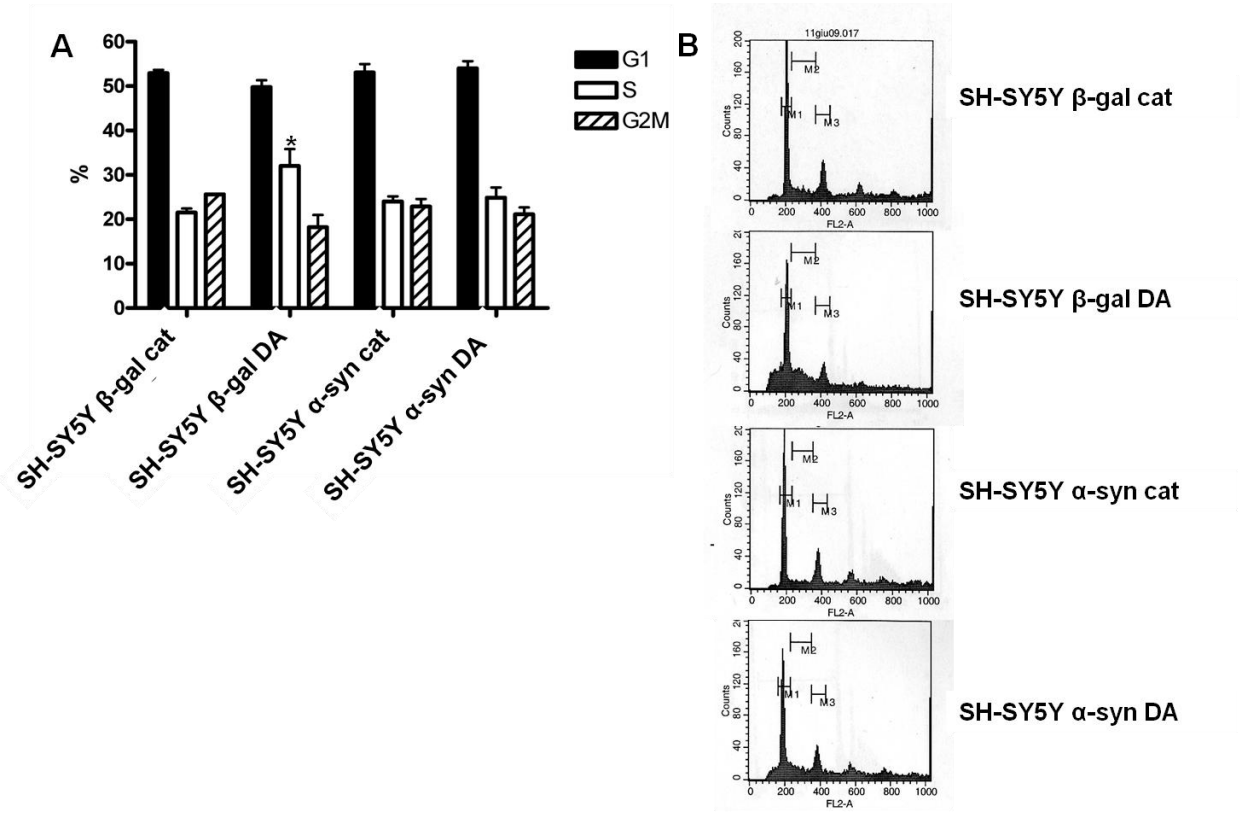

Figure **14**: Effects of dopamine on cell cycle distribution in α-syn and β-gal cells. A) Distribution in the different cell cycle phases. Black bars: G0/G1 phase; white bars: S phase; shaded bars: G2/M phase. Values are the mean ± SE of three independent experiments. * $p < 0.05$ vs. β-gal cat. B) Representative histograms for the cell cycle analysis. Fluorescent emission of PI is collected through a 575 band-pass filter, acquired in linear mode. Gaps are set in the control condition (SH-SY5Y β-gal cat) and applied to other samples: M1= G0/G1 phase; M2= S phase; M3= G2/M phase. For details see Materials and Methods, Paragraph 3.1.9.

4.1.10 Dopamine downregulates Voltage-Dependent Anion Channels

Voltage-Dependent Anion Channels (VDACs) are the most abundant proteins of the outer mitochondrial membrane, thus acting as key players in many cellular processes, ranging from metabolism regulation to cell death (Celsi et al., 2009).

In order to validate the qualitative change observed in VDAC2 level in the proteomic analysis (see Figure 15 and Paragraph 4.1.3), we evaluated VDAC2 levels by Western blotting after 4, 7, 12 and 24 h dopamine exposure (see Paragraph 3.1.10). Since mitochondrial impairment is a well known pathogenetic mechanism in PD, we investigated how dopamine influenced levels of all VDACs family members.

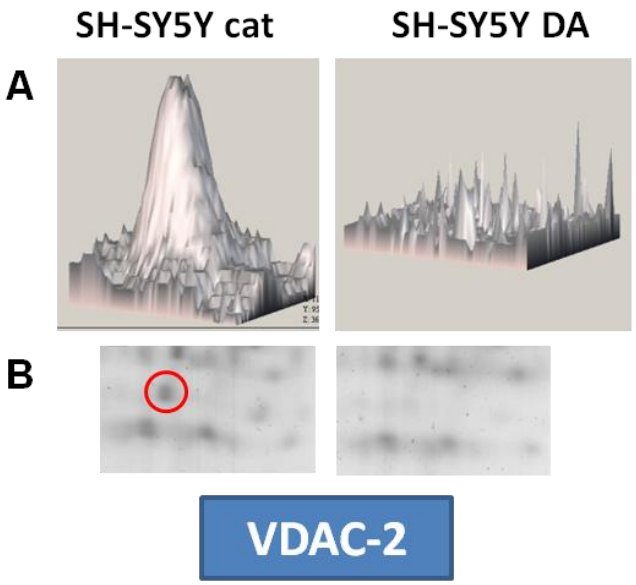

Figure 15: Dopamine downregulation of VDAC2 after 24 h dopamine treatment. A) 3D representation of spot #173 in 2-DE maps of SH-SY5Y cells treated (DA) or not (cat) with 0.25 mM dopamine for 24 h, regardless of α-synuclein overexpression. B) Zoom of 2-DE maps of SH-SY5Y cells treated or not with 0.25 mM dopamine for 24 h in the area of spot #173 (circled), corresponding to VDAC2.

Figure 16 shows VDACs levels after 24 h dopamine treatment. VDAC2 disappeared, thus confirming two-dimensional electrophoresis results. VDAC3 was completely eliminated, too. VDAC1, which is the most abundant form among VDACs family members, was downregulated, but not completely removed by dopamine altered levels.

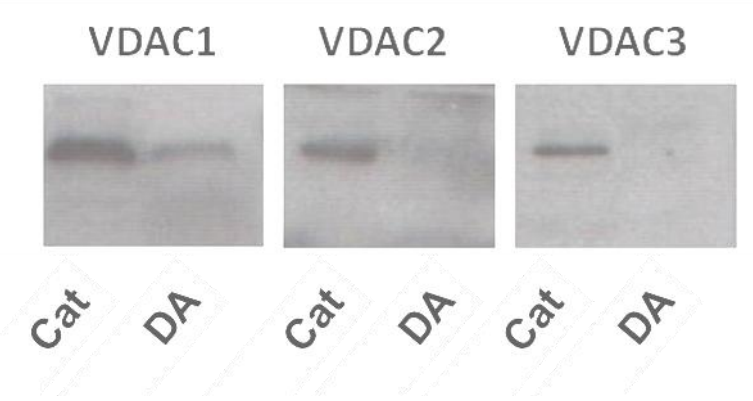

Figure 16: Anti-VDAC1, -VDAC2 and -VDAC3 immunoblot in SH-SY5Y cells after 24 h dopamine treatment (DA) and in controls (Cat, 700 U/ml catalase, 24h).

To better characterize time-dependent changes of VDACs levels, we performed a time-course evaluation of VDACs by Western blotting after 4, 7, 12 and 24 h dopamine exposure.

VDAC1

As shown in Figure 17, VDAC1 level did not differ significantly in controls, but progressively diminished in SH-SY5Y cells treated with 0.25 mM dopamine. The downregulation became significant after 12 h, VDAC1 level being further reduced to one third (compared to Cat 24h) after 24 h.

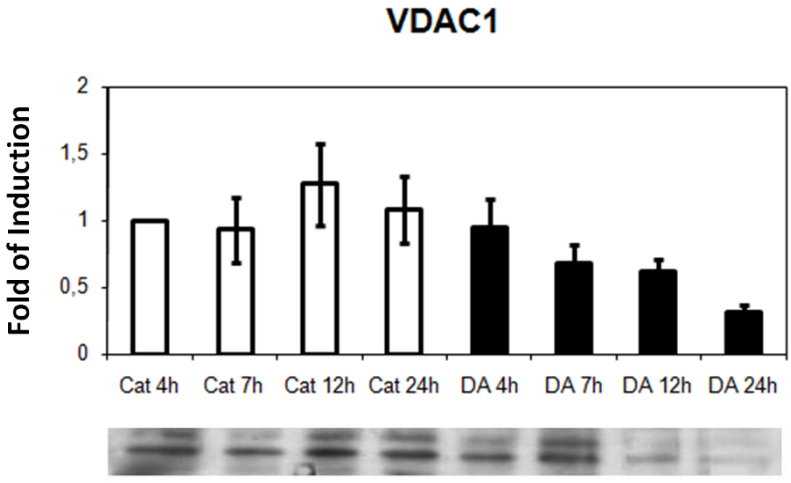

Figure 17: Upper panel: Expression of VDAC1 relative to expression observed in SH-SY5Y cells cat 4h (set to 1). Values are the mean ± SD of three independent experiments. Lower panel: a representative anti-VDAC1 immunoblot.

VDAC2

As shown in Figure 18, VDAC2 level differed significantly also in controls and progressively increases in SH-SY5Y cells maintained in culture (similar behavior was observed in the absence of catalase, data not shown). After 24 h (Cat 24 h), VDAC2 level was raised 2-fold compared to Cat 4h cells. In dopamine-treated cells the downregulation became significant after 7 h. After 12 h dopamine treatment VDAC2 is barely detectable.

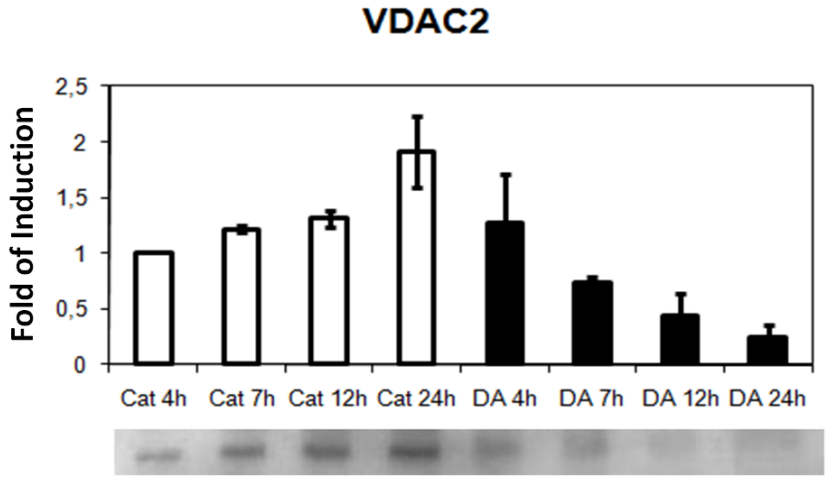

Figure 18: Upper panel: Expression of VDAC2 relative to expression observed in SH-SY5Y cells cat 4h (set to 1). Values are the mean ± SD of three independent experiments. Lower panel: A representative anti-VDAC2 immunoblot.

VDAC3

Due to the low expression level of VDAC3 compared to VDAC1 and VDAC2 and considering the low specificity/sensitivity of anti-VDAC3 antibody used here, the time course analysis of VDAC3 response to dopamine treatment did not give reproducible results, thus limiting the observation to the qualitative result shown in Figure 16.

TOTAL NUMBER OF MITOCHONDRIA

To verify that VDACs downregulation was not due to a general decrease in the number of mitochondria, we determined the level of other mitochondrial proteins, such as grp75 and HSP60 (see Figure 19).

Western blotting analysis did not show changes in their levels, neither in controls (culture time effect) nor in SH-SY5Y dopamine-treated cells for different times (treatment effect), thus confirming a specific effect of dopamine on VDACs expression.

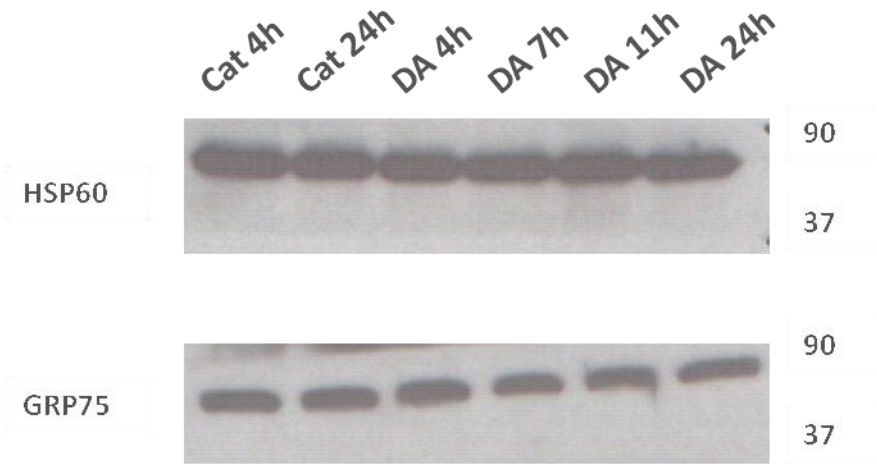

Figure 19: Immunoblot anti mitochondrial proteins grp75 and HSP60.

4.1.11 Two-dimensional Western blotting of VDAC2 reveals a treatment-dependent phosphorylated form

To observe possible post-translational modifications of VDAC2, we performed a two-dimensional Western blotting. Indeed, in one-dimensional Western blotting of VDAC2 we observed a high standard deviation in DA 4h samples (see Figure 18); thus, the observation of a diffuse band prompted us to hypothesize the presence of different forms migrating at similar molecular weight and immunoreactive to anti-VDAC2 antibody.

Immunoblot was performed after 4 and 7 h, VDAC2 becoming undetactable after 7 hours of dopamine treatment (see Paragraph 4.1.10).

As shown in Figure 20, VDAC 2 migrated at pH ≈ 8 (VDAC2 4h Cat), as expected (theoretical pI= 7.66). After 4 hours of dopamine treatment the prevalent form of VDAC2 was the more acidic one, with a pI ≈ 7 (VDAC2 4h DA). When present in controls, the acidic form was always a spot with a lower intensity with respect to the main form at pH 8.

After 7 h, the more acidic form became appreciable in controls too, although the main form still remained the one at pH ≈ 8 (VDAC2 7h Cat). In dopamine-treated cells, on the other hand, VDAC2 was strongly downregulated and the only form being observed here is the acidic one. Remarkably, the more acidic form has been reported to be the phosphorylated form (Sarioglu et al., 2008).

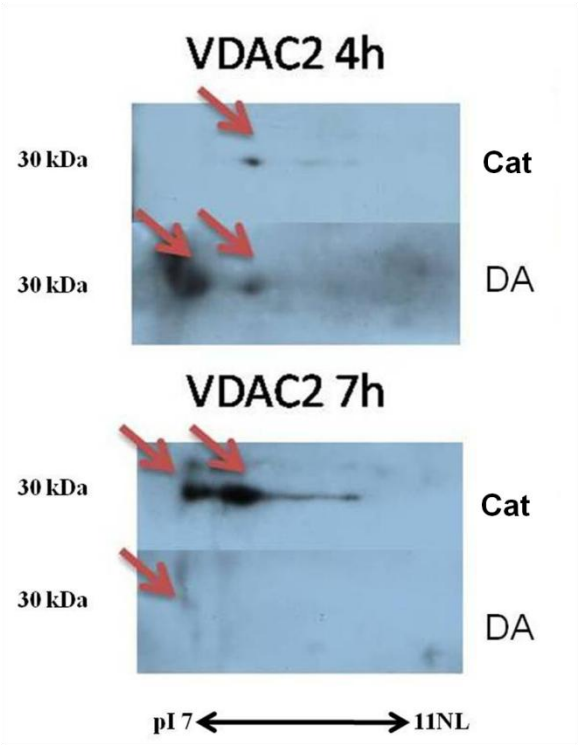

Figure 20: Two-dimensional immunoblot anti VDAC2 of SH-SY5Y cells treated with 700 U/ml of catalase only (Cat) or with 700 U/ml catalase + 0.25 mM dopamine (DA) for 4 h (upper panel) and for 7 h (lower panel). Arrows indicate VDAC2 forms.

4.1.12 Dopamine alters the mitochondrial membrane potential

Since VDACs are porins of the outer mitochondrial membrane, we measured the membrane potential with the TMRM potentiometric staining (see Paragraph 3.1.11). TMRM is a positively charged molecule that accumulates in mitochondria when their membrane potential (ΔΨm) is normal (negatively charged). If the potential drops down, the mitochondria become barely visible.

Figure 21 left shows TMRM-stained mitochondria in SH-SY5Y cells treated for 24 h with 700 U/ml catalase only (Cat). Conversely, right panel displays a marked depolarization of the mitochondrial membrane as a consequence of 24 h 0.25 mM dopamine exposure (DA).

Hence, dopamine induced a reduction of ΔΨm.

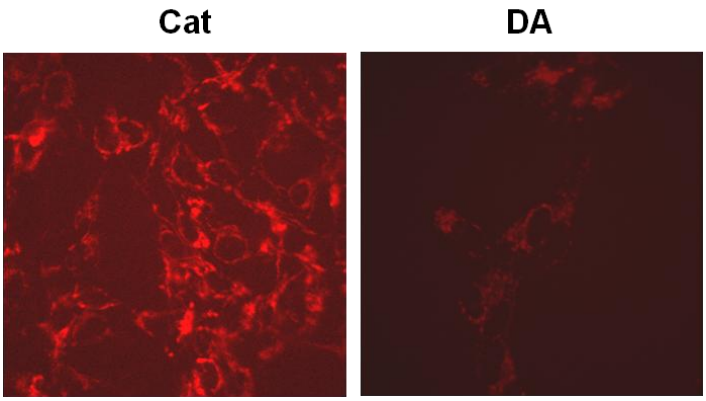

Figure 21: TMRM staining of SH-SY5Y cells treated with 700 U/ml of catalase only (Cat, left panel) or with 700 U/ml catalase + 0.25 mM dopamine (DA, right panel) for 24 h.

4.1.13 Dopamine alters calcium flux to mitochondria

VDACs mediate the flow of ions and metabolites between the cytoplasm and the mitochondrial network and regulate Ca^{2+} signaling (Celsi et al., 2009). In this respect we measured the flow of Ca^{2+} to the mitochondria in dopamine treated cells, taking into account the downregulation of VDACs. Recombinant aequorin was targeted to the mitochondria (mtAEQ) to reveal calcium flux to mitochondria and 100 nM bradykinin was used as a trigger to detect a peak in this flux (see Material and Methods, Paragraph 3.1.12).

In Figure 22 are reported different traces of calcium mitochondrial influx measurements in control conditions (black, Cat) and following 24 h dopamine treatment (red, DA). The calcium flux to mitochondria was reduced by dopamine to 75% of the basal value after 24 h as it is possible to observe in Figure 23, lower panel, where the mean and standard deviation of 14 different experiments are reported. Calcium mitochondrial influx was not influenced by 4 h dopamine exposue (Figure 23, upper panel).

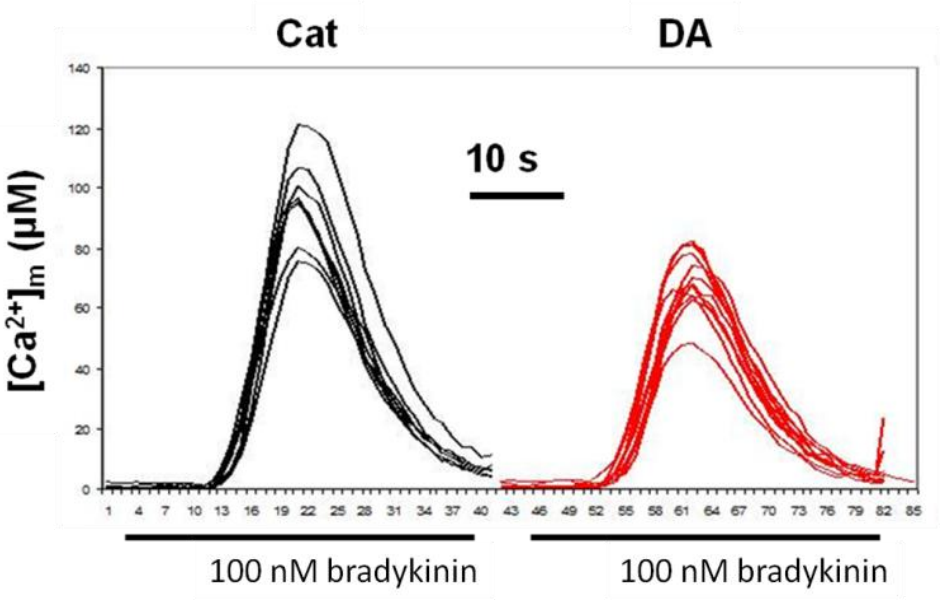

Figure 22: Effect of dopamine treatment on mitochondrial Ca^{2+} uptake. $[Ca^{2+}]_m$ measurements in SH-SY5Y cells, transfected with mitochondria-targeted aequorin, are shown. Left, black traces: different $[Ca^{2+}]_m$ measurements of control condition replicates (700 U/ml catalase, 24 h). Right, red traces: different $[Ca^{2+}]_m$ measurements of treated cells condition replicates (700 U/ml catalase + 0.25 mM dopamine for 24h). Ca^{2+} influx is stimulated by 100 nM bradykinin.

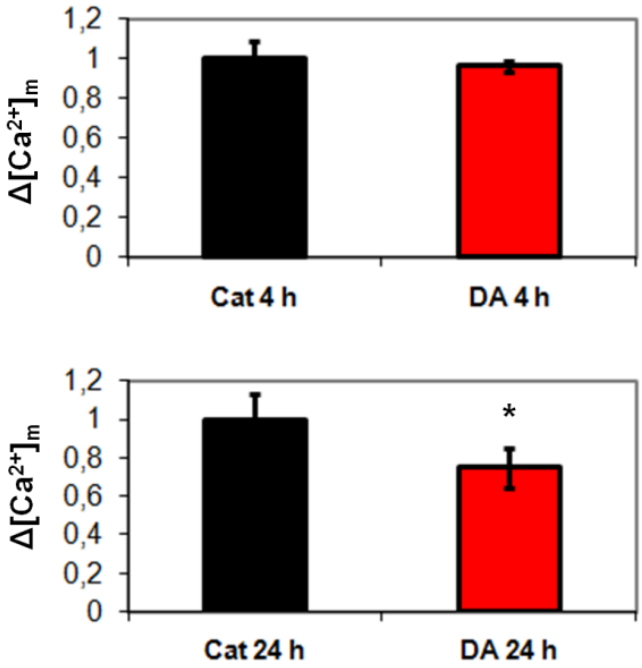

Figure 23: Effect of dopamine treatment on relative mitochondrial Ca^{2+} uptake after 4 h (upper panel) or 24 h 0.25 mM dopamine exposure (lower panel). Black bars refer to SH-SY5Y cells treated with 700 U/ml catalase only; red bars refer to SH-SY5Y cells treated with 700 U/ml catalase + 0.25 mM dopamine. Values are normalized to the reference condition (Cat 4 h and 24 h, respectively), set to 1. Bars represent the mean ± SD of 14 experiments from two independent sample preparations. *= $p < 0.01$.

4.1.14 Dopamine specifically affects the two-dimensional pattern of DJ-1

SH-SY5Y model has been further exploited to better characterize cellular responses to altered dopamine homeostasis. DJ-1 is a well documented reporter of this condition (see Introduction, Paragraph 1.5).

We chose to investigate changes in the 2-DE pattern of DJ-1 following 24 h treatment with 0.1 mM dopamine (for experimental details see Materials and Methods, Paragraph 3.1.13), a concentration that did not increase intracellular ROS levels (data not shown). Under these conditions, we observed the occurrence of 5 main spots (pI = 5.8, 6.0, 6.3, 6.6, and 6.8) progressively numbered from -2 to 2 on going from the acidic to the basic side of the pattern, with spot 0 corresponding to the central and most intense one (Figure 24, Panel A). Each spot was observed to be present in all replicates and under both experimental conditions, although the relative intensity of the most acidic (-2) and most basic (2) spot was significantly affected by dopamine treatment (Figure 24, Panels B and C). In particular, a marked reduction of spot 2 was observed, whereas spots -2, fairly visible under control conditions, and -1 were significantly enhanced. No significant differences were observed after 48 h dopamine exposure for each spot with respect to 24 h exposure. As a positive control, we treated cells with 1.0 mM H_2O_2, 15 min (see Figure 25). Upon treatment with a strong oxidizing agent a new basic form appeared, which in turn was barely detectable following dopamine treatment. Conversely, a marked increase in acidic forms was observed, in agreement with what reported in the literature (Mitsumoto and Nakagawa., 2001; Mitsumoto et al., 2001).

Three main forms are reported in the literature in the absence of a dopamine challenge. Figure 24, Panel D shows a meta-gel, *i.e.*, an average intensity projection image, wherein each pixel stores the average intensity in the 6 original images (Bandopadhyay et al., 2004; Canet-Avilés et al., 2004; Colapinto et al., 2006; Motani et al., 2008) at corresponding pixel location. The color scale of this meta-gel accounts for the occurrence frequency of each spot in the considered experiments, with less frequent spot positions in blue and more frequent spot positions in white. In the absence of dopamine challenge, the acidic spot -2 is underrepresented, thus accounting for a specific effect of dopamine.

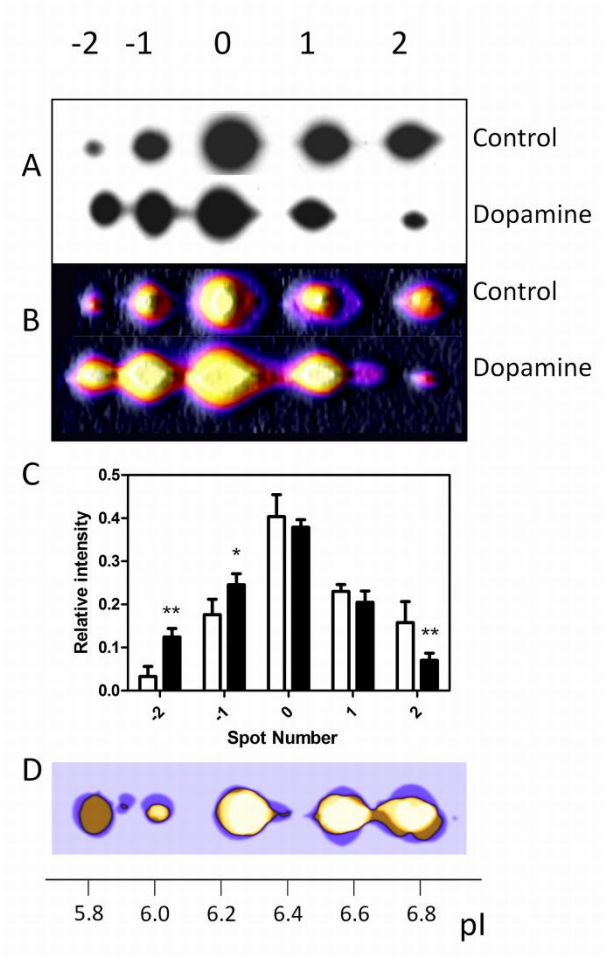

Figure 24: The two-dimensional electrophoresis pattern of DJ-1. Panel A: Representative two-dimensional anti-DJ-1 immunoblots of proteins extracted from human neuroblastoma SH-SY5Y cells. Upper row: control; middle row: 0.1 mM dopamine. All treatments were performed for 24 hours unless specified otherwise. Spots observed at pI= 5.8, 6.0, 6.3, 6. 6, and 6.8 were progressively labeled with a number from -2 to 2. Panel B: Synthetic image of average distribution of DJ-1 isoforms. Upper row: control; lower row: 0.1 mM dopamine. Panel C: Relative intensity of DJ-1 spots. Each intensity is normalized with respect to total intensity. Values are the mean ± SD of three independent experiments. White bars: control; black bars: 0.1 mM dopamine. * $p < 0.05$ vs. controls; ** $p < 0.001$ vs. controls. Panel D: meta-gel of DJ-1 isoforms in human neuroblastoma SH-SY5Y cells.

Figure 25 Oxidative modifications in the two-dimensional electrophoresis pattern of DJ-1. Representative two-dimensional anti-DJ-1 immunoblots of proteins extracted from human neuroblastoma SH-SY5Y cells. Control: fresh medium for 15 min; H_2O_2: 1.0 mM H_2O_2 in fresh medium for 15 min. Spots observed at pI= 5.8, 6.0, 6.3, 6.6, and 6.8 were progressively labeled with a number from -2 to 2.

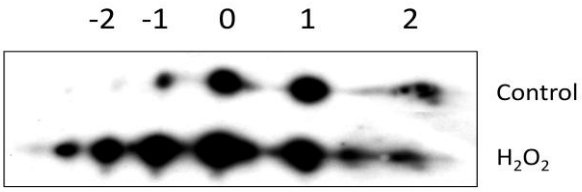

4.2 DOPAMINE RESPONSE OF DOPAMINERGIC CIRCULATING CELLS: THE JURKAT CELL MODEL

4.2.1 Jurkat cells possess a complete dopaminergic system

To investigate the nature of the dopaminergic system in Jurkat cells, we evaluated the mRNA expression of D1, D2(1) and D2(2) splicing variants, D3(a) splicing variant, D4 and D5 receptors, DAT, VMAT1 and VMAT2 transporters and TH (Figure 26, upper panel). We selectively evaluated the D3(a) level because the D3(e) splicing isoform does not bind dopamine (Missale et al., 1998). Detectable transcript levels of D1, D2(1), D3(a) and D5 receptors, as well as of DAT, VMAT1 and VMAT2 transporters, allowed us to establish the occurrence of a complete dopaminergic system in Jurkat cells. The appropriateness of primers and RT-PCR conditions was verified by checking the expression of the dopaminergic system components in the catecholaminergic human neuroblastoma SH-SY5Y cell line (Figure 26, lower panel). For further details see Material and Methods, Paragraph 3.2.2 and Table 6.

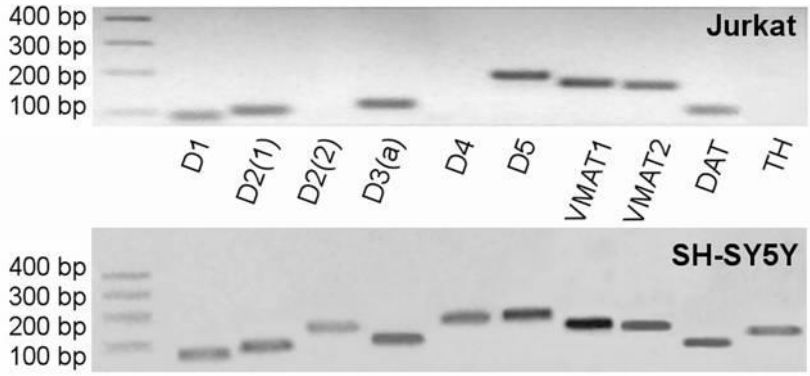

Figure 26: Expression at the transcriptional level of the dopaminergic system components in Jurkat T leukemic cells and neuroblastoma SH-SY5Y cells (as positive control). Receptors D1, D2(1) and D2(2) splicing variants, D3(a) splicing variant, D4 and D5, transporters VMAT1, VMAT2 and DAT, and TH in Jurkat cells (upper panel) and SH-SH5Y cells (lower panel) are visualized on a 2% agarose gel stained with ethidium bromide after RNA extraction, reverse transcription and PCR amplification. Results were confirmed by three independent replicates.

4.2.2 Proteomics analysis reveals quantitative changes in 7 proteins

Dopamine challenge of Jurkat cells induced quantitative changes in the protein expression pattern, as deduced by image analysis of 2-DE gels (Figure 27). A 50 μM dopamine concentration was chosen in order to stimulate all receptors and to load cells through the DAT and VMAT transporter system. On the other hand, the dopamine concentration is limited by the appearance of oxidative stress conditions associated to dopamine auto-oxidation (Alberio et al., 2010b). Cell viability was not affected by the treatment (data not shown), thus confirming that the chosen concentration was not toxic. We observed reproducible changes in the level of 7 spots (Student's *t* test) that were further analyzed by peptide mass fingerprinting. Consequently, we were able to establish that calreticulin and 14-3-3 ε were downregulated by dopamine treatment, whereas STI1, a basic isoform of β/γ actin, phosphoglycerate mutase 1, HSP60 and TCP1θ were upregulated (Table 11).

Table 11: Identification of differentially expressed proteins in Jurkat cells challenged with 50 μM dopamine. a Uniprot database; b Theoretical values; c Student's t test. FI: Fold of Induction in dopamine-treated cells vs control condition.

Spot No.	Protein	Accession No. [a]	MW [b] kDa	pI [b]	FI	p [c]	Seq. cov. (%)	Mowse score
1	Calreticulin	P27797	47.9	4.29	2.72 ↓	0.02	30	83
2	14-3-3 ε	P62258	29.2	4.63	2.30 ↓	0.05	34	74
3	STI1	P31948	62.6	6.40	1.78 ↑	0.05	34	119
4	β/γ Actin	P60709	41.7	5.29	1.92 ↑	0.03	38	86
5	Phosphoglycerate mutase 1	P18669	28.7	6.75	1.65 ↑	0.02	46	131
6	HSP60	P10809	58.0	5.24	1.47 ↑	0.01	24	62
7	TCP1θ	P50990	59.5	5.42	1.63 ↑	0.01	18	98

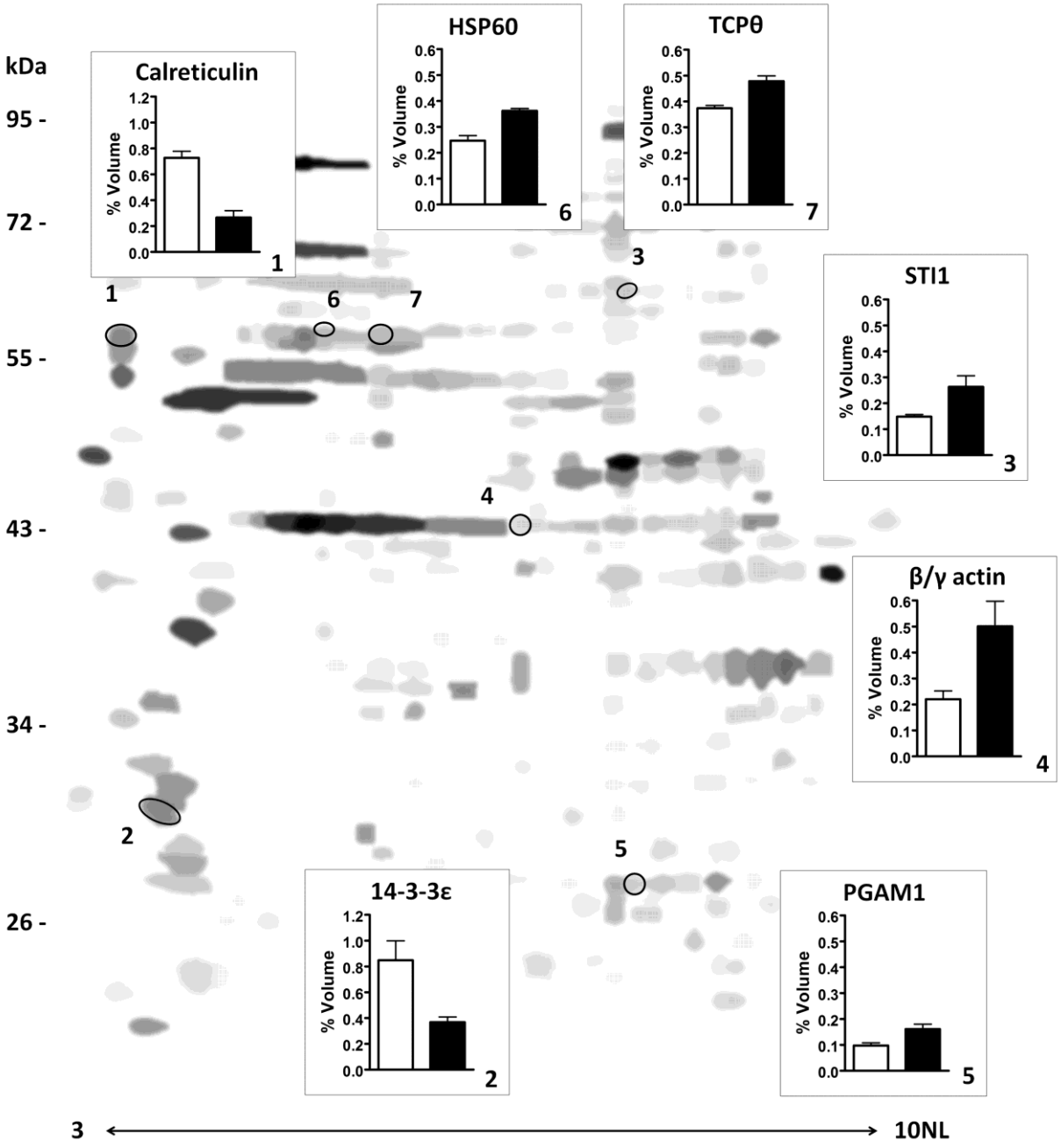

Figure 27: Representative spots in a synthetic two-dimensional gel of proteins extracted from whole Jurkat cells. The synthetic gel is obtained from Coomassie stained gels (three replicates per experimental condition) by averaging the normalized volumes of spots present in all considered gels. Greyscale refers to mean spot volumes. Spots which display a significant change in intensity after dopamine challenge (50 μM, 24 h) are numbered. Insets report the mean percent spot volumes ± SE in three different gels. Open bars: control cells; filled bars: dopamine treated cells. For protein identifications see Table 11. For further details and experimental conditions see Material and Methods, Paragraph 3.2.3 and 3.2.4.

4.2.3 Network enrichment procedure underlines the importance of a chaperone proteins network

In order to build a comprehensive model to encompass the experimentally identified proteins, we analyzed the entire list in terms of both interaction network and GO classification enrichment using PPI spider (Antonov et al., 2009) (see Materials and Methods, Paragraph 3.2.5).

A significant (p<0.05) enriched network for proteins altered by the dopamine challenge is reported in Figure 28. A significant functional association to Gene Ontology (GO) class "unfolded protein binding" (GO:0051082) was obtained for this network.

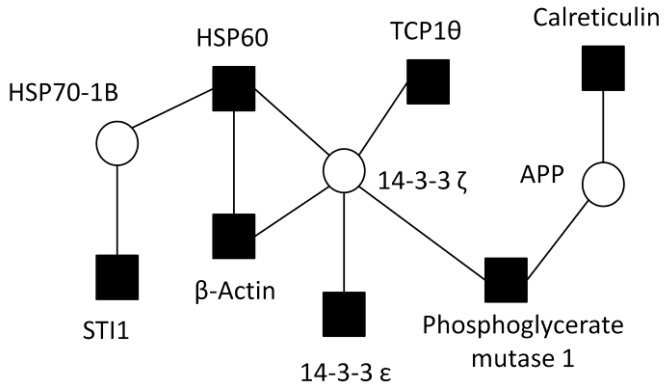

Figure 28: Protein-protein interaction network enrichment. Filled squares refer to experimentally identified proteins, whereas empty circles indicate enriched proteins (common interactors). The network enrichment procedure was performed using PPIspider as described in Paragraph 3.2.5, $p < 0.05$.

4.2.4 Dopamine modifies the two-dimensional pattern of β-actin and 14-3-3

The observation of a significant change in a basic isoform of β/γ actin (see Paragraph 4.2.2) appeared quite unusual. Therefore, we proceeded to validate the finding by two-dimensional Western blotting. Actually, dopamine treatment markedly affected the 2-DE pattern of β/γ actin with a shift towards basic forms (Figure 29, panel A).

Two members of the 14-3-3 chaperone family seemed to be affected by dopamine treatment: 2-DE analysis revealed the upregulation of 14-3-3 ε (Figure 27), whereas the network enrichment procedure assigned a central role to 14-3-3 ζ (Figure 28). To confirm both findings, we performed two-dimensional Western blotting using an antibody that recognizes all 14-3-3 isoforms (Figure 29, Panel B). Dopamine treatment induced a global change in isoform distribution. Images were acquired using two different exposure times, in order to discriminate differences in both low- and high-abundance species. By saturating the main component, we were able to observe the downregulation of minor spots following dopamine treatment (Figure 29, Panel B, left). By lowering the exposure time, on the other hand, the most abundant isoforms appeared as four resolved spots. In this pattern, dopamine downregulated the most acidic spot and upregulated the most basic one (Figure 29, Panel B, right).

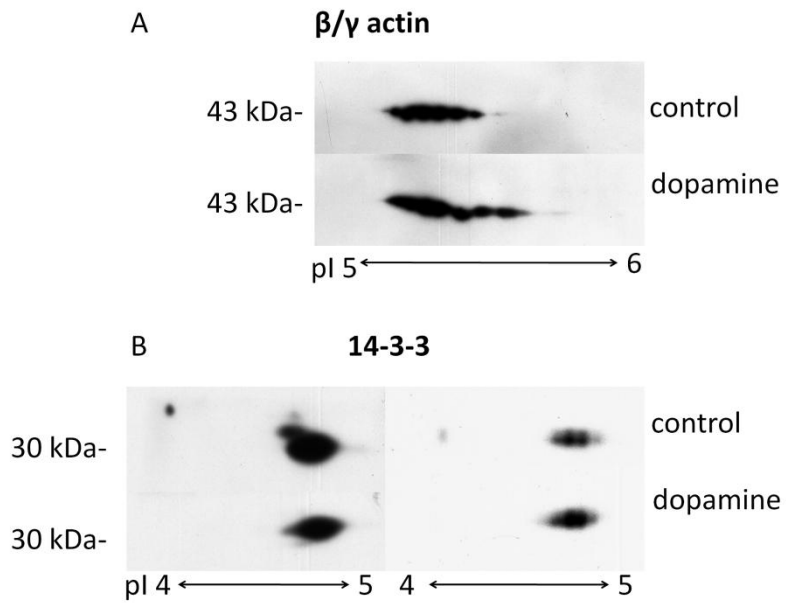

Figure 29: Two-dimensional Western blot analysis of β-actin and 14-3-3 isoform patterns. Panel A: alteration of the β-actin pattern in control (upper row) and dopamine-treated cells (50 μM, 24 h, lower row). Panel B: alteration of the 14-3-3 pattern in control (upper row) and dopamine-treated cells (lower row) at different exposure times (left: 20 sec; right: 5 sec). Results were confirmed by three independent replicates. For further details and experimental conditions see Paragraph 3.2.6.

5. DISCUSSION

Clinical research takes advantage of basic neurobiology research mainly when dealing with two aspects: the characterization of biochemical mechanisms at the ground of the disease onset and progression, and the identification of biomarkers, which in turn could help in following the clinical response to new therapeutic agents. These two aspects, that define the framework of the present thesis, are actually two sides of the same extent to improve the clinical approach to the disease and to give to basic research a translational meaning (Alberio et al., 2010a, 2010b). The ways of dealing with this important challenge are substantially two: a targeted approach or a widespread approach. Of course, in the first case valid hypotheses raising from other studies need to be available and the new goal is that of validating them or giving a deeper molecular characterization of the phenomenon (hypothesis-driven method). The second is, on the contrary, an hypothesis-generating method, descriptive at the very beginning to become mechanistic in the foreground, to functionally characterize the observations made in the first part.

The case of Parkinson's disease is a clear example of the advantages of an unbiased, hypothesis-generating approach. PD is a progressive neurological disorder whose causes are unknown, but considerable evidence suggests a multifactorial etiology involving genetic and environmental factors. Moreover, pathogenesis has not yet been clarified even if many aspects, such as oxidative stress, mitochondrial dysfunction, excitotoxicity, glia hyperactivation and apoptosis, have been investigated in the last decades. Understanding the mechanisms at the basis of neurodegeneration in PD would then request an *a priori* speculation on probable causes and pathological cascades that follow. To bypass this initial bias the emerging field of neuroproteomics promises to provide powerful strategies to further characterize neuronal dysfunction and cell loss associated with neurodegenerative diseases (Becker et al., 2006). Several papers have been published in the last years on the pathogenetic mechanisms of neurodegenerative disorders, with a focus on Alzheimer's disease (AD) (Sheta et al., 2006) and Parkinson's disease (PD) (see Fasano et al., 2007 and Robinson, 2010).

Proteomics is a powerful methodology to investigate how protein expression is affected in the pathogenesis and is a technology-driven approach that takes advantage from unprecedented advances in separation techniques such as two-dimensional electrophoresis and liquid chromatography, in the design and exploitation of high-sensitivity sources and analyzers for mass spectrometry, and in bioinformatics. These advances have allowed the quantitative analysis of protein levels and post-translational modifications that altogether help to understand molecular alterations in cells, tissues and biofluids that are associated to disease

etiology, progression, outcome, and response to therapy. On the other hand, proteomics provides a high-throughput methodology for the search of new therapeutic targets.
As a whole, the proteomic methods are a valuable toolbox for either the analysis of pathogenetic mechanisms in neurodegenerative disorders and (cell and animal) models thereof, or the search for suitable biomarkers that should be useful for early and differential diagnosis as well as for therapy assessment.

A SH-SY5Y MODEL TO INVESTIGATE PD PATHOGENETIC MECHANISMS

A common issue in proteomic investigations of PD models is the choice of the best suited model system to be used in the study. *In vitro* models represent the more controlled environment systems for proteomic analysis, but may lack the cellular microenvironment critical to disease development, and the cell type chosen may not express the particular protection systems expressed in cells such as dopaminergic cells. Similar to established cell lines, primary cells must adapt to grow in culture conditions, which will be reflected by continuous changes in the cellular proteome. The longer they are in culture, the more the proteome is likely to change. The use of inducible pluripotent stem cells derived from inherited and sporadic patients may be particularly useful to look for evidence of subtle background genetic influences on disease development.
By contrast, animal models offer a microenvironment more akin to that of humans, although differences in brain structures and methods used to induce parkinsonism constitute an important limit. Though, they can be very useful for answering specific questions, such as changes to the expression of proteins that specifically affect dopaminergic neurons or cause some of the phenotypic changes observed in PD. Combining these limitations with the potential absence of other key environmental factors make the creation of an accurate model of disease difficult to develop. Consequently, the model used to address a particular question always needs to be considered carefully. The analysis of human tissue may be useful, but also has limitations. Difficulties in the acquisition of a suitable number of autoptic specimens from PD affected individuals strongly limited proteome analysis of human brain areas of PD patients. Moreover, human tissue samples are heterogeneous from patient to patient, which increases the difficulty of identifying changes in protein expression for a specific disease state. Another important point is that patient tissue samples often can provide information at the terminal stage of a disease, owing to the difficulty in collecting tissues undergoing disease

development.

Taking into account all these difficulties, we chose to use the catecholaminergic SH-SY5Y human neuroblastoma cell line to address a specific pathogenetic mechanism related to altered dopamine homeostasis, being aware that we could simply mimic a particular aspect of a complicated, multifactorial disease, such as PD. SH-SY5Y cells express the DA transporter (DAT) and DA receptors and are able to form storage vesicles, although the low activity of the vesicular monoamine transporter type 2 impairs DA storage into vesicles. For this reason, SH-SY5Y cytoplasmic DA concentration may be increased by administering DA in the culture medium (Gomez-Santos et al., 2003, Fasano et al., 2008a). The optimal concentration of dopamine to be used in this study was determined by MTT assay (see Results, Figure 6) Following 0.25 mM dopamine exposure, both β-gal and α-syn cells displayed about 70±5% viability. Since the percentage of viable cells was still acceptable to conduct the proteomic analysis and the toxicity was almost identical for the two cell lines, the concentration chosen for all further experiments was 0.25 mM. Cells were always exposed to dopamine in the presence of 700 U/ml catalase to eliminate aspecific effects due to H_2O_2 arising from dopamine auto-oxidation (Blum et al., 2000).

Additionally, SH-SY5Y cells were stably transformed to enhance expression of wild-type α-synuclein. Unlike transient expression reported in the literature that leads to protein aggregation and increased susceptibility to DA toxicity, stable (*i.e.*, at sub-toxic level) expression of wild-type α-synuclein avoid problems linked to an excessive expression that inevitably leads to fibrillation and cell death (Colapinto et al., 2006). As a control, we used SH-SY5Y cells stably transfected with the plasmid containing β-galactosidase cDNA (β-gal). We intentionally did not clone the cell lines to avoid working with only few clones and raising the possibility to study cells different from those originally selected. Because it is known from literature that dopamine upregulates α-synuclein expression (Gomez-Santos et al., 2003), we measured the level of α-synuclein in α-syn cells with respect to β-gal cells after dopamine exposure. Interestingly, dopamine treatment significantly increased the expression of α-synuclein in β-gal control cells but not in α-syn cells that already overexpress it owing to transfection (see Results, Figure 7). If a small increase in α-synuclein levels is protective, a further induction in α-syn cells is not necessary following dopamine treatment.

Proteomic investigations were conducted on β-gal and α-syn cells treated or not with dopamine, giving rise to four experimental conditions. Through the comparison of treated and non-treated cells it is possible to unravel the dopamine toxicity effect on the proteome; by

comparing β-gal and α-syn cells it is possible to appreciate the effect of α-synuclein overexpression, while taking into account all the different conditions at the same time permits to reveal proteins whose levels are modified by the combination of the two factors. Statistical analysis (by two-way ANOVA) of silver-stained gel images revealed 28 spots whose intensity was significantly different in at least one of the four groups considered (see Results, Figure 8).

Proteins differentially expressed in this model are individually linked to PD

Most of the identified proteins may be linked to different pathogenetic mechanisms in PD, either specific or associated to generic stress conditions. Upregulation of peroxyredoxin 1 is in keeping with increased ROS production by dopamine oxidation that activates apoptosis and together induces the synthesis of antioxidant (Lev et al., 2009) and anti-apoptotic factors (Mattson, 2000). Higher glycolytic activity is shown by higher aldolase A, enolase 1 and pyruvate kinase levels together with lower parathymosin level (Brand and Heinickel, 1991). It should be noticed, however, that quantitative alterations of glycolytic enzymes are frequently observed following a generic stress event (Petrak et al., 2008). Two groups of spots showing remarkable changes in the isoform pattern in the four conditions were easily assigned to glyceraldehyde-3-phosphate dehydrogenase and to mitochondrial ATP synthase alpha subunit by comparison with 2-DE maps available in the SWISS 2D-PAGE database. Variations of ATP synthase A and GAPDH isoforms, but not in their total level, could reflect a proteome adaptation as a response to perturbation of protein levels caused by stimuli of different origin (Mao et al., 2007). In parallel, proteins involved in protein synthesis, *i.e.*, eIF5A, RPLP2 and its mitochondrial paralog L7/L12, were less abundant, suggesting attenuated translation at both cytoplasmic and mitochondrial level under cellular stress conditions (Shenton et al., 2006). Proteins involved in cytoskeleton structure and regulation were found in both groups (proteins whose level change on account of dopamine treatment or of α-synuclein overexpression). Cytoskeleton dysregulation was suggested to be an early event in PD pathogenesis, as alterations in either cytoskeleton components or regulatory proteins were reported in a fruitfly model expressing mutant α-synuclein in the early postnatal days (Xun et al., 2007). Dopamine induced an increase of fascin 1, a regulator of the organization of filamentous actin into bundles (Tseng et al., 2005). Comparison with 2-DE image databases assigned this spot to the phosphorylated, inactive form of fascin 1 (Aratyn et al., 2007). Dopamine also induced changes of two calcium-dependent phospholipid-binding, actin-

associated proteins, namely annexin A2 and annexin A5, both acting on regulation of membrane dynamics, cell migration, proliferation and apoptosis (Monastyrskaya et al., 2009), and contributing to the regulation of neural development (Naciff et al., 1996). Profilin 1, another regulator of the actin cytoskeleton that is necessary for neuronal differentiation and synaptic plasticity (Birbach, 2008), is upregulated in α-syn cells. Also in this case, comparison of the experimental maps with those available in 2-DE image databases indicates that the spot relative to profilin 1 corresponds to the phosphorylated protein, showing increased affinity for G-actin with a consequent destabilization of the actin cytoskeleton (Sathish et al., 2004). It has been recently reported that α-synuclein binds actin, slowing down its polymerization and accelerating its depolymerization, thus suggesting a role of α-synuclein in actin dynamics (Sousa et al., 2009). Moreover, we observed decreased levels of (dephosphorylated) stathmin 1 in α-syn cells. This protein destabilizes microtubules, thus accounting for their dynamics, and regulates cell cycle progression by acting on the mitotic spindle (Andersen, 2000). In this context, increased levels of lamin A/C both after dopamine treatment and α-synuclein overexpression can be signs of a more complex regulation possibly involving physical contacts between the nuclear structure and cytoskeletal proteins (Broers et al., 2006). Lamin levels could also change in response to oxidative stress conditions as lamin A/C is more phosphorylated and forms a complex with molecular chaperone HSP90 in 6-hydroxydopamine-treated SH-SY5Y cells (Nakamura et al., 2009).

Besides cytoskeleton-related proteins, an increase of GSTπ was observed in α-syn cells. GSTπ polymorphism is associated with PD both in humans after pesticide exposure (Menegon et al., 1998) and in a *Drosophila* model expressing mutant parkin (Whitworth et al., 2005). GSTπ expression is responsible for nigral neuron sensitivity in an experimental model of PD (Smeyne et al., 2007) and quantitative changes in GSTπ levels were observed in SNpc specimens of PD patients by proteome analysis (Werner et al., 2008).

Alterations in mitochondrial proteins, on the other hand, are specifically linked to one of the major pathogenetic mechanisms of PD (Henchcliffe and Beal, 2008) and our proteomic analysis showed that mitochondrial activity is affected. Mitofilin plays a fundamental role in the maintenance of mitochondrial cristae structure (John et al., 2005), and is covalently modified by dopamine oxidation products (Van Laar et al., 2009). Mitofilin interacts with PINK1 (PTEN-induced putative kinase 1) (Weihofen et al., 2009), an ubiquitous kinase associated to a familial, early-onset PD form (Valente et al., 2004). Mitochondrial p32 (*i.e.*, C1q binding protein) was overexpressed in α-syn cells. Although this protein is primarily

localized in mitochondria, it also localizes at the cell surface and in the nucleus where it acts as a multifunctional chaperone for several ligands (Bialucha et al., 2007).

Another cellular process coming out from our proteomic analysis was the control of Wnt/β-catenin pathway, associated to neurite outgrowth and synaptic plasticity (Endo and Rubin, 2007). In the absence of a Wnt signal, β-catenin is targeted to degradation by phosphorylation by glycogen synthase kinase-3β (GSK-3β), a multifunctional kinase involved in various neuronal functions (Takashima, 2009). Following a Wnt signal, β-catenin is imported into the nucleus through RanGTP-dependent transport and activates the transcription of target genes by recruiting other factors such as the histone acetyltransferase RuvB-like 1 (Tip49/pontin). Levels of the RAN binding protein 1 were reduced in α-syn cells with respect to β-gal cells, regardless of dopamine treatment, and RuvB-like 1 is upregulated in α-syn cells in the absence of dopamine, thus suggesting a potential role of the Wnt/β-catenin pathway. Noticeably, the anti-apoptotic action of parkin in dopaminergic neurons has been associated to the regulation of excessive Wnt/β-catenin signalling by blocking Wnt/β-catenin-induced cell cycle re-entry and apoptosis, two events that are deregulated in PD (Rawal et al., 2009). CRMP4 (collapsin response mediator protein 4), observed here to be significantly reduced in α-syn cells, is a member of a family of neuron-enriched proteins that regulate neurite outgrowth and growth cone dynamics. Interestingly, CRMP4 is also a substrate of GSK-3β (Cole et al., 2006).

The more evident qualitative change observed after dopamine treatment both in β-gal and α-syn cells was the complete disappearance of one spot (see Results, Figure 15), corresponding to the protein VDAC-2, a porin of the outer mitochondrial membrane that regulates mitochondrial Ca^{2+} homeostasis, thus controlling mitochondrial-dependent cell death (Celsi et al., 2009). This reduction, already associated to dopamine-induced apoptosis (Premkumar and Simantov, 2002), could affect the outer membrane electrochemical potential with consequent impairment of mitochondrial function and calcium homeostasis, major pathogenetic mechanisms of neurodegeneration in PD (Celsi et al., 2009; Chan et al., 2009).

A focus on Voltage-dependent anion channels role

Because of the great importance of mitochondrial dysfunction in PD pathogenesis, we further investigated dopamine-induced VDAC2 downregulation, also considering VDAC1 and VDAC3, to get more insight on their correlation with dopamine altered levels and on their role in leading mitochondrial impairment. Since VDAC2 expression was not influenced by α-

synuclein overexpression, we performed this focused investigation on SH-SY5Y wild type cells.

First of all, we confirmed that VDAC2 completely disappeared after 24 hours dopamine treatment (0.25 mM) and observed that also VDAC1 and VDAC3 had a similar behavior (see Results, Figure 16). Since all VDACs were downregulated, we verified that no change in mitochondria number occurred. The level of other mitochondrial proteins (grp75, HSP60; see Results, Figure 19), was not affected by dopamine treatment, thus confirming that the effect observed was specific for these proteins. However, even if the number of organelles remained the same, mitochondria displayed loss of the membrane potential in dopamine-treated cells (see Results, Figure 21). In our model, dopamine accumulation in the cytosol and its oxidation generates oxidative stress, ROS production and complex I impairment (inhibited by dopamine-quinone), thus accounting for the decreased mitochondrial membrane potential. It is well established that mitochondria have a pivotal role in the apoptotic cell death pathway; when the outer mitochondrial membrane is rendered permeable by the action of 'death agonists', such as Bax, cytochrome c is released into the cytosol, leading to caspase activation and apoptosis. Similar pathways are also activated by opening of the mitochondrial permeability transition pore, an event that can occur under conditions of oxidative stress or electron transport chain inhibition, leading to collapse of the mitochondrial membrane potential (Henchcliffe and Beal, 2008). VDACs have been implicated as essential mediators of mitochondrial-dependent cell death by functioning as a channel-forming unit within the mitochondrial permeability transition (MPT) pore and targets of Bcl-2 family members; nevertheless, mitochondria from VDAC1-, VDAC3-, and VDAC1/VDAC3-null mice exhibited a Ca^{2+} and oxidative stress-induced MPT that was indistinguishable from wild type mitochondria. Similarly, Ca^{2+} and oxidative-stress-induced MPT and cell death was unaltered or even exacerbated in fibroblasts lacking VDAC1, VDAC2, VDAC3, VDAC1/3, and VDAC1/2/3. Wild type and VDAC-deficient mitochondria and cells also exhibited equivalent cytochrome c release, caspase cleavage, and cell death in response to Bax and Bid activation. These results indicate that VDACs are dispensable for both MPT and Bcl-2 family member-driven cell death (Baines et al., 2007). This is in agreement with our observation that dopamine-treated cells underwent apoptosis (see Results, Figure 10), despite of VDACs downregulation.

To better characterize time-dependent changes of VDACs levels, we performed a time-course evaluation of VDACs by Western blotting after 4, 7, 12 and 24 h dopamine exposure.

VDAC2 downregulation appears more gradual than that of VDAC1, which in turn occurs later and to a lesser extent. Due to the low expression level of VDAC3 compared to VDAC1 and VDAC2 and considering the low specificity/sensitivity of anti-VDAC3 antibody used, the time course analysis of VDAC3 response to dopamine treatment did not give reproducible results. It is worth to note that VDAC2 level increases in control cells as a time-depending effect. One possible explanation of this observation, supported by ongoing experiments, is that VDAC2 upregulation could be associated to activation of autophagy as a response to a decrease of nutrients in cell culture.

VDACs mediate the flow of ions and metabolites between the cytoplasm and the mitochondrial network and regulate Ca^{2+} signaling (Celsi et al., 2009). In this respect, we measured mitochondrial Ca^{2+} influx in dopamine-treated cells. The calcium flux to mitochondria is reduced to 75% of the basal value after 24 h dopamine exposure, probably mirroring VDACs downregulation. Accordingly, after 4 h dopamine exposure there is no difference in Ca^{2+} flux between controls and dopamine-treated cells, in agreement with the observation that VDACs are not considerably downregulated, (see Results, Figures 22 and 23).

To take into account possible post-translational modifications of VDAC2 that would in some way target the protein to degradation, we performed a two-dimensional Western blotting. Indeed, in one-dimensional Western blotting of VDAC2 we observed a high standard deviation in SH-SY5Y cells after 4 h dopamine treatment; thus, the occurrence of a diffuse band prompted us to hypothesize the presence of different forms migrating at similar molecular weight and immunoreactive to the anti-VDAC2 antibody. Immunoblots were performed after 4 and 7 h, VDAC2 becoming undetactable after 7 hours of dopamine treatment. VDAC2 migrates at pI ≈ 8, as expected (theoretical pI= 7.66), but after 4 h dopamine exposure a more acidic VDAC2 form becomes prevalent, with a pI ≈ 7. When present in controls, the acidic form was always a spot with a lower intensity than the main form at pH 8. After 7 h, the more acidic form becomes appreciable in controls too, although the main form still remains the one at pH ≈ 8. In dopamine-treated cells, on the other hand, VDAC2 is strongly downregulated and the only form being observed here is the acidic one. Remarkably, the more acidic form has been reported to be the phosphorylated form (Sarioglu et al., 2008). In the same paper, Sarioglu and coworkers demonstrate that treatment of 5L cell line with 2,3,7,8-tetrachlorodibenzo-*p*-dioxin (TCDD) causes an upregulation of VDAC2 total level, thus downregulating the phosphorylated form. This observation prompted us to

correlate the appearance of VDAC2 phosphorylated form with its disposal process. Additionally, we examined the X-ray structure of VDAC1 (PDB code 2K4T; Hiller et al., 2008) and annotated on the structure all the putative phosphorylation sites (Distler et al., 2006; Pastorino et al., 2005) by multiple sequence alignment (Figure 30). Thr51 is a conserved residue in all VDACs, and it was reported to be phosphorylated by GSK3β (Das et al., 2008). As already discussed, GSK3β involvement is also suggested by the results of the proteomic analysis and the hyper-activation of this kinase has already been related to neurodegeneration, being involved in Tau phosphorylation (Hernández et al., 2009).

To characterize the possible involvement of GSK3β in phosphorylating VDAC2 in our model, we used the specific GSK3β inhibitor TDZD-8. Preliminary data on VDAC2 phosphorylation by GSK3β show that dopamine enhances VDAC2 phosphorylation by GSK3β. Nonetheless, this finding does not appear to be a key event for VDAC2 disposal, as dopamine-induced VDAC2 downregulation was not blocked by GSK3β inhibition (data not shown). Further experiments are needed to confirm these data, to understand the role of GSK3β in our model of dopamine toxicity and to verify GSK3β role in influencing VDAC2 function.

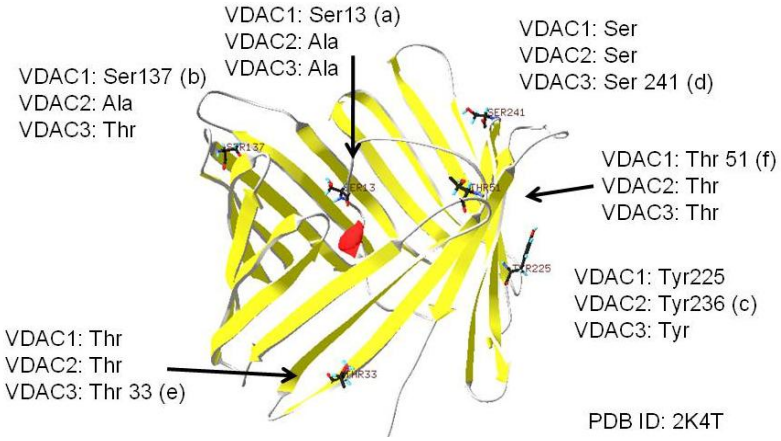

Figure 30: The structural model of VDACs shows their structure and putative phosphorylation sites, obtained by multiple sequence alignment of the three VDACs sequences.

a) CaMKII e GSK3 consensus (Distler et al., 2006)
b) PKC consensus (Distler et al. , 2006)
c) VDAC2 phosphorylated by INSR (Distler et al. , 2006)
d) VDAC3 phosphorylated by CKI e PKA (Distler et al. , 2006)
e) VDAC3 phosphorylated by PKC (Distler et al. , 2006)
f) VDACs phosphorylated by PKC (Pastorino et al. , 2005)

A recent paper suggests that VDAC1 is ubiquitinylated through Lys27-linked chains, following mitochondrial membrane depolarization. The authors also show that silencing of endogenous VDAC1 by siRNA disrupts the redistribution of Parkin to damaged mitochondria and prevents mitochondrial clearance. Both effects could be restored by re-transfection with wild type VDAC1, indicating that the mitochondrial substrate VDAC1 is required for proper PINK1/parkin-directed mitophagy (Figure 31) (Geisler et al., 2010; Wild and Dikic., 2010). This latter result points to an important role for VDAC1 in the formation of this trimeric complex, in addition to being a parkin substrate.

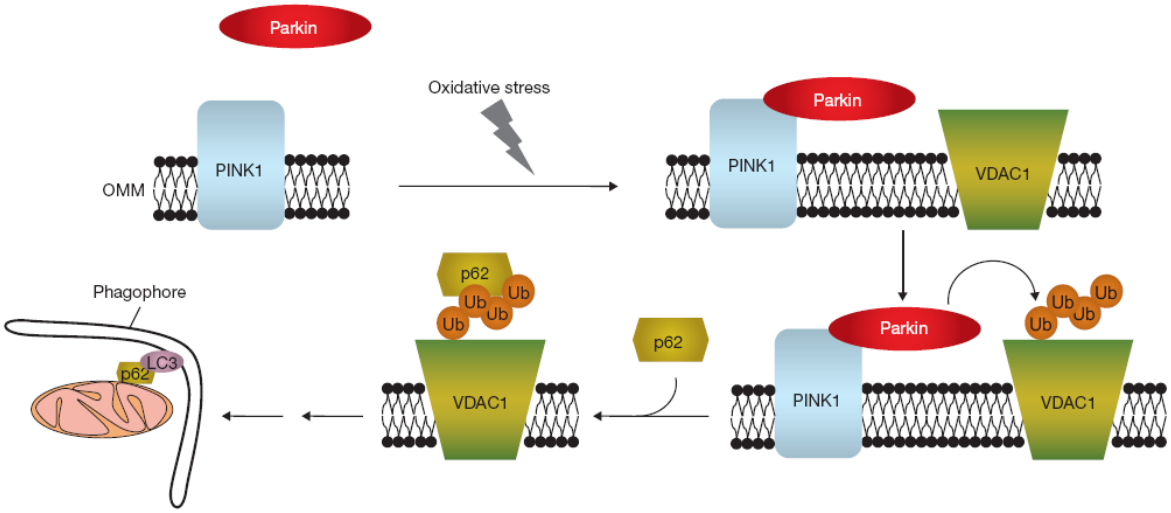

Figure 31: Model of PINK1/parkin-mediated mitophagy. In the absence of mitochondrial damage, E3 ligase parkin is diffusely distributed throughout the cytosol. Upon mitochondrial membrane depolarization, PINK1, a kinase of the outer mitochondrial membrane (OMM), induces parkin translocation to stressed mitochondria. Subsequently, parkin mediates the formation of Lys27-linked ubiquitin (Ub) chains on VDAC1. This leads to the recruitment of the autophagy receptor p62, which in turn, by binding to LC3, directs damaged mitochondria into forming autophagosomes (phagophore). Disruption of this sequential process at distinct steps may contribute to the development of PD due to accumulation of dysfunctional mitochondria and a concomitant increased cellular toxicity. Taken from Wild and Dikic, 2010.

Conequently, dopamine could impair proper mitophagy in our model by downregulating VDACs. We could therefore hypothesize that the activation of autophagy described above (as a consequence of mitochondrial depolarization induced by dopamine) does not end up with

the expected removal of damaged mitochondria owing to the lack of VDAC1. The simultaneous downregulation of VDACs could be responsible of this misregulation and thus cause mitochondrial impairment and consequent neuronal cell death. It is worth to notice, however, that the role of VDAC1 in mitophagy has been very recently debated, as Narendra and coworkers found that VDAC1 and VDAC3 are dispensable for the recruitment of p62, mitochondrial clustering and mitophagy (Narendra et al., 2010). For this reason, we are further evaluating autophagy in our experimental conditions and the possible role of VDACs in influencing this mechanism, also considering the role played by α-synuclein overall. Actually, it has been recently described how α-synuclein overexpression induces mitochondrial fragmentation that is rescued by coexpression of PINK1, parkin or DJ-1 (Kamp et al., 2010).

A focus on the pool of DJ-1 different species

The analysis of the literature on dopamine toxicity in SNpc neurons, together with our findings on altered mitophagy in dopamine-treated SH-SY5Y cells described above, drew our attention to DJ-1, the subject of another targeted study. This protein has multiple functions, but its most relevant function seems to be to protect cells from oxidative-stress-related death (Uversky and Eliezer, 2009). This function is of primary importance in cells with high demand of energy and a strong ROS production, like dopaminergic SNpc neurons. On the ground of these considerations we evaluated DJ-1 forms specifically responding to a dopamine stimulus. Indeed, under condition of oxidative stress, DJ-1 relocalizes from the nucleus to the mitochondrial matrix and intermembrane space and is thought to be neuroprotective under such conditions (Zhang et al., 2005). Multiple DJ-1 forms are simultaneously present, so that DJ-1 can be better considered as a pool of different species, with different modifications and in different amounts. Likely, the composition of this pool and the precise balance between different forms is the main factor determining DJ-1 global activity. Alterations of this pool, instead of DJ-1 mutations, are expected to play a role in non-genetic conditions correlated to DJ-1 activity, including idiopathic PD. Indeed, since many different DJ-1 forms can be separated on the basis of their pI, it is a common finding that DJ-1 oxidation, correlated to ageing, PD and Alzheimer's diseases (AD), produces an increase in DJ-1 species of acidic pH, and a decrease in basic species, so that these conditions are characterized by a pool of DJ-1 forms different than that observed in controls. Up to 10 different DJ-1 forms, including the acidic forms (pI 5.5 and 5.7) of DJ-1 monomer and the

basic forms (pI 8.0 and 8.4) of SDS-resistant DJ-1 dimer, were reported to selectively accumulate in PD and AD frontal cortex tissues compared with age-matched controls (see Alberio et al., 2010a).

While two-dimensional electrophoresis (2-DE) is able to separate modified DJ-1 forms on the basis of pI changes, there is little experimental evaluation of DJ-1 modifications to completely describe the pool of DJ-1 possible forms and to evaluate the pool composition in a given condition (Natale et al., 2010). By performing a meta-analysis of DJ-1 in heterogeneous two-dimensional electrophoresis experiments we observed changes in this pattern that are specifically related to neurodegenerative processes and aging (Natale et al., 2010). The meta-analysis of proteomic data can provide valuable information pertinent to various biological processes (or methods involved) that otherwise remains hidden if a single paper is considered. The occurrence of frequently-identified proteins, for instance, may represent common cellular stress responses or simply reflect technical limitations of 2-DE, as recently stated by Petrak and coworkers in their paper on déjà-vu in proteomics reports (Petrak et al., 2008). However, there is such a variability in the 2-DE pattern that it usually prevents the association of each isoform to a specific pathological or experimental condition. To this purpose, we analyzed the 2-DE pattern of DJ-1 in the SH-SY5Y catecholaminergic cell line following a dopamine challenge to understand whether specific and reproducible modifications of the DJ-1 isoform distribution could be associated to altered dopamine homeostasis.

Based on the background we got from dopamine exposure of SH-SY5Y cells that has been discussed in previous sections, we chose to investigate changes in the 2-DE pattern of DJ-1 following 24 h treatment with a dopamine concentration (0.1 mM) that did not increase intracellular ROS levels, preventively measured using the fluorogenic probe 2'-7'-dichlorodihydrofluorescein diacetate (data not shown). Actually, we wanted to observe an effect specifically due to dopamine rather than a generic response to an oxidative challenge. Under these conditions, we observed the occurrence of 5 main spots (pI = 5.8, 6.0, 6.3, 6.6, and 6.8) progressively numbered from -2 to 2 on going from the acidic to the basic side of the pattern, with spot 0 corresponding to the central and most intense one (see Results, Figure 24). Each spot was observed to be present in all replicates and under both experimental conditions, although the relative intensity of the most acidic (-2) and most basic (2) spot was significantly affected by dopamine treatment (see Results, Figure 24). In particular, a marked reduction of spot 2 was observed, whereas spots -2, fairly visible under control conditions, and -1 were significantly enhanced. No significant differences were observed after 48 h

dopamine exposure for each spot with respect to 24 h exposure. As a positive control, we treated cells with 1.0 mM H_2O_2, 15 min. Upon treatment with a strong oxidizing agent a new basic form appeared, which in turn was barely detectable following dopamine treatment. Conversely, a marked increase in acidic forms was observed, in agreement with what reported in the literature (Mitsumoto and Nakagawa., 2001; Mitsumoto et al., 2001). Three main forms are reported in the literature in the absence of a dopamine challenge. We were able to evaluate the frequency and the intensity of each form thanks to the creation of a meta-gel, *i.e.*, an average intensity projection image wherein each pixel stores the average intensity in the 6 original images at corresponding pixel location (Bandopadhyay et al., 2004; Canet-Avilés et al., 2004; Colapinto et al., 2006; Motani et al., 2008). In the absence of dopamine challenge, the acidic spot -2 is underrepresented, thus accounting for a specific effect of dopamine in the observed increase. Unlike early experiments showing a comprehensive shift of every isoform (Bandopadhyay et al., 2004; Mitsumoto and Nakagawa., 2001; Mitsumoto et al., 2001), we describe here specific and significant increase of acidic spots (-2 and -1) together with decrease of the most basic (2) spot in the 2-DE pattern of DJ-1 upon dopamine treatment.

Increase in DJ-1 expression may be induced by ROS, and DJ-1 overexpression specifically protects against dopamine toxicity (Lev et al., 2008; Lev et al., 2009); more specifically, a compensatory upregulation of DJ-1 and parkin has been reported in a A53T α-synuclein mouse model treated with the mitochondrial toxin rotenone (George et al., 2010); eventually, DJ-1 is indispensable for the survival of dopaminergic neurons lacking the GDNF-receptor Ret (Aron et al., 2010). Very recently, loss of DJ-1 has been shown to lead to loss of mitochondrial polarization, fragmentation of mitochondria and accumulation of markers of autophagy around mitochondria in human dopaminergic cells. Similar to PINK1 and parkin, DJ-1 also limits mitochondrial fragmentation in response to the mitochondrial toxin rotenone (Thomas et al., 2010). DJ-1 appears thus to display a multi-faceted function that is regulated by interaction with cytosolic and mitochondrial proteins (Cookson et al., 2010).

As a whole, the dopamine-dependent variation observed here may suggest the result of a specific post-translational modification functionally linked to an active protective role in dopaminergic neurons, rather than reflecting generic oxidative modifications. During the preparation of this thesis Guzman and coworkers reported that oxidative stress evoked by pacemaking in dopaminergic SNpc neurons is attenuated by DJ-1 (Guzman et al., in press). Indeed, SNpc neurons differ from neighbouring dopaminergic neurons (*e.g.*, neurons of the mesolimbic pathway) by their pacemaking activity. To produce rhythmic bursts, SNpc

neurons take in calcium and release it via L-type calcium channels. This process requires energy generated by mitochondria, which in turn causes oxidative stress that is specifically counterbalanced by DJ-1.

Validation of proteomic data through an enriched network model

Although the involvement of most identified proteins with PD pathogenesis is an interesting result *per se*, we tried to build a single, representative network that possibly grouped together all the proteins differentially expressed. Instead of validating every single protein by Western blot, we applied a different approach by searching for known relationships between the identified proteins. Experimentally identified proteins were analyzed in terms of both interaction network and GO classification enrichment using *PPI spider*, a network enrichment algorithm based on known protein-protein physical interactions (Antonov et al., 2009). Significant ($p<0.05$) network models were found for proteins that displayed significant changes following dopamine treatment, regardless of α-synuclein overexpression, and for proteins that displayed significant changes as a consequence of α-synuclein overexpression or as a result of the association of dopamine treatment with α-synuclein overexpression (see Results, Figure 9). Surprisingly, all proteins were included in two different networks and proteins responding to dopamine treatment only are segregated from those showing a response to α-synuclein expression. A statistically-significant ($p < 0.05$) functional association to Gene Ontology (GO) classifications was obtained from *PPI spider* starting from proteins grouped as above.

- NF-κB

In both cases, bioinformatic analysis revealed that the NF-κB pathway could be involved in determining the effects of dopamine treatment and α-synuclein overexpression. Accordingly, we transfected β-gal and α-syn cells with the pNF-κB-Luc reporter gene and measured the NF-κB-dependent luciferase activity. The basal activation of NF-κB was significantly lower in α-syn cells than in β-gal cells, and the expression of the reporter gene in β-gal and α-syn cells was dramatically reduced after 24 h dopamine treatment (see Results, Figure 11). Dopamine quenched NF-κB activation both in β-gal and α-syn cells similar to what reported for the PD-related neurotoxin MPP^+ (Halvorsen et al., 2002).

HSP70 is known to be induced by several stress conditions in the nervous system (Calabrese et al., 2004; Garrido et al., 2001) and to inhibit NF-κB activation (Malhotra et al., 2002; Salminen et al., 2008). Thus, we measured by Western blotting HSP70 levels in β-gal and α-

syn cells treated or not with dopamine. HSP70 basal levels are similar in α-syn and β-gal cells (see Results, Figure 12). However, dopamine increases HSP70 level 1.5-fold, regardless of α-synuclein overexpression. Increased levels of the molecular chaperone HSP70 observed here in response to dopamine could contribute to the inhibition of NF-κB (Salminen et al., 2008). Because the upregulation of HSP70 is only observed after dopamine treatment, the inhibition of NF-κB activity by α-synuclein overexpression should be linked to a different pathway, *e.g.*, to the increase of GSK-3β levels as recently suggested (Yuan et al., 2008). Noteworthy, the NF-κB pathway is less active in all the experimental conditions where higher levels of α-synuclein are present, either as a consequence of transfection or of dopamine treatment, suggesting that α-synuclein could be at least in part responsible for the deactivation of this cascade.

- 14-3-3

Network enrichment revealed also a central role for 14-3-3 chaperone proteins after both dopamine treatment and α-synuclein overexpression. The amino-terminal portion of α-synuclein shares 40% sequence conservation with molecular chaperones 14-3-3 (Slavotinek et al., 2003), suggesting that the two proteins could subserve the same function. Molecular chaperones 14-3-3 are particularly abundant in brain, where they comprise ≈1% of total soluble proteins. Chaperone 14-3-3 family accumulates in LBs, participates in neuronal development and cell growth control, and prevents apoptosis by antagonizing BAD, a proapoptotic member of the Bcl-2 family. α-Synuclein binds to many of the same proteins as 14-3-3, including three proteins known to affect cell viability, protein kinase C (PKC), BAD, and extracellular regulated kinase (ERK) (Recchia et al., 2004). α-Synuclein interacts with 14-3-3, and the interaction between the two proteins produces a 54 to 83 kDa protein complex in PD brain. This complex is selectively increased in SNpc but not in cerebellum or cortex. Thus, α-synuclein may sequester 14-3-3, leading to a reduction in the amount of 14-3-3 proteins available to inhibit apoptosis and rendering the cells more susceptible to cellular stresses (Recchia et al., 2004). Both 14-3-3 and α-synuclein bind to tyrosine hydroxylase (TH), the rate-limiting enzyme in catecholamine synthesis, with divergent consequences: activity is stimulated by 14-3-3 but inhibited by α-synuclein (Perez et al., 2002). Therefore, lack of available α-synuclein following its sequestration into LBs has been described as a cause of increased dopamine synthesis.

For all these reasons, we measured 14-3-3 levels in β-gal and α-syn cells treated or not with dopamine. 14-3-3 total levels are similar in α-syn and β-gal cells, even after dopamine

treatment. However, 14-3-3 is present in several isoforms with poorly characterized specificity of action. Analysis of total 14-3-3 is not informative as a whole, and a detailed analysis of changes in ζ vs. ε isoforms could be more interesting. Therefore, present data are not sufficient to exclude a role for 14-3-3 in our model. Further investigations using two-dimensional Western blotting and isoform specific antibodies are needed.

- Apoptosis

The suggestions obtained from enriched GO categories prompted us to evaluate apoptotic cell death in our experimental setting. Dopamine is known to induce apoptosis (Cookson and Van der Brug., 2008) and our results are in agreement with this finding (see Results, Figure 10, panel A). The basal level of apoptotic cells is not significantly different in α-syn cells with respect to β-gal cells (in agreement with cell viability assays) and dopamine triggers apoptotic cell death to the same extent in both α-syn and β-gal cells. Remarkably, also the percentage of necrotic cells was not significantly affected by α-synuclein overexpression (see Results, Figure 10, panel B). Due to the cancerous nature of SH-SY5Y cells, we made clear that in all our experimental conditions cell cycle was not affected with the only exception of a slight increase in S phase of β-gal dopamine-treated cells, a result that does not add anything to our toxicity model (see Results, Figure 14). Although both anti-apoptotic and pro-apoptotic properties were attributed to α-synuclein (Cookson., 2006; Cookson and Van der Brug., 2008), we did not observe any significant effect due to α-synuclein overexpression on the percentage of apoptotic cells. This finding suggests that a 50% increase of α-synuclein level does not exert any apoptotic action by itself, nor it increases cell susceptibility towards dopamine-induced apoptosis. Rather, the 1.5-fold increase could represent a threshold value that discriminates protective from toxic effects (Cookson., 2006). There is clear evidence that high levels of α-synuclein can be damaging, but it is equally true that raising its level from low to moderate is beneficial. One must also consider that under these different conditions α-synuclein is present in different molecular forms, from monomeric to heavily aggregated and deposited into fibrillar forms, and that the microenvironment of the neuron can modulate both baseline expression levels and the aggregation state of α-synuclein (Cookson, 2006). Here, α-synuclein does not induce any detrimental effect *per se*, nor it results to be protective at the basal level and after dopamine exposure, suggesting that an equilibrium between beneficial and detrimental actions has been reached.

DOPAMINE RESPONSE OF DOPAMINERGIC CIRCULATING CELLS: THE JURKAT CELL MODEL

Basic research can concretely help the improvement of clinical approaches to neurodegenerative diseases such as PD, not only by trying to unravel its pathogenetic mechanisms but also by looking for possible peripheral biomarkers.
The second goal of the present thesis can be summarized in three points:

- substantiate the use of T-cells as an appropriate source of peripheral biomarkers in conditions where the dopaminergic system is involved, as it is the case with PD (Fasano et al., 2008b).
- verify if Jurkat cells could be an useful cell culture model to investigate dopamine-activated biochemical processes in T-cells.
- find proteins whose level is modified by dopamine in Jurkat cells that might itself represent a reporter of dopaminergic functionality at the peripheral level, for instance in T-cells of PD patients whether or not stimulated with dopamine.

Jurkat cells express different components of the dopaminergic system. Both D1- and D2-like receptors are present, thus accounting for a variety of cellular responses following a dopaminergic stimulation. Remarkably, D3(a) and D5 receptors were detected, in addition to what was recently reported (Basu et al., 2010). Moreover, they express plasma membrane and vesicular transporters, which makes them capable to internalize dopamine and to store it into vesicles. Noteworthy, Jurkat cells are not able to synthesize dopamine as they lack TH expression (see Results, Figure 26). The body of these results suggests that Jurkat cells posses a dopaminergic system similar to the vast majority of T-cells (Pacheco et al., 2009), TH activity having been reported in T_{reg} cells only (Cosentino et al., 2007). On this basis, Jurkat cells appear to be a suitable model for dopaminergic peripheral cells.
Dopamine stimulation may elicit both receptor- and transporter-mediated responses. For this reason, the dopamine concentration employed here was chosen as the highest possible (without affecting cell viability) in order to induce a wide variety of responses. Indeed, D1 receptors are reported to bind dopamine with a thermodynamic equilibrium dissociation constant in the micromolar range (Missale et al., 1998). Although the identification of the transduction mechanisms activated by dopamine could be of interest to understand the role of the neurotransmitter in regulating immune responses (Basu et al., 2010; Pacheco et al., 2009),

our purpose was to identify variations at the protein level that altogether constituted a sort of dopamine biosensor. As a matter of fact, dopamine induces a significant change in the Jurkat cell proteome (see Results, Figure 27). Specifically, alterations are observed in chaperone proteins, glycolytic enzymes and proteins involved in cytoskeleton maintenance. Upregulation of stress proteins (*e.g.*, HSP60) and of glycolytic enzymes (*e.g.* phosphoglycerate mutase 1) are commonly identified in proteomics studies and may reflect an unspecific response to a generic stress condition (Petrak et al., 2008), or a proteome adaptation as a response to perturbation in the protein levels caused by stimuli of various origin (Mao et al., 2007). β-Actin itself may behave as a proteome balancer in this view, although its deregulation was associated to early stages of pathogenesis in a *Drosophila* model of PD (Xun et al., 2007). The actin isoform pattern is not only modified in its principal components, but it shifts towards basic forms. Indeed, the observed upregulation of a basic β/γ-actin form after dopamine treatment is confirmed by two-dimensional Western blotting, in which a general basic shift is observed (see Results, Figure 29, panel A). Alterations in the 2-DE pattern of β-actin, with the upregulation of a basic isoform, were also described in lymphocytes of PD patients regardless of the therapy (Mila et al., 2009). Noticeably, TCP1θ, a subunit of the main actin folding chaperonin CCT (Hynes and Willison, 2000), is upregulated in Jurkat cells by dopamine treatment. In general, dysregulation of cytoskeletal proteins could be an important common feature of the presymptomatic (or premotor) stages of PD that could be involved at the origin of the disorder (Xun et al., 2008). Of course, it would be particularly intriguing if the same dysregulation could be detectable at the peripheral level.

STI1 and TCP1θ, both upregulated in dopamine treated cells, may take part to the formation of a large multichaperone complex which recruits further chaperones, such as other TCP1 isoforms and heat shock proteins (*e.g.* HSP70, HSC70, HSP90). This complex has been demonstrated to play an active role in the protection of dopaminergic neurons (Imai et al., 2003). Moreover, dopamine treatment of differentiated PC12 cells induces a marked upregulation of chaperone proteins, suggesting a protective response towards unfolded protein stress (Dukes et al., 2008). Thus, the upregulation here reported might constitute a specific response of dopaminergic cells. It should be considered that the low dopamine concentration used in this work (50 μM) was not likely to produce the aspecific oxidative stress conditions that are observed in neuronal dopaminergic cells, when exposed to higher levels (Alberio et al., 2010b; Blum et al., 2000; Gomez-Santos et al., 2003).

An independent confirmation of the specificity of the proteome changes observed in

dopamine challenged Jurkat cells comes from the bioinformatic network enrichment procedure that clusters in a single network (see Results, Figure 28) all the experimentally identified proteins. Additionally, several proteins among those listed here are interactors of the 14-3-3 protein family, a set of adaptor proteins that regulate many cellular processes, including dopamine synthesis (Pozuelo-Rubio et al., 2004). The analysis of the 14-3-3 expression pattern by two-dimensional Western blotting represents at the same time a validation of the central result coming from the proteome analysis and a deeper inspection of the pattern changes suggested by the network enrichment. Although the specificity of action of different isoforms is not completely understood, a significant, general remodeling of their 2-DE pattern is associated to dopamine treatment. Nevertheless, we exclude that the pattern remodeling could be associated with the regulation of dopamine synthesis, given the absence of detectable expression of TH (see Results, Figure 26). Due to intrinsic limits of the resolution of 2-DE and of the specificity of peptide mass fingerprinting, a more detailed description of 14-3-3 balance will require further investigation.

In conclusion, Jurkat cells react to a non-oxidative, saturating dopamine stimulus by inducing specific changes in a network of chaperone proteins that are able to interact with 14-3-3 and β-actin. This network is known to protect dopaminergic neurons from the dopamine-associated damage (Imai et al., 2003). These findings substantiate the use of T-cells as an appropriate source of peripheral biomarkers in conditions where the dopaminergic system is involved, as it is the case with PD . The evidence of a specific response to dopamine, on the other hand, suggests that Jurkat cells are a useful cell culture model to investigate dopamine-activated biochemical processes in T-cells. Eventually, the set of proteins whose level is modified by dopamine in Jurkat cells might represent by itself a reporter of dopaminergic functionality at the peripheral level.

6. FUTURE PERSPECTIVES

PD PATHOGENESIS

1) Evaluate mRNA expression pattern in the four experimental conditions of our model of altered dopamine homeostasis (SH-SY5Y overexpressing or not α-synuclein, treated or not with dopamine). We aim at the comparison of transcriptomic and proteomic data to better evaluate time-dependent effects.
2) Better characterize the role of VDACs in leading apoptosis and autophagy and describe GSK3β activity on VDACs in our model of altered dopamine homeostasis (SH-SY5Y). Indeed, ongoing experiments are revealing a role of GSK3β on VDAC2 phosphorylation and the presence of autophagy, triggered by dopamine treatment. We aim at understanding a possible impairment of these processes, in particular of mitophagy.
3) Measure VDACs level in Substantia Nigra pc, comparing post-mortem samples from PD patients and samples from healthy donors with no other neurological disease.

PD BIOMARKERS

1) Search for a panel of peripheral biomarkers of PD in T-cells.

   We are now performing a proteomic analysis of T-cells comparing those from PD patients and from control volunteers aiming at the identification of differentially expressed proteins. We have already collected blood samples from EOPD patients, LOPD patients, healthy controls, and patients with atypical parkinsonisms, to improve specificity of the panel of biomarkers. Although each single protein may be promising as a biomarker, it might not have a sufficient predictive power if taken alone. A correct balance of sensitivity and specificity may be pursued if a panel of several biomarkers, uncorrelated in the general population, is measured. Moreover, inclusion of patients affected by atypical degenerative parkinsonisms will improve specificity of the proposed panel.

7. BIBLIOGRAPHY

Alavian KN, Scholz C, Simon HH. Transcriptional regulation of mesencephalic dopaminergic neurons: the full circle of life and death. Mov Disord. 2008 23:319-28.

Alberio T, Colapinto M, Natale M, Ravizza R, Gariboldi MB, Bucci EM, Lopiano L, Fasano M. Changes in the two-dimensional electrophoresis pattern of the Parkinson's disease related protein DJ-1 in human SH-SY5Y neuroblastoma cells after dopamine treatment. IUBMB Life. 2010a 62:688-92.

Alberio T, Bossi AM, Milli A, Parma E, Gariboldi MB, Tosi G, Lopiano L, Fasano M. Proteomic analysis of dopamine and α-synuclein interplay in a cellular model of Parkinson's disease pathogenesis. FEBS J. 2010b. doi:10.1111/j.1742-4658.2010.07896.x.

Allcock LM, Kenny RA, Burn DJ: Clinical phenotype of subjects with Parkinson's disease and orthostatic hypotension: autonomic symptom and demographic comparison. Mov Disord. 2006 21:1851-1855.

Andersen SS. Spindle assembly and the art of regulating microtubule dynamics by MAPs and Stathmin/Op18. Trends Cell Biol. 2000 10:261-267.

Antonini A, Schwarz J, Oertel WH, Beer HF, Madeja UD, Leenders KL. [11C]raclopride and positron emission tomography in previously untreated patients with Parkinson's disease: Influence of L-dopa and lisuride therapy on striatal dopamine D2-receptors. Neurology. 1994 44:1325-9.

Antonov AV, Dietmann S, Rodchenkov I, Mewes HW. PPI spider: a tool for the interpretation of proteomics data in the context of protein-protein interaction networks. Proteomics. 2009:2740-9.

Aratyn YS, Schaus TE, Taylor EW, Borisy GG. Intrinsic dynamic behavior of fascin in filopodia. Mol Biol Cell. 2007 18:3928-3940.

Aron L, Klein P, Pham TT, Kramer ER, Wurst W, Klein R. Pro-survival role for Parkinson's associated gene DJ-1 revealed in trophically impaired dopaminergic neurons. PLoS Biol. 2010 8:e1000349.

Baba Y, Kuroiwa A, Uitti RJ, Wszolek ZK, Yamada T. Alterations of T-lymphocyte populations in Parkinson disease. Parkinsonism Relat Disord. 2005 11:493-8.

Baines CP, Kaiser RA, Sheiko T, Craigen WJ, Molkentin JD. Voltage-dependent anion channels are dispensable for mitochondrial-dependent cell death. Nat Cell Biol. 2007 9:550-5.

Bandopadhyay R, Kingsbury AE, Cookson MR, Reid AR, Evans IM, Hope AD, Pittman AM, Lashley T, Canet-Aviles R, Miller DW, McLendon C, Strand C, Leonard AJ, Abou-Sleiman PM, Healy DG, Ariga H, Wood NW, de Silva R, Revesz T, Hardy JA, Lees AJ. The expression of DJ-1 (PARK7) in normal human CNS and idiopathic Parkinson's disease. Brain. 2004 127(Pt 2):420-30.

Barbanti P, Fabbrini G, Ricci A, Cerbo R, Bronzetti E, Caronti B, Calderaro C, Felici L, Stocchi F, Meco G, Amenta F, Lenzi GL. Increased expression of dopamine receptors on lymphocytes in Parkinson's disease. Mov Disord. 1999 14:764-71.

Barnham KJ, Masters CL, Bush AI. Neurodegenerative diseases and oxidative stress. Nat Rev Drug Discov. 2004 3:205-14.

Basu B, Sarkar C, Chakroborty D, Ganguly S, Shome S, Dasgupta PS, Basu S. D1 and D2 dopamine receptor-mediated inhibition of activated normal T cell proliferation is lost in jurkat T leukemic cells. J Biol Chem. 2010 285:27026-32.

Batelli S, Albani D, Rametta R, Polito L, Prato F, Pesaresi M, Negro A, Forloni G. DJ-1 modulates alpha-synuclein aggregation state in a cellular model of oxidative stress: relevance for Parkinson's disease and involvement of HSP70. PLoS One. 2008 3:e1884.

Battisti C, Formichi P, Radi E, Federico A. Oxidative-stress-induced apoptosis in PBLs of two patients with Parkinson disease secondary to alpha-synuclein mutation. J Neurol Sci. 2008 267:120-4.

Becker M, Schindler J, Nothwang HG. Neuroproteomics - the tasks lying ahead. Electrophoresis. 2006 27:2819-29.

Benamer HT, Patterson J, Wyper DJ, Hadley DM, Macphee GJ, Grosset DG. Correlation of Parkinson's disease severity and duration with 123I-FP-CIT SPECT striatal uptake. Mov Disord. 2000 15:692-8.

Bialucha CU, Ferber EC, Pichaud F, Peak-Chew SY, Fujita Y. p32 is a novel mammalian Lgl binding protein that enhances the activity of protein kinase Cζ and regulates cell polarity. J Cell Biol. 2007 178:575-581.

Birbach A. Profilin, a multi-modal regulator of neuronal plasticity. Bioessays 2008 30:994-1002.

Blandini F, Mangiagalli A, Cosentino M, Marino F, Samuele A, Rasini E, Fancellu R, Martignoni E, Riboldazzi G, Calandrella D, Frigo GM, Nappi G. Peripheral markers of apoptosis in Parkinson's disease: the effect of dopaminergic drugs. Ann N Y Acad Sci. 2003 1010:675-8.

Blandini F, Sinforiani E, Pacchetti C, Samuele A, Bazzini E, Zangaglia R, Nappi G, Martignoni E. Peripheral proteasome and caspase activity in Parkinson disease and Alzheimer disease. Neurology. 2006 66:529-34.

Blandini F, Bazzini E, Marino F, Saporiti F, Armentero MT, Pacchetti C, Zangaglia R, Martignoni E, Lecchini S, Nappi G, Cosentino M. Calcium homeostasis is dysregulated in Parkinsonian patients with l-DOPA-induced dyskinesias. Clin Neuropharmacol. 2008 32:133-139.

Blum D, Torch S, Nissou MF, Benabid AL, Verna JM. Extracellular toxicity of 6-hydroxydopamine on PC12 cells. Neurosci Lett. 2000 283:193-6.

Bogdanov M, Matson WR, Wang L, Matson T, Saunders-Pullman R, Bressman SS, Flint Beal M. Metabolomic profiling to develop blood biomarkers for Parkinson's disease. Brain. 2008 131(Pt 2):389-96.

Bonifati V, Rizzu P, van Baren MJ, Schaap O, Breedveld GJ, Krieger E, Dekker MC, Squitieri F, Ibanez P, Joosse M, van Dongen JW, Vanacore N, van Swieten JC, Brice A, Meco G, van Duijn CM, Oostra BA, Heutink P. Mutations in the DJ-1 gene associated with autosomal recessive early-onset parkinsonism. Science 2003 299:256-9.

Bonuccelli U, Del Dotto P. New pharmacologic horizons in the treatment of Parkinson disease. Neurology 2006 67(7 Suppl 2):S30-38.

Borro M, Gentile G, Stigliano A, Misiti S, Toscano V, Simmaco M. Proteomic analysis of peripheral T lymphocytes, suitable circulating biosensors of strictly related diseases. Clin Exp Immunol. 2007 150:494-501.

Braak H, Del Tredici K, Rüb U, de Vos RA, Jansen Steur EN, Braak E. Staging of brain pathology related to sporadic Parkinson's disease. Neurobiol Aging. 2003 24:197-211.

Braak H, Ghebremedhin E, Rüb U, Bratzke H, Del Tredici K. Stages in the development of Parkinson's disease-related pathology. Cell Tissue Res. 2004 318:121-34.

Braak H, Rüb U, Jansen Steur EN, Del Tredici K, de Vos RA. Cognitive status correlates with neuropathologic stage in Parkinson disease. Neurology. 2005 64:1404-10.

Braak H, Rüb U, Del Tredici K. Cognitive decline correlates with neuropathological stage in Parkinson's disease. J Neurol Sci. 2006 248:255-8.

Brand IA and Heinickel A. Key enzymes of carbohydrate metabolism as targets of the 11.5-kDa Zn(2+)-binding protein (parathymosin). J Biol Chem. 1991 266:20984-9.

Brochard V, Combadière B, Prigent A, Laouar Y, Perrin A, Beray-Berthat V, Bonduelle O, Alvarez-Fischer D, Callebert J, Launay JM, Duyckaerts C, Flavell RA, Hirsch EC, Hunot S. Infiltration of CD4+ lymphocytes into the brain contributes to neurodegeneration in a mouse model of Parkinson disease. J Clin Invest. 2009 119:182-92.

Broers JL, Ramaekers FC, Bonne G, Yaou RB, Hutchison CJ. Nuclear lamins: laminopathies and their role in premature ageing. Physiol Rev. 2006 86:967-1008.

Brown DR. Oligomeric alpha-synuclein and its role in neuronal death. IUBMB Life. 2010 62:334-9.

Calabrese V, Stella AM, Butterfield DA, Scapagnini G. Redox regulation in neurodegeneration and longevity: role of the heme oxygenase and HSP70 systems in brain stress tolerance. Antioxid Redox Signal. 2004 6:895-913.

Calabrese V, Lodi R, Tonon C, D'Agata V, Sapienza M, Scapagnini G, Mangiameli A, Pennisi G, Stella AM, Butterfield DA. Oxidative stress, mitochondrial dysfunction and cellular stress response in Friedreich's ataxia. J Neurol Sci. 2005 233:145-62.

Canet-Avilés RM, Wilson MA, Miller DW, Ahmad R, McLendon C, Bandyopadhyay S, Baptista MJ, Ringe D, Petsko GA, Cookson MR. The Parkinson's disease protein DJ-1 is neuroprotective due to cysteine-sulfinic acid-driven mitochondrial localization. Proc Natl Acad Sci U S A 2004 101:9103-8.

Caronti B, Antonini G, Calderaro C, Ruggieri S, Palladini G, Pontieri FE, Colosimo C. Dopamine transporter immunoreactivity in peripheral blood lymphocytes in Parkinson's disease. J Neural Transm. 2001 108:803-7.

Caudle WM, Bammler TK, Lin Y, Pan S, Zhang J. Using 'omics' to define pathogenesis and biomarkers of Parkinson's disease. Expert Rev Neurother. 2010 10:925-42.

Celsi F, Pizzo P, Brini M, Leo S, Fotino C, Pinton P, Rizzuto R. Mitochondria, calcium and cell death: a deadly triad in neurodegeneration. Biochim Biophys Acta. 2009 1787:335-44.

Chan CS, Guzman JN, Ilijic E, Mercer JN, Rick C, Tkatch T, Meredith GE, Surmeier DJ. 'Rejuvenation' protects neurons in mouse models of Parkinson's disease. Nature. 2007 447:1081-6.

Chan CS, Gertler TS, Surmeier DJ. Calcium homeostasis, selective vulnerability and Parkinson's disease. Trends Neurosci. 2009 32:249-56.

Chinta SJ, Kumar MJ, Hsu M, Rajagopalan S, Kaur D, Rane A, Nicholls DG, Choi J, Andersen JK. Inducible alterations of glutathione levels in adult dopaminergic midbrain neurons results in nigrostriatal degeneration. J Neurosci. 2007 27:13997–4006.

Chinta SJ, Andersen JK. Redox imbalance in Parkinson's disease. Biochim Biophys Acta. 2008 1780:1362-7.

Choi J, Sullards MC, Olzmann JA, Rees HD, Weintraub ST, Bostwick DE, Gearing M, Levey AI, Chin LS, Li L. Oxidative damage of DJ-1 is linked to sporadic Parkinson and Alzheimer diseases. J Biol Chem 2006 281:10816-24.

Cohen IR, Schwartz M. Autoimmune maintenance and neuroprotection of the central nervous system. J Neuroimmunol. 1999 100:111-4.

Colapinto M, Mila S, Giraudo S, Stefanazzi P, Molteni M, Rossetti C, Bergamasco B, Lopiano L, Fasano M. alpha-Synuclein protects SH-SY5Y cells from dopamine toxicity. Biochem Biophys Res Commun 2006 349:1294-300.

Cole AR, Causeret F, Yadirgi G, Hastie CJ, McLauchlan H, McManus EJ, Hernández F, Eickholt BJ, Nikolic M, Sutherland C. Distinct priming kinases contribute to differential regulation of collapsin response mediator proteins by glycogen synthase kinase-3 in vivo. J Biol Chem. 2006 281:16591-8.

Cole NB, Dieuliis D, Leo P, Mitchell DC, Nussbaum RL. Mitochondrial translocation of alpha-synuclein is promoted by intracellular acidification. Exp Cell Res. 2008 314:2076-89.

Conway KA, Rochet JC, Bieganski RM, Lansbury PT Jr. Kinetic stabilization of the alpha-synuclein protofibril by a dopamine-alpha-synuclein adduct. Science 2001 294:1346-9.

Cookson MR. Hero versus antihero: the multiple roles of alpha-synuclein in neurodegeneration. Exp Neurol. 2006 199:238-42.

Cookson MR, van der Brug M. Cell systems and the toxic mechanism(s) of alpha-synuclein. Exp Neurol. 2008 209:5-11.

Cookson MR, Bandmann O. Parkinson's disease: insights from pathways. Hum Mol Genet. 2010 19:R21-7.

Cosentino M, Marino F, Bombelli R, Ferrari M, Lecchini S, Frigo GM. Unravelling dopamine (and catecholamine) physiopharmacology in lymphocytes: open questions. Trends Immunol. 2003 24:581-2.

Cosentino M, Fietta AM, Ferrari M, Rasini E, Bombelli R, Carcano E, Saporiti F, Meloni F, Marino F, Lecchini S. Human CD4+CD25+ regulatory T cells selectively express tyrosine hydroxylase and contain endogenous catecholamines subserving an autocrine/paracrine inhibitory functional loop. Blood 2007 109:632-42.

Danzer KM, Haasen D, Karow AR, Moussaud S, Habeck M, Giese A, Kretzschmar H, Hengerer B, Kostka M. Different species of alpha-synuclein oligomers induce calcium influx and seeding. J Neurosci. 2007 27:9220-32.

Das S, Wong R, Rajapakse N, Murphy E, Steenbergen C. Glycogen synthase kinase 3 inhibition slows mitochondrial adenine nucleotide transport and regulates voltage-dependent anion channel phosphorylation. Circ Res. 2008 103:983-91.

Dauer W, Przedborski S. Parkinson's disease: mechanisms and models. Neuron. 2003 39:889-909.

Devi L, Raghavendran V, Prabhu BM, Avadhani NG, Anandatheerthavarada HK. Mitochondrial import and accumulation of alpha-synuclein impair complex I in human dopaminergic neuronal cultures and Parkinson disease brain. J Biol Chem. 2008 283:9089-100.

Devine MJ, Lewis PA. Emerging pathways in genetic Parkinson's disease: tangles, Lewy bodies and LRRK2. FEBS J. 2008 275:5748-57.

Distler AM, Kerner J, Peterman SM, Hoppel CL. A targeted proteomic approach for the analysis of rat liver mitochondrial outer membrane proteins with extensive sequence coverage. Anal Biochem. 2006 356:18-29.

Dodson MW, Guo M. Pink1, Parkin, DJ-1 and mitochondrial dysfunction in Parkinson's disease. Curr Opin Neurobiol. 2007 17:331-7.

Dorsey ER, Holloway RG, Ravina BM: Biomarkers in Parkinson's disease. Expert Rev. Neurother. 2006 6:823-31.

Dukes AA, Van Laar VS, Cascio M, Hastings TG. Changes in endoplasmic reticulum stress proteins and aldolase A in cells exposed to dopamine. J. Neurochem. 2008 106:333-46.

Endo Y, Rubin JS. Wnt signaling and neurite outgrowth: insights and questions. Cancer Sci. 2007 98:1311-7.

Esteves AR, Arduíno DM, Swerdlow RH, Oliveira CR, Cardoso SM. Dysfunctional mitochondria uphold calpain activation: contribution to Parkinson's disease pathology. Neurobiol Dis. 2010 37:723-30.

Fasano M, Giraudo S, Coha S, Bergamasco B, Lopiano L. Residual substantia nigra neuromelanin in Parkinson's disease is cross-linked to alpha-synuclein.Neurochem Int. 2003 42:603-6.

Fasano M, Bergamasco B, Lopiano L. Modifications of the iron-neuromelanin system in Parkinson's disease. J Neurochem. 2006 96:909-16.

Fasano M, Bergamasco B, Lopiano L: The proteomic approach in Parkinson’s disease. Proteomics Clin. Appl. 2007 1:1428-35.

Fasano M, Alberio T, Colapinto M, Mila S, Lopiano L. Proteomics as a tool to investigate cell models for dopamine toxicity. Parkinsonism Relat Disord. 2008a 14 Suppl 2:S135-S138.

Fasano M, Alberio T, Lopiano L. Peripheral biomarkers of Parkinson's disease as early reporters of central neurodegeneration. Biomark Med. 2008b 2:465-78.

Fasano M, Lopiano L: Alpha-synuclein and Parkinson’s disease: a proteomic view. Expert Rev. Proteomics 2008 5:239-48.

Fedorow H, Tribl F, Halliday G, Gerlach M, Riederer P, Double KL. Neuromelanin in human dopamine neurons: comparison with peripheral melanins and relevance to Parkinson's disease. Prog Neurobiol. 2005 75:109-24.

Fiszer U. Does Parkinson's disease have an immunological basis? The evidence and its therapeutic implications. BioDrugs 2001 15:351-5.

Garrido C, Gurbuxani S, Ravagnan L, Kroemer G. Heat shock proteins: endogenous modulators of apoptotic cell death. Biochem Biophys Res Commun. 2001 286:433-42.

Gasser T. Mendelian forms of Parkinson's disease. Biochim Biophys Acta. 2009 1792:587-96.

Geisler S, Holmström KM, Skujat D, Fiesel FC, Rothfuss OC, Kahle PJ, Springer W. PINK1/Parkin-mediated mitophagy is dependent on VDAC1 and p62/SQSTM1. Nat Cell Biol. 2010 12:119-31.

George S, Mok SS, Nurjono M, Ayton S, Finkelstein DI, Masters CL, Li QX, Culvenor JG. alpha-synuclein transgenic mice reveal compensatory increases in Parkinson's disease-associated proteins DJ-1 and Parkin and have enhanced alpha-synuclein and PINK1 levels after rotenone treatment. J Mol Neurosci. 2010:243-54.

Gibb WR. Melanin, tyrosine hydroxylase, calbindin and substance P in the human midbrain and substantia nigra in relation to nigrostriatal projections and differential neuronal susceptibility in Parkinson's disease. Brain Res. 1992 581:283-91.

Gluck MR, Zeevalk GD. Inhibition of brain mitochondrial respiration by dopamine and its metabolites: implications for Parkinson's disease and catecholamine-associated diseases. J Neurochem. 2004 91:788–795.

Goedert M. Alpha-synuclein and neurodegenerative diseases. Nat Rev Neurosci. 2001 2:492-501.

Gómez-Santos C, Ferrer I, Santidrián AF, Barrachina M, Gil J, Ambrosio S. Dopamine induces autophagic cell death and alpha-synuclein increase in human neuroblastoma SH-SY5Y cells. J Neurosci Res. 2003 73:341-50.

Görg A, Obermaier C, Boguth G, Harder A, Scheibe B, Wildgruber R, Weiss W. The current state of two-dimensional electrophoresis with immobilized pH gradients. Electrophoresis. 2000 21:1037-53.

Green DR, Kroemer G. The pathophysiology of mitochondrial cell death. Science. 2004 305:626-9.

Gromova I, Celis JE. Protein detection in gels by silver staining: A procedure compatible with mass-spectrometry. In *Cell Biology: A Laboratory Handbook* (Celis JE, Carter N, Hunter T, Simons K, Small JV, Shotton D, eds) 2006, pp. 219-224 Elsevier, Academic Press, New York.

Guzman JN, Sanchez-Padilla J, Wokosin D, Kondapalli J, Ilijic E, Schumacker PT, Surmeier DJ. Oxidant stress evoked by pacemaking in dopaminergic neurons is attenuated by DJ-1. Nature. 2010 Nov 10. doi:10.1038/nature09536.

Haas RH, Nasirian F, Nakano K, Ward D, Pay M, Hill R, Shults CW. Low platelet mitochondrial complex I and complex II/III activity in early untreated Parkinson's disease. Ann Neurol. 1995 37:714-22.

Häbig K, Walter M, Poths S, Riess O, Bonin M. RNA interference of LRRK2-microarray expression analysis of a Parkinson's disease key player. Neurogenetics. 2008 9:83-94.

Halvorsen EM, Dennis J, Keeney P, Sturgill TW, Tuttle JB, Bennett JB Jr. Methylpyridinium (MPP(+))- and nerve growth factor-induced changes in pro- and anti-apoptotic signaling pathways in SH-SY5Y neuroblastoma cells. Brain Res. 2002 952:98-110.

Hanash S. Disease proteomics. Nature. 2003 422:226-32.

Hao R, MacDonald RG, Ebadi M, Schmit JC, Pfeiffer RF. Stable interaction between G-actin and neurofilament light subunit in dopaminergic neurons. Neurochem. Int. 1997 31:825-34.

Hawkes CH. The prodromal phase of sporadic Parkinson's disease: does it exist and if so how long is it? Mov Disord. 2008 23:1799-807.

Henchcliffe C, Beal MF. Mitochondrial biology and oxidative stress in Parkinson disease pathogenesis. Nat Clin Pract Neurol. 2008 4:600-9.

Henchcliffe C, Shungu DC, Mao X, Huang C, Nirenberg MJ, Jenkins BG, Beal MF. Multinuclear magnetic resonance spectroscopy for in vivo assessment of mitochondrial dysfunction in Parkinson's disease. Ann N Y Acad Sci. 2008 1147:206-20.

Hernández F, de Barreda EG, Fuster-Matanzo A, Goñi-Oliver P, Lucas JJ, Avila J. The role of GSK3 in Alzheimer disease. Brain Res Bull. 2009 80:248-50.

Hilker R, Thomas AV, Klein JC, Weisenbach S, Kalbe E, Burghaus L, Jacobs AH, Herholz K, Heiss WD. Dementia in Parkinson disease: functional imaging of cholinergic and dopaminergic pathways. Neurology. 2005 65:1716-22.

Hiller S, Garces RG, Malia TJ, Orekhov VY, Colombini M, Wagner G. Solution structure of the integral human membrane protein VDAC-1 in detergent micelles. Science 2008 321:1206-10.

Hirsch E, Graybiel AM, Agid YA. Melanized dopaminergic neurons are differentially susceptible to degeneration in Parkinson's disease. Nature 1988 334:345-8.

Hod Y, Pentyala SN, Whyard TC, El-Maghrabi MR. Identification and characterization of a novel protein that regulates RNA-protein interaction. J Cell Biochem. 1999 72:435-44.

Hynes, G.M., Willison, K.R. Individual subunits of the eukaryotic cytosolic chaperonin mediate interactions with binding sites located on subdomains of beta-actin. J. Biol. Chem. 2000 275:18985-94.

Ichimura T, Isobe T, Okuyama T, Takahashi N, Araki K, Kuwano R, Takahashi Y. Molecular cloning of cDNA coding for brain-specific 14-3-3 protein, a protein kinase-dependent activator of tyrosine and tryptophan hydroxylases. Proc Natl Acad Sci U S A. 1988 85:7084-8.

Imai, Y., Soda, M., Murakami, T., Shoji, M., Abe, K., Takahashi, R. A product of the human gene adjacent to parkin is a component of Lewy bodies and suppresses Pael receptor-induced cell death. J. Biol. Chem. 2003 278:51901-10.

Ito G, Ariga H, Nakagawa Y, Iwatsubo T. Roles of distinct cysteine residues in S-nitrosylation and dimerization of DJ-1. Biochem Biophys Res Commun. 2007 339:667-672.

Jankovic J, McDermott M, Carter J, Gauthier S, Goetz C, Golbe L, Huber S, Koller W, Olanow C, Shoulson I, et al. Variable expression of Parkinson's disease: a base-line analysis of the DATATOP cohort. The Parkinson Study Group.Neurology. 1990 40:1529-34.

Jankovic J, Chen S, Le WD. The role of Nurr1 in the development of dopaminergic neurons and Parkinson’s disease. Prog Neurobiol. 2005 77:128-38.

Jankovic J. Parkinson's disease: clinical features and diagnosis. J. Neurol. Neurosurg. Psychiatry 2008 79:368-76.

Jellinger KA. Post mortem studies in Parkinson's disease--is it possible to detect brain areas for specific symptoms? J Neural Transm Suppl. 1999 56:1-29.

Jenner P, Olanow CW. Oxidative stress and the pathogenesis of Parkinson's disease. Neurology 1996 47:S161–70.

Jenner P. Oxidative stress in Parkinson's disease. Ann Neurol. 2003 53 Suppl 3:S26-36.

Jimenez Del Rio M, Moreno S, Garcia-Ospina G, Buritica O, Uribe CS, Lopera F, Velez-Pardo C. Autosomal recessive juvenile parkinsonism Cys212Tyr mutation in parkin renders lymphocytes susceptible to dopamine- and iron-mediated apoptosis. Mov Disord. 2004 19:324-30.

John GB, Shang Y, Li L, Renken C, Mannella CA, Selker JM, Rangell L, Bennett MJ, Zha J. The mitochondrial inner membrane protein mitofilin controls cristae morphology. Mol Biol Cell 2005 16:1543-54.

Johnson MD, Yu LR, Conrads TP, Kinoshita Y, Uo T, McBee JK, Veenstra TD, Morrison RS. The proteomics of neurodegeneration. Am J Pharmacogenomics. 2005 5:259-70.

Junn E, Mouradian MM. Human alpha-synuclein over-expression increases intracellular reactive oxygen species levels and susceptibility to dopamine. Neurosci Lett. 2002 320:146-50.

Junn E, Taniguchi H, Jeong BS, Zhao X, Ichijo H, Mouradian MM. Interaction of DJ-1 with Daxx inhibits apoptosis signal-regulating kinase 1 activity and cell death. Proc Natl Acad Sci U S A. 2005 102:9691-6.

Kamp F, Exner N, Lutz AK, Wender N, Hegermann J, Brunner B, Nuscher B, Bartels T, Giese A, Beyer K, Eimer S, Winklhofer KF, Haass C. Inhibition of mitochondrial fusion by α-synuclein is rescued by PINK1, Parkin and DJ-1. EMBO J. 2010 29:3571-89.

Kanda S, Bishop JF, Eglitis MA, Yang Y, Mouradian MM. Enhanced vulnerability to oxidative stress by alpha-synuclein mutations and C-terminal truncation. Neuroscience. 2000 97:279-84.

Karpinar DP, Balija MB, Kügler S, Opazo F, Rezaei-Ghaleh N, Wender N, Kim HY, Taschenberger G, Falkenburger BH, Heise H, Kumar A, Riedel D, Fichtner L, Voigt A, Braus GH, Giller K, Becker S, Herzig A, Baldus M, Jäckle H, Eimer S, Schulz JB, Griesinger C, Zweckstetter M. Pre-fibrillar alpha-synuclein variants with impaired beta-structure increase neurotoxicity in Parkinson's disease models. EMBO J. 2009 28:3256-68.

Kastner A, Hirsch EC, Lejeune O, Javoy-Agid F, Rascol O, Agid Y. Is the vulnerability of neurons in the substantia nigra of patients with Parkinson's disease related to their neuromelanin content? J Neurochem. 1992 59:1080-9.

Kaufmann H, Nahm K, Purohit D, Wolfe D. Autonomic failure as the initial presentation of Parkinson disease and dementia with Lewy bodies. Neurology. 2004 63:1093-5.

Kay DM, Zabetian CP, Factor SA, Nutt JG, Samii A, Griffith A, Bird TD, Kramer P, Higgins DS, Payami H. Parkinson's disease and LRRK2: frequency of a common mutation in U.S. movement disorder clinics. Mov Disord. 2006 21:519-23.

Keeney PM, Xie J, Capaldi RA, Bennett JP Jr. Parkinson's disease brain mitochondrial complex I has oxidatively damaged subunits and is functionally impaired and misassembled. J Neurosci. 2006 26:5256-64.

Kendall JM, Sala-Newby G, Ghalaut V, Dormer RL, Campbell AK. Engineering the CA(2+)-activated photoprotein aequorin with reduced affinity for calcium. Biochem Biophys Res Commun. 1992 187:1091-7.

Kim RH, Smith PD, Aleyasin H, Hayley S, Mount MP, Pownall S, Wakeham A, You-Ten AJ, Kalia SK, Horne P, Westaway D, Lozano AM, Anisman H, Park DS, Mak TW. Hypersensitivity of DJ-1-deficient mice to 1-methyl-4-phenyl-1,2,3,6-tetrahydropyrindine (MPTP) and oxidative stress. Proc Natl Acad Sci U S A. 2005 102:5215-20.

Kinumi T, Kimata J, Taira T, Ariga H, Niki E. Cysteine-106 of DJ-1 is the most sensitive cysteine residue to hydrogen peroxide-mediated oxidation in vivo in human umbilical vein endothelial cells. Biochem Biophys Res Commun. 2004 317:722-8.

Kipnis J, Cohen H, Cardon M, Ziv Y, Schwartz M. T cell deficiency leads to cognitive dysfunction: implications for therapeutic vaccination for schizophrenia and other psychiatric conditions. Proc Natl Acad Sci U S A 2004 101:8180-5.

Kuroda Y, Mitsui T, Kunishige M, Shono M, Akaike M, Azuma H, Matsumoto T. Parkin enhances mitochondrial biogenesis in proliferating cells. Hum Mol Genet. 2006 15:883-95.

Langston JW. The Parkinson's complex: parkinsonism is just the tip of the iceberg. Ann Neurol. 2006 59:591-6.

Lashuel HA, Petre BM, Wall J, Simon M, Nowak RJ, Walz T, Lansbury PT Jr. Alpha-synuclein, especially the Parkinson's disease-associated mutants, forms pore-like annular and tubular protofibrils. J Mol Biol. 2002 322:1089-102.

Lee M, Hyun DH, Halliwell B, Jenner P. Effect of overexpression of wild-type and mutant Cu/Zn-superoxide dismutases on oxidative stress and cell death induced by hydrogen peroxide, 4-hydroxynonenal or serum deprivation: potentiation of injury by ALS-related mutant superoxide dismutases and protection by Bcl-2. J Neurochem. 2001 78:209-20.

Lee MP. Genome-wide analysis of epigenetics in cancer. Ann N Y Acad Sci. 2003 983:101-9.

Lesage S, Brice A. Parkinson's disease: from monogenic forms to genetic susceptibility factors. Hum Mol Genet. 2009 18(R1):R48-59.

Lev N, Ickowicz D, Melamed E, Offen D. Oxidative insults induce DJ-1 upregulation and redistribution: implications for neuroprotection. Neurotoxicology 2008 29:397-405

Lev N, Ickowicz D, Barhum Y, Lev S, Melamed E, Offen D. DJ-1 protects against dopamine toxicity. J Neural Transm 2009 116:151-60.

Lewis SJG, Foltynie T, Blackwell AD, Robbins TW, Owen AM, Barker RA: Heterogeneity of Parkinson’s disease in the early clinical stages using a data driven approach. J. Neurol. Neurosurg. Psychiatry 2005 76:343-8.

Li HM, Niki T, Taira T, Iguchi-Ariga SM, Ariga H. Association of DJ-1 with chaperones and enhanced association and colocalization with mitochondrial Hsp70 by oxidative stress. Free Radic Res. 2005 39:1091-9.

Liu WB, Zhou J, Qu Y, Li X, Lu CT, Xie KL, Sun XL, Fei Z. Neuroprotective effect of osthole on MPP+-induced cytotoxicity in PC12 cells via inhibition of mitochondrial dysfunction and ROS production. Neurochem Int. 2010 57:206-15.

Lotharius J, Brundin P. Pathogenesis of Parkinson's disease: dopamine, vesicles and alpha-synuclein. Nat Rev Neurosci. 2002 3:932-42.

Maguire-Zeiss KA, Short DW, Federoff HJ. Synuclein, dopamine and oxidative stress: co-conspirators in Parkinson's disease? Brain Res Mol Brain Res. 2005 134:18-23.

Malhotra V, Eaves-Pyles T, Odoms K, Quaid G, Shanley TP, Wong HR. Heat shock inhibits activation of NF-kappaB in the absence of heat shock factor-1. Biochem Biophys Res Commun. 2002 291:453-7.

Mao L, Zabel C, Herrmann M, Nolden T, Mertes F, Magnol L, Chabert C, Hartl D, Herault Y, Delabar JM, Manke T, Himmelbauer H, Klose J. Proteomic shifts in embryonic stem cells with gene dose modifications suggest the presence of balancer proteins in protein regulatory networks. PLoS One 2007 2:e1218.

Marek K, Jennings D. Can we image premotor Parkinson disease? Neurology. 2009 72(7 Suppl):S21-6.

Marino F, Cosentino M, Bombelli R, Ferrari M, Lecchini S, Frigo G. Endogenous catecholamine synthesis, metabolism storage, and uptake in human peripheral blood mononuclear cells. Exp Hematol. 1999 27:489-95.

Martí MJ, Saura J, Burke RE, Jackson-Lewis V, Jiménez A, Bonastre M, Tolosa E. Striatal 6-hydroxydopamine induces apoptosis of nigral neurons in the adult rat. Brain Res. 2002 958:185-91.

Martignoni E, Blandini F, Godi L, Desideri S, Pacchetti C, Mancini F, Nappi G. Peripheral markers of oxidative stress in Parkinson's disease. The role of L-DOPA. Free Radic Biol Med. 1999 27:428-37.

Mattson MP. Apoptotic and anti-apoptotic synaptic signaling mechanisms. Brain Pathol. 2000 10:300-12.

McGeer PL, McGeer EG. Inflammation and neurodegeneration in Parkinson's disease. Parkinsonism Relat Disord. 2004 10:S3-7.

Menegon A, Board PG, Blackburn AC, Mellick GD, Le Couteur DG. Parkinson's disease, pesticides, and glutathione transferase polymorphisms. Lancet 1998 352:1344-6.

Meulener MC, Graves CL, Sampathu DM, Armstrong-Gold CE, Bonini NM, Giasson BI. DJ-1 is present in a large molecular complex in human brain tissue and interacts with alpha-synuclein. J Neurochem. 2005 93:1524-32.

Meulener MC, Xu K, Thomson L, Ischiropoulos H, Bonini NM. Mutational analysis of DJ-1 in Drosophila implicates functional inactivation by oxidative damage and aging. Proc Natl Acad Sci USA. 2006 103:12517-22.

Michell AW, Lewis SJG, Foltynie T, Barker RA: Biomarkers and Parkinson's disease. Brain 2004 127:1693-705.

Migliore L, Petrozzi L, Lucetti C, Gambaccini G, Bernardini S, Scarpato R, Trippi F, Barale R, Frenzilli G, Rodilla V, Bonuccelli U. Oxidative damage and cytogenetic analysis in leukocytes of Parkinson's disease patients. Neurology 2002 58:1809-15.

Mila S, Giuliano Albo A, Corpillo D, Giraudo S, Zibetti M, Bucci EM, Lopiano L, Fasano M. Lymphocyte proteomics of Parkinson's disease patients reveals cytoskeletal protein dysregulation and oxidative stress. Biomarkers Med. 2009 3:117-28.

Missale C, Nash SR, Robinson SW, Jaber M, Caron MG. Dopamine receptors: from structure to function. Physiol Rev. 1998 78:189-225.

Mitsumoto A, Nakagawa Y, Takeuchi A, Okawa K, Iwamatsu A, Takanezawa Y. Oxidized forms of peroxiredoxins and DJ-1 on two-dimensional gels increased in response to sublethal levels of paraquat. Free Radic Res. 2001 35:301-10.

Mitsumoto A, Nakagawa Y. DJ-1 is an indicator for endogenous reactive oxygen species elicited by endotoxin. Free Radicals Research 2001 35:885-93.

Monastyrskaya K, Babiychuk EB, Draeger A. The annexins: spatial and temporal coordination of signaling events during cellular stress. Cell Mol Life Sci. 2009 66:2623-42.

Montine TJ, Farris DB, Graham DG. Covalent crosslinking of neurofilament proteins by oxidized catechols as a potential mechanism of Lewy body formation. J. Neuropathol. Exp. Neurol. 1995 54:311-9.

Moore DJ, Zhang L, Troncoso J, Lee MK, Hattori N, Mizuno Y, Dawson TM, Dawson VL. Association of DJ-1 and parkin mediated by pathogenic DJ-1 mutations and oxidative stress. Hum Mol Genet. 2005 14:71-84.

Motani K, Tabata K, Kimura Y, Okano S, Shibata Y, Abiko Y, Nagai H, Akihisa T, Suzuki T. Proteomic analysis of apoptosis induced by xanthoangelol, a major constituent of Angelica keiskei, in neuroblastoma. Biol Pharm Bull. 2008 31:618-26.

Naciff JM, Kaetzel MA, Behbehani MM, Dedman JR. Differential expression of annexins I-VI in the rat dorsal root ganglia and spinal cord. J Comp Neurol. 1996 368:356-70.

Nagai Y, Ueno S, Saeki Y, Soga F, Hirano M, Yanagihara T. Decrease of the D3 dopamine receptor mRNA expression in lymphocytes from patients with Parkinson's disease. Neurology. 1996 46:791-5.

Nagakubo D, Taira T, Kitaura H, Ikeda M, Tamai K, Iguchi-Ariga SM, Ariga H. DJ-1, a novel oncogene which transforms mouse NIH3T3 cells in cooperation with ras. Biochem Biophys Res Commun 1997 231:509-13.

Nakamura M, Morisawa H, Imajoh-Ohmi S, Takamura C, Fukuda H, Toda T. Proteomic analysis of protein complexes in human SH-SY5Y neuroblastoma cells by using blue-native gel electrophoresis: an increase in lamin A/C associated with heat shock protein 90 in response to 6-hydroxydopamine-induced oxidative stress. Exp Gerontol. 2009 44:375-82.

Narendra D, Tanaka A, Suen DF, Youle RJ. Parkin is recruited selectively to impaired mitochondria and promotes their autophagy. J Cell Biol. 2008 183:795-803.

Narendra DP, Kane LA, Hauser DN, Fearnley IM, Youle RJ. p62/SQSTM1 is required for Parkin-induced mitochondrial clustering but not mitophagy; VDAC1 is dispensable for both. Autophagy. 2010 6:1090-106

Natale M, Bonino D, Consoli P, Alberio T, Ravid RG, Fasano M, Bucci EM. A meta-analysis of two-dimensional electrophoresis pattern of the Parkinson's disease-related protein DJ-1. Bioinformatics. 2010 26:946-52.

Niki T, Takahashi-Niki K, Taira T, Iguchi-Ariga SM, Ariga H. DJBP: a novel DJ-1-binding protein, negatively regulates the androgen receptor by recruiting histone deacetylase complex, and DJ-1 antagonizes this inhibition by abrogation of this complex. Mol Cancer Res. 2003 1:247-61.

Obeso JA, Rodriguez-Oroz MC, Goetz CG, Marin C, Kordower JH, Rodriguez M, Hirsch EC, Farrer M, Schapira AH, Halliday G. Missing pieces in the Parkinson's disease puzzle. Nat Med. 2010 16:653-61.

Olzmann JA, Li L, Chudaev MV, Chen J, Perez FA, Palmiter RD, Chin LS. Parkin-mediated K63-linked polyubiquitination targets misfolded DJ-1 to aggresomes via binding to HDAC6. J Cell Biol 2007 178:1025-38.

Ostrerova N, Petrucelli L, Farrer M, Mehta N, Choi P, Hardy J, Wolozin B. alpha-Synuclein shares physical and functional homology with 14-3-3 proteins. J Neurosci. 1999 19:5782-91.

O'Sullivan SS, Williams DR, Gallagher DA, Massey LA, Silveira-Moriyama L, Lees AJ. Nonmotor symptoms as presenting complaints in Parkinson's disease: a clinicopathological study. Mov Disord. 2008 23:101-6.

Outeiro TF, Putcha P, Tetzlaff JE, Spoelgen R, Koker M, Carvalho F, Hyman BT, McLean PJ. Formation of toxic oligomeric alpha-synuclein species in living cells. PLoS One. 2008 3:e1867.

Pacheco R, Prado CE, Barrientos MJ, Bernales S. Role of dopamine in the physiology of T-cells and dendritic cells. J Neuroimmunol. 2009 216:8-19.

Parker WD Jr, Parks JK, Swerdlow RH. Complex I deficiency in Parkinson's disease frontal cortex. Brain Res. 2008 1189:215-8.

Pastorino JG, Hoek JB, Shulga N. Activation of glycogen synthase kinase 3beta disrupts the binding of hexokinase II to mitochondria by phosphorylating voltage-dependent anion channel and potentiates chemotherapy-induced cytotoxicity. Cancer Res. 2005 65:10545-54.

Payami H, Zareparsi S, James D, Nutt J. Familial aggregation of Parkinson disease: a comparative study of early-onset and late-onset disease. Arch Neurol. 2002 59:848-50.

Pellicano C, Buttarelli FR, Circella A, Tiple D, Giovannelli M, Benincasa D, Colosimo C, Pontieri FE. Dopamine transporter immunoreactivity in peripheral blood lymphocytes discriminates Parkinson's disease from essential tremor. J Neural Transm. 2007 114:935-8.

Penn AM, Roberts T, Hodder J, Allen PS, Zhu G, Martin WR. Generalized mitochondrial dysfunction in Parkinson's disease detected by magnetic resonance spectroscopy of muscle. Neurology. 1995 45:2097-9.

Perez RG, Waymire JC, Lin E, Liu JJ, Guo F, Zigmond MJ. A role for alpha-synuclein in the regulation of dopamine biosynthesis. J Neurosci. 2002 22:3090-9.

Petrak J, Ivanek R, Toman O, Cmejla R, Cmejlova J, Vyoral D, Zivny J, Vulpe CD. Déjà vu in proteomics. A hit parade of repeatedly identified differentially expressed proteins. Proteomics 2008 8:1744-9.

Porcelli AM, Pinton P, Ainscow EK, Chiesa A, Rugolo M, Rutter GA, Rizzuto R. Targeting of reporter molecules to mitochondria to measure calcium, ATP, and pH. Methods Cell Biol. 2001 65:353-80.

Pozuelo Rubio, M., Geraghty, K.M., Wong, B.H., Wood, N.T., Campbell, D.G., Morrice, N., Mackintosh, C. 14-3-3-affinity purification of over 200 human phosphoproteins reveals new links to regulation of cellular metabolism, proliferation and trafficking. Biochem. J. 2004 379:395-408.

Premkumar A, Simantov R. Mitochondrial voltage-dependent anion channel is involved in dopamine-induced apoptosis. J Neurochem. 2002 82:345-52.

Quilty MC, King AE, Gai WP, Pountney DL, West AK, Vickers JC, Dickson TC. Alpha-synuclein is upregulated in neurones in response to chronic oxidative stress and is associated with neuroprotection. Exp Neurol. 2006 199:249-56.

Ransohoff RM, Kivisäkk P, Kidd G. Three or more routes for leukocyte migration into the central nervous system. Nat Rev Immunol. 2003 3:569-81.

Rawal N, Corti O, Sacchetti P, Ardilla-Osorio H, Sehat B, Brice A, Arenas E. Parkin protects dopaminergic neurons from excessive Wnt/beta-catenin signaling. Biochem Biophys Res Commun. 2009 388:473-8.

Recchia A, Debetto P, Negro A, Guidolin D, Skaper SD, Giusti P. Alpha-synuclein and Parkinson's disease. FASEB J. 2004 18:617-26.

Rinne JO, Ma SY, Lee MS, Collan Y, Röyttä M. Loss of cholinergic neurons in the pedunculopontine nucleus in Parkinson's disease is related to disability of the patients. Parkinsonism Relat Disord. 2008 14:553-7.

Robinson PA. Understanding the molecular basis of Parkinson's disease, identification of biomarkers and routes to therapy. Expert Rev Proteomics. 2010 7:565-78.

Rochet JC, Outeiro TF, Conway KA, Ding TT, Volles MJ, Lashuel HA, Bieganski RM, Lindquist SL, Lansbury PT. Interactions among alpha-synuclein, dopamine, and biomembranes: some clues for understanding neurodegeneration in Parkinson's disease. J. Mol. Neurosci. 2004 23:23-4.

Roos RA, Jongen JC, van der Velde EA. Clinical course of patients with idiopathic Parkinson's disease. Mov Disord. 1996 11:236-42.

Salminen A, Paimela T, Suuronen T, Kaarniranta K. Innate immunity meets with cellular stress at the IKK complex: regulation of the IKK complex by HSP70 and HSP90. Immunol Lett. 2008 117:9-15.

Sarioglu H, Brandner S, Haberger M, Jacobsen C, Lichtmannegger J, Wormke M, Andrae U. Analysis of 2,3,7,8-tetrachlorodibenzo-p-dioxin-induced proteome changes in 5L rat hepatoma cells reveals novel targets of dioxin action including the mitochondrial apoptosis regulator VDAC2. Mol Cell Proteomics. 2008 7:394-410.

Sathish K, Padma B, Munugalavadla V, Bhargavi V, Radhika KV, Wasia R, Sairam M, Singh SS. Phosphorylation of profilin regulates its interaction with actin and poly L-proline. Cell Signal 2004 16:589-96.

Schapira AH, Cooper JM, Dexter D, Clark JB, Jenner P, Marsden CD. Mitochondrial complex I deficiency in Parkinson's disease. J Neurochem. 1990 54:823-7.

Schapira AH. Mitochondrial dysfunction in neurodegenerative diseases. Neurochem Res. 2008 33:2502-9.

Scherman D, Desnos C, Darchen F, Pollak P, Javoy-Agid F, Agid Y. Striatal dopamine deficiency in Parkinson's disease: role of aging. Ann Neurol. 1989 26:551-7.

Schrag A, Schott JM. Epidemiological, clinical, and genetic characteristics of early-onset parkinsonism. Lancet Neurol. 2006 5:355-63.

Schulenborg T, Schmidt O, van Hall A, Meyer HE, Hamacher M, Marcus K: Proteomics in neurodegeneration - disease driven approaches. J. Neural Transm. 2006 113:1055-73.

Schwartz M. Beneficial autoimmune T cells and posttraumatic neuroprotection. Ann N Y Acad Sci. 2000 917:341-7.

Schwartz M. Harnessing the immune system for neuroprotection: therapeutic vaccines for acute and chronic neurodegenerative disorders. Cell Mol Neurobiol. 2001 21:617-27.

Sekito A, Taira T, Niki T, Iguchi-Ariga SM, Ariga H. Stimulation of transforming activity of DJ-1 by Abstrakt, a DJ-1-binding protein. Int J Oncol 2005 26:685-9.

Shastry BS. Parkinson disease: etiology, pathogenesis and future of gene therapy. Neurosci Res. 2001 41:5-12.

Shenton D, Smirnova JB, Selley JN, Carroll K, Hubbard SJ, Pavitt GD, Ashe MP, Grant CM. Global translational responses to oxidative stress impact upon multiple levels of protein synthesis. J Biol Chem. 2006 281:29011-21.

Sheta EA, Appel SH, Goldknopf IL: 2D gel blood serum biomarkers reveal differential clinical proteomics of the neurodegenerative diseases. Expert Rev. Proteomics 2006 3:45-62.

Shimomura O, Musicki B, Kishi Y. Semi-synthetic aequorin. An improved tool for the measurement of calcium ion concentration. Biochem J. 1988 251:405-10.

Shinbo Y, Niki T, Taira T, Ooe H, Takahashi-Niki K, Maita C, Seino C, Iguchi-Ariga SM, Ariga H. Proper SUMO-1 conjugation is essential to DJ-1 to exert its full activities. Cell Death Differ 2006 13:96-108.

Shulman LM, Gruber-Baldini AL, Anderson KE, Vaughan CG, Reich SG, Fishman PS, Weiner WJ. The evolution of disability in Parkinson disease. Mov Disord. 2008 23:790-6.

Slavotinek, A. M., Biesecker, L. G. Unfolding the role of chaperones and chaperonins in human disease. Trends Genet. 2003 17:528-35.

Smeyne M, Boyd J, Raviie Shepherd K, Jiao Y, Pond BB, Hatler M, Wolf R, Henderson C, Smeyne RJ. GSTpi expression mediates dopaminergic neuron sensitivity in experimental parkinsonism. Proc Natl Acad Sci U S A 2007 104:1977-82.

Sousa VL, Bellani S, Giannandrea M, Yousuf M, Valtorta F, Meldolesi J, Chieregatti E. α-Synuclein and its A30P mutant affect actin cytoskeletal structure and dynamics. Mol Biol Cell 2009 20:3725-39.

Spiegel J, Hellwig D, Samnick S, Jost W, Möllers MO, Fassbender K, Kirsch CM, Dillmann U. Striatal FP-CIT uptake differs in the subtypes of early Parkinson's disease. J Neural Transm. 2007 114:331-5.

Spillantini MG, Schmidt ML, Lee VM, Trojanowski JQ, Jakes R, Goedert M. Alpha-synuclein in Lewy bodies. Nature. 1997 388:839-40.

Tabrizi SJ, Orth M, Wilkinson JM, Taanman JW, Warner TT, Cooper JM, Schapira AH. Expression of mutant alpha-synuclein causes increased susceptibility to dopamine toxicity. Hum Mol Genet. 2000 9:2683-9.

Takahashi K, Taira T, Niki T, Seino C, Iguchi-Ariga SM, Ariga H. DJ-1 positively regulates the androgen receptor by impairing the binding of PIASx alpha to the receptor. J Biol Chem 2001 276:37556-63.

Takashima A. Drug development targeting the glycogen synthase kinase-3beta (GSK-3beta)-mediated signal transduction pathway: role of GSK-3beta in adult brain. J Pharmacol Sci. 2009 109:174-8.

Tanaka Y, Engelender S, Igarashi S, Rao RK, Wanner T, Tanzi RE, Sawa A, L Dawson V, Dawson TM, Ross CA. Inducible expression of mutant alpha-synuclein decreases

proteasome activity and increases sensitivity to mitochondria-dependent apoptosis. Hum Mol Genet. 2001 10:919-26.

Tao WA, Aebersold R. Advances in quantitative proteomics via stable isotope tagging and mass spectrometry. Curr Opin Biotechnol. 2003 14:110-8.

Tao X, Tong L. Crystal structure of human DJ-1, a protein associated with early onset Parkinson's disease. J Biol Chem 2003 278:31372-9.

Thannickal TC, Lai YY, Siegel JM. Hypocretin (orexin) cell loss in Parkinson's disease. Brain. 2007 130:1586-95.

Thomas B, Beal MF. Parkinson's disease. Hum Mol Genet. 2007 16 Spec. No. 2, R183-94.

Thomas KJ, McCoy MK, Blackinton J, Beilina A, van der Brug M, Sandebring A, Miller D, Maric D, Cedazo-Minguez A, Cookson MR. DJ-1 acts in parallel to the PINK1/parkin pathway to control mitochondrial function and autophagy. Hum Mol Genet. 2010 doi: 10.1093/hmg/ddq430.

Tillman JE, Yuan J, Gu G, Fazli L, Ghosh R, Flynt AS, Gleave M, Rennie PS, Kasper S. DJ-1 binds androgen receptor directly and mediates its activity in hormonally treated prostate cancer cells. Cancer Res. 2007 67:4630-7.

Tseng Y, Kole TP, Lee JS, Fedorov E, Almo SC, Schafer BW, Wirtz D. How actin crosslinking and bundling proteins cooperate to generate an enhanced cell mechanical response. Biochem Biophys Res Commun. 2005 334:183-92.

Uversky VN, Li J, Fink AL. Metal-triggered structural transformations, aggregation, and fibrillation of human alpha-synuclein. A possible molecular NK between Parkinson's disease and heavy metal exposure. J Biol Chem. 2001 276:44284-96.

Uversky VN, M Cooper E, Bower KS, Li J, Fink AL. Accelerated alpha-synuclein fibrillation in crowded milieu. FEBS Lett. 2002 515:99-103.

Uversky VN, Eliezer D. Biophysics of Parkinson's disease: structure and aggregation of alpha-synuclein. Curr Protein Pept Sci. 2009 10:483-99.

Valente EM, Abou-Sleiman PM, Caputo V, Muqit MM, Harvey K, Gispert S, Ali Z, Del Turco D, Bentivoglio AR, Healy DG, Albanese A, Nussbaum R, González-Maldonado R, Deller T, Salvi S, Cortelli P, Gilks WP, Latchman DS, Harvey RJ, Dallapiccola B, Auburger G, Wood NW. Hereditary early-onset Parkinson's disease caused by mutations in PINK1. Science 2004 304:1158-60.

Van der Brug MP, Blackinton J, Chandran J, Hao LY, Lal A, Mazan-Mamczarz K, Martindale J, Xie C, Ahmad R, Thomas KJ, Beilina A, Gibbs JR, Ding J, Myers AJ, Zhan M, Cai H, Bonini NM, Gorospe M, Cookson MR. RNA binding activity of the recessive parkinsonism protein DJ-1 supports involvement in multiple cellular pathways. Proc Natl Acad Sci U S A. 2008 105:10244-9.

Van Laar VS, Berman SB. Mitochondrial dynamics in Parkinson's disease. Exp Neurol. 2009 218:247-56.

Volles MJ, Lee SJ, Rochet JC, Shtilerman MD, Ding TT, Kessler JC, Lansbury PT Jr. Vesicle permeabilization by protofibrillar alpha-synuclein: implications for the pathogenesis and treatment of Parkinson's disease. Biochemistry 2001 40:7812-9.

Volles MJ, Lansbury PT Jr. Vesicle permeabilization by protofibrillar alpha-synuclein is sensitive to Parkinson's disease-linked mutations and occurs by a pore-like mechanism. Biochemistry 2002 41:4595-602.

Waak J, Weber SS, Görner K, Schall C, Ichijo H, Stehle T, Kahle PJ. Oxidizable residues mediating protein stability and cytoprotective interaction of DJ-1 with apoptosis signal-regulating kinase 1. J Biol Chem. 2009 284:14245-57.

Walkinshaw G, Waters CM. Neurotoxin-induced cell death in neuronal PC12 cells is mediated by induction of apoptosis. Neuroscience 1994 63:975-87.

Wasinger VC, Cordwell SJ, Cerpa-Poljak A, Yan JX, Gooley AA, Wilkins MR, Duncan MW, Harris R, Williams KL, Humphery-Smith I. Progress with gene-product mapping of the Mollicutes: Mycoplasma genitalium. Electrophoresis. 1995 16:1090-4.

Weihofen A, Thomas KJ, Ostaszewski BL, Cookson MR, Selkoe DJ. Pink1 forms a multiprotein complex with Miro and Milton, linking Pink1 function to mitochondrial trafficking. Biochemistry 2009 48:2045-52.

Werner CJ, Heyny-von Haussen R, Mall G, Wolf S. Proteome analysis of human substantia nigra in Parkinson's disease. Proteome Sci. 2008 6:8.

West AB, Moore DJ, Biskup S, Bugayenko A, Smith WW, Ross CA, Dawson VL, Dawson TM. Parkinson's disease-associated mutations in leucine-rich repeat kinase 2 augment kinase activity. Proc Natl Acad Sci U S A. 2005 102:16842-7.

Whitworth AJ, Theodore DA, Greene JC, Benes H, Wes PD, Pallanck LJ. Increased glutathione S-transferase activity rescues dopaminergic neuron loss in a Drosophila model of Parkinson's disease. Proc Natl Acad Sci U S A 2005 102:8024-9.

Wild P, Dikic I. Mitochondria get a Parkin' ticket. Nat Cell Biol. 2010 12:104-6.

Wood-Kaczmar A, Gandhi S, Wood NW. Understanding the molecular causes of Parkinson's disease. Trends Mol. Med. 2006 12:521-8.

Wright JA, Wang X, Brown DR. Unique copper induced oligomers mediate alpha-synuclein toxicity. FASEB J. 2009 23:2384-93.

Xiong H, Wang D, Chen L, Choo YS, Ma H, Tang C, Xia K, Jiang W, Ronai Z, Zhuang X, Zhang Z. Parkin, PINK1, and DJ-1 form a ubiquitin E3 ligase complex promoting unfolded protein degradation. J Clin Invest. 2009 119:650-60.

Xu J, Kao SY, Lee FJ, Song W, Jin LW, Yankner BA. Dopamine-dependent neurotoxicity of alpha-synuclein: a mechanism for selective neurodegeneration in Parkinson disease. Nat Med. 2002 8:600-6.

Xu J, Zhong N, Wang H, Elias JE, Kim CY, Woldman I, Pifl C, Gygi SP, Geula C, Yankner BA. The Parkinson's disease-associated DJ-1 protein is a transcriptional co-activator that protects against neuronal apoptosis. Hum Mol Genet. 2005 14:1231-41.

Xun Z, Sowell RA, Kaufman TC, Clemmer DE. Lifetime proteomic profiling of an A30P alpha-synuclein Drosophila model of Parkinson's disease. J Proteome Res. 2007 6:3729-38.

Xun Z, Sowell RA, Kaufman TC, Clemmer DE. Quantitative proteomics of a presymptomatic A53T alpha-synuclein Drosophila model of Parkinson disease. Mol Cell Proteomics. 2008 7:1191-203.

Yang Y, Ouyang Y, Yang L, Beal MF, McQuibban A, Vogel H, Lu B. Pink1 regulates mitochondrial dynamics through interaction with the fission/fusion machinery. Proc Natl Acad Sci U S A. 2008 105:7070-5.

Youdim MB, Ben-Shachar D, Riederer P. The enigma of neuromelanin in Parkinson's disease substantia nigra. J Neural Transm Suppl. 1994 43:113-22.

Youdim MB, Riederer P. Understanding Parkinson's disease. Sci Am. 1997 276:52-9.

Yuan Y, Jin J, Yang B, Zhang W, Hu J, Zhang Y, Chen NH. Overexpressed alpha-synuclein regulated the nuclear factor-kappaB signal pathway. Cell Mol Neurobiol. 2008 28:21-33.

Zarow C, Lyness SA, Mortimer JA, Chui HC. Neuronal loss is greater in the locus coeruleus than nucleus basalis and substantia nigra in Alzheimer and Parkinson diseases. Arch Neurol. 2003 60:337-41.

Zecca L, Tampellini D, Gerlach M, Riederer P, Fariello RG, Sulzer D. Substantia nigra neuromelanin: structure, synthesis, and molecular behaviour. Mol Pathol. 2001 54:414-8.

Zecca L, Zucca FA, Wilms H, Sulzer D. Neuromelanin of the substantia nigra: a neuronal black hole with protective and toxic characteristics. Trends Neurosci. 2003 26:578-80.

Zhang L, Shimoji M, Thomas B, Moore DJ, Yu SW, Marupudi NI, Torp R, Torgner IA, Ottersen OP, Dawson TM, Dawson VL. Mitochondrial localization of the Parkinson's disease related protein DJ-1: implications for pathogenesis. Hum Mol Genet. 2005 14:2063-73.

Zhang Y, Dawson VL, Dawson TM. Oxidative stress and genetics in the pathogenesis of Parkinson's disease. Neurobiol Dis. 2000 7:240-50.

Zhong N, Xu J. Synergistic activation of the human MnSOD promoter by DJ-1 and PGC-1alpha: regulation by SUMOylation and oxidation. Hum Mol Genet. 2008 17:3357-67.

Zhou W, Freed CR. DJ-1 up-regulates glutathione synthesis during oxidative stress and inhibits A53T alpha-synuclein toxicity. J Biol Chem. 2005 280:43150-8.

Zhou Y, Gu G, Goodlett DR, Zhang T, Pan C, Montine TJ, Montine KS, Aebersold RH, Zhang J. Analysis of alpha-synuclein-associated proteins by quantitative proteomics. J Biol Chem. 2004 279:39155-64.

Publications on international ISI journals

Related to the project:

Alberio T, Bossi AM, Milli A, Parma E, Gariboldi MB, Tosi G, Lopiano L, Fasano M. Proteomic analysis of dopamine and α-synuclein interplay in a cellular model of Parkinson's disease pathogenesis. FEBS J. 2010 Sep 27. doi:10.1111/j.1742-4658.2010.07896.x

Alberio T, Colapinto M, Natale M, Ravizza R, Gariboldi MB, Bucci EM, Lopiano L, Fasano M. Changes in the two-dimensional electrophoresis pattern of the Parkinson's disease related protein DJ-1 in human SH-SY5Y neuroblastoma cells after dopamine treatment. IUBMB Life. 2010 Sep;62(9):688-92.

Natale M, Bonino D, Consoli P, Alberio T, Ravid RG, Fasano M, Bucci EM. A meta-analysis of two-dimensional electrophoresis pattern of the Parkinson's disease-related protein DJ-1. Bioinformatics. 2010 Apr 1;26(7):946-52.

Fasano M, Alberio T, Lopiano L. Peripheral biomarkers of Parkinson's disease as early reporters of central neurodegeneration. Biomark Med. 2008 Oct;2(5):465-78.

Fasano M, Alberio T, Colapinto M, Mila S, Lopiano L. Proteomics as a tool to investigate cell models for dopamine toxicity. Parkinsonism Relat Disord. 2008;14 Suppl 2:S135-8.

Non-related to the project:

Rubino T, Realini N, Braida D, Alberio T, Capurro V, Viganò D, Guidali C, Sala M, Fasano M, Parolaro D. The depressive phenotype induced in adult female rats by adolescent exposure to THC is associated with cognitive impairment and altered neuroplasticity in the prefrontal cortex. Neurotox Res. 2009 May;15(4):291-302.

Marrazzo E, Marchini S, Tavecchio M, Alberio T, Previdi S, Erba E, Rotter V, Broggini M. The expression of the DeltaNp73beta isoform of p73 leads to tetraploidy. Eur J Cancer. 2009 Feb;45(3):443-53.